Investigation of Equation of State for Materials under High Pressure and Temperature

Thesis Submitted for the Award of the Degree of

DOCTOR OF PHILOSOPHY

in

Physics

By

Tajamul Islam Seh

Registration Number: 41900747

Supervised by

Dr.Ajeet Kumar Srivastava

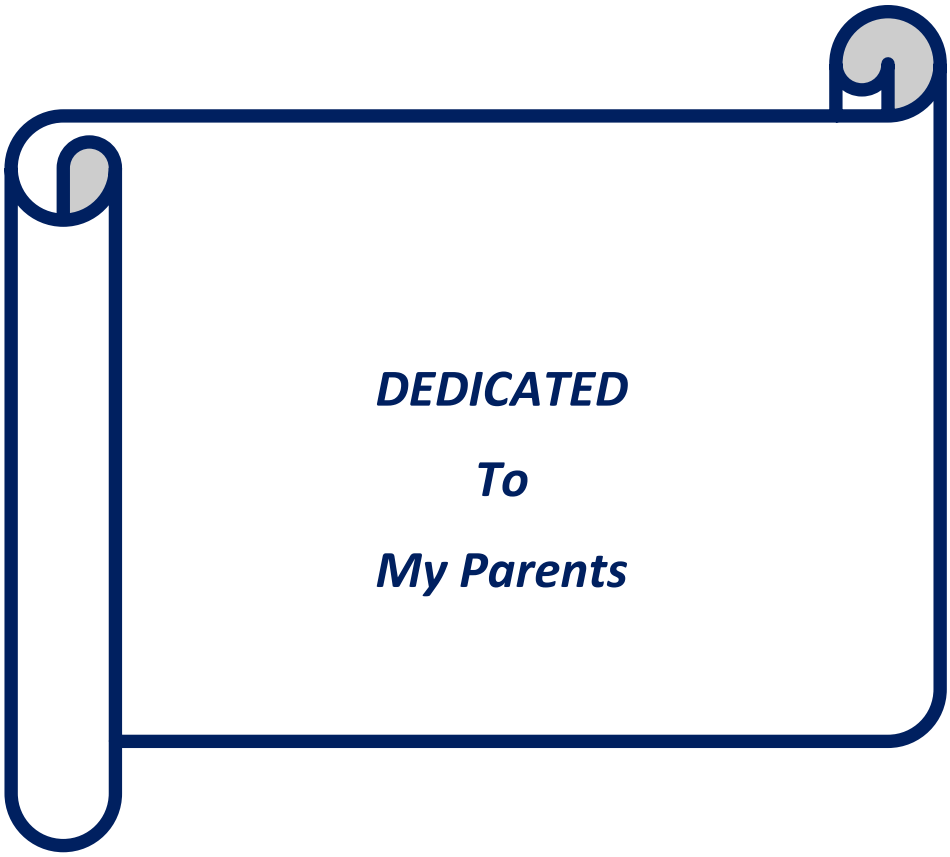
Department of Physics (Professor)

Lovely Professional University



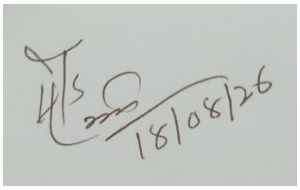
LOVELY PROFESSIONAL UNIVERSITY, PUNJAB

February, 2026


DEDICATED
To
My Parents

DECLARATION

I hereby declare that the thesis entitled "***Investigation of Equation of State for Materials under High Pressure and Temperature***" is an authentic record of research work carried out by me, under the supervision of Dr.Ajeet Kumar Srivastava, School of Chemical Engineering and Physical Science Department of Physics, Lovely Professional University, Phagwara,Punjab, India. The matter embodied in this Ph.D. thesis has not been submitted for the award of any other degree. Keeping in view, the general practice of reporting scientific observations, due acknowledgement has been made whenever work described here has been based on the findings of other investigators. Any omission that might have occurred due to oversight or error in judgment is regretted.



(Signature of Scholar)

Tajamul Islam

Registration No: (41900747)

Department/School: Physics

Lovely Professional University,

Phagwara-144411, Punjab, India

Date: 12-02-2026

CERTIFICATE

This is to certify that the thesis entitled **"Investigation of Equation of State for Materials under High Pressure and Temperature"** submitted by **Tajamul Islam Seh** bearing registration No: 41900747, Department of Physics, Lovely Professional University, Phagwara, Punjab, India for the award of the degree of **Doctor of Philosophy (Ph. D) in Physics** is a bonafide record of research work carried out by him under my supervision. The contents of the thesis, in full or in parts, have not been submitted to any other Institute or University for the award of any degree or diploma.



(Signature of Supervisor)

Dr.Ajeet Kumar Srivastava
(Supervisor)
Department of Physics
Lovely Professional University,
Phagwara-144411, Punjab, India

Acknowledgement

All praises to Allah, the creator and sustainer of the World

I owe my gratitude to many people who have made this thesis possible and because of whom my research experience has been one that I will cherish forever.

First and foremost, I would like to express my deepest gratitude to my advisor, Dr.Ajeet Kumar Srivastava, for his unwavering support, guidance, and encouragement throughout this research journey. His expertise and insights have been invaluable, and his patience and understanding have been a constant source of motivation. I am also profoundly grateful to the members of Dr.Kaialsh Chandra Juglan, Professor and HOD for their thoughtful feedback and constructive criticism, which have significantly improved the quality of this work. A special thanks to Department of Physics, Lovely Professional University (LPU), Phagwara, Punjab, whose resources and support have been fundamental to the completion of this thesis.

I extend my heartfelt appreciation to my brother in law Dr. Mudasir Ahmad Mir for his camaraderie, support, and the stimulating discussions that helped shape my ideas and provided a much-needed balance during this challenging journey. I am deeply indebted to my family, especially my parents, for their unwavering support and encouragement. Their understanding, sacrifices, and constant motivation have been my rock throughout this process. Thank you for your endless love, patience, and belief in me. I would like to express my sincere gratitude to my partner Ms Nusrat Ahad, for her encouragement, best wishes, and heartfelt prayers. No words can truly capture the depth of my love and affection for her.

Finally, I would like to thank everyone who has contributed, directly or indirectly, to the successful completion of this thesis. I am deeply grateful for your support and contributions, no matter how small. Your patience and unwavering moral support throughout my life have been invaluable, and I am profoundly indebted to you.

Thank you all.

Tajamul Islam

(41900747)

Abstract

Nanotechnology, the manipulation of matter at the nanoscale, grasps immense importance across various arenas owing to wide range of applications in medicine, electronics, energy and environmental science. In medicine, nanotechnology aids targeted drug delivery, precise imaging, and innovative treatments. In electronics, it improves device performance, miniaturization, and energy efficiency. Moreover, nanotechnology enables breakthroughs in renewable energy, pollution control, and water purification. Its aptitude to manipulate materials at the atomic and molecular level opens doors to solutions for pressing global challenges, making it a crucial frontier of scientific innovation with vast potential for the future.

Heusler compounds hold unique properties due to their structure and composition, exhibiting intriguing characteristics such as high electrical conductivity, low thermal conductivity, and tunable optical properties. Potential applications of Heusler compounds span numerous fields, including electronics, optoelectronics, and thermoelectric devices. In electronics, they could be used in high-performance transistors and sensors due to their outstanding electrical conductivity. In optoelectronics, their tunable optical properties make them promising candidates for photonic devices like LEDs and photo detectors. Moreover, in thermoelectric applications, Heusler compounds can proficiently convert waste heat into electricity, offering solutions for energy harvesting and cooling systems. With ongoing research, the adaptability of Heusler compounds continues to inspire innovation across multiple industries.This study investigated the compression behaviour of some Co, Rh, and Mn-based Heusler compounds such as Co_2TaB, Co_2NbB, Rh2MnZn, Rh2FeZn, Mn_2PtCo and Mn_2CoCr, using various equations of state such as Tait's equation of state, Murnaghan's equation of state, Shanker's equation of state and Kholiya and Chandra equation of state as a function of pressure. The Tait's equation of state generally fits best for the compression behavior of the materials, followed by the Murnaghan equation of state, and the Kholiya and Chandra and Shankers equations of state. All Heusler compounds exhibit similar patterns in compression behaviorwith increasing pressure. There is a slight deviation in compression that may be due to their crystal structure and chemical composition. The compression behavior of Heusler compounds FeCrTiSn and FeCrTiSb reveal that V/V_0 of both FeCrTiSn and FeCrTiSb compounds decreases linearly with increasing pressure.

The physical properties of nanomaterials are profoundly influenced by their structure and the distances between atoms. Under high pressure, the interatomic distance of the

nanomaterials can be altered, presenting an opportunity to explore the intricate relationship between the structure and various properties of nanomaterials. The impact of pressure on nanomaterials has emerged as a focal point of interest among researchers, owing to the profound alterations in their properties induced by pressure. Thus, exploring the behavior of nanomaterials under high pressure is essential due to the vast potential applications linked with these nanomaterials for broadening the spectrum of solid-state materials accessible to us.We have also investigated the compression behaviour of nanomaterials such as single-walled carbon nanotubes (SWCNT's), graphite, aluminium oxide (Al_2O_3), nano-ε-Fe and nano Ni by using different equation of states.

Fullerenes are fascinating molecules with a unique structure and diverse potential applications in fields ranging from materials science to medicine and electronics. We have employed the modified Suzuki equation of state to investigate the effect of temperature on volume expansion (V/V_0) for C_{60} (fullerenes as a solid material in nanoform). The results so obtained are compared with the experimental values which present a good agreement.

Manuscripts Published

- **Islam, T.,** Srivastava, A. K., Kaloo, M. A., &Wani, A. A.,Study of The Compression Behaviour Of FeCrTiSn And FeCrTiSb Materials Using Various Equation Of States. *Elementary Education Online*, (2023), *20*(6), 4961-4961.
- **Islam, T.,** Srivastava, A.K.,Kaloo, M. A., Mir.M.A.,Invesigation of Compression Behavior of Heusler Compounds Using Various Equations of State.*European Chemical Bulletin,*(2023),2063-5346.
- **Islam,T.,** Srivastava,A.K., Investigation of Compression Behaviour of Bulk Inorganic Materials(Al,Cu,Pb,Ni, and Zn) Under High Pressure. *South Eastern European Journal of Public Health*, (2025), 2197-5248.
- **Islam,T.,** Srivastava, A.K., Mudasir,M.,Santosh,C., and R.A. Zargar., Pressure Volume Response in Nanomaterials: Contrasting Graphenic Sheets, Oxide Ceramics, and transition Metals Architectures, (2026);20(2).

List of Conferences

- 8thInternational Conference on Nanotechnology for Better Living NBL – 2023 In collaboration with IIT BHU, Parul University, SKUAST- K and Kashmir University from: 25th -29th May 2023 "Study of the Compression Behaviour of FeCrTiSn and FeCrTiSb Using Various Equations of States".
- 3rd International Conference on Innovative Research in Sciences, Technology, Agriculture, Environment, Business Management and Humanities (STAEBM-2023) organised by the Department of "Metallurgical and Materials Engineering", NIT Srinagar, Jammu and Kashmir – 190006 and "Krishi Sanskriti" New Delhi from 13th-14thMay, 2023 on "Study of the thermal Compression Behaviour of C60(Fullerene) using modified equation of state

List of Tables

Table No	Caption	Page No
Table 4.1.1	Input data of Co, Rh, Mn based Heusler compounds	27
Table 4.1.2	Compression behaviour of Mn_2CoCr predicted by various EOS	27
Table 4.1.3	Compression behaviour of Mn_2PtCo predicted by various EOS	29
Table 4.1.4	Compression behaviour of Rh_2MnZn predicted by various EOS	30
Table 4.1.5	Compression behaviour of Rh_2FeZn predicted by various EOS	32
Table 4.1.6	Compression behaviour of Co_2NbB predicted by various EOS	33
Table 4.1.7	Compression behaviour of Co_2TaB predicted by various EOS	35
Table 4.2.1	Compression behaviour of FeCrTiSb predicted by various EOS	39
Table 4.2.2	Compression behaviour of FeCrTiSnpredicted by various EOS	41
Table 4.3.1	Input data of SWCNTs, Graphite, Al_2O_3, Nano-ε-Fe, Nano Ni	46
Table 4.3.2	Data regarding compression of Graphite material by different EOS	46
Table 4.3.3	Data regarding compression of Al_2O_3 material by different EOS	47
Table 4.3.4	Data regarding compression of SWCNT'smaterial by different EOS.	48
Table 4.3.5	Data regarding compression of Nano-Nimaterial by different EOS.	49
Table 4.3.6	Data regarding compression of Nano-ε-Fe material by different EOS.	50
Table 4.4.1	Input data of aluminium, copper, nickel, lead and zinc	53
Table 4.4.2	Compression behaviour of aluminium predicted by various EOS	53
Table 4.4.3	Compression behavior of Copper predicted by various EOS	55
Table 4.4.4	Compression behaviour of Lead (Pb) predicted by various EOS	56
Table 4.4.5	Compression behaviour of Nickel (Ni) predicted by various EOS	57
Table 4.4.6	Compression behaviour of Zinc (Zn) predicted by various EOS	58
Table 4.5.1	Compression Behaviour of C60 Fullerenes in nano form predicted by EOS	60

List of Figures

Figure No	Caption	Page No
Fig.1.1	Structure of pure Single walled carbon nanotubes (SWCNT)	3
Fig 1.2	The types of CNTs, (a): armchair nanotube (b): zigzag nanotube (c): chiral nanotubes	4
Fig 1.3	Schematic Structure of fullerene C60	5
Fig 4.1.1	Volume compression with respect to Pressure for Mn_2CoCr	28
Fig 4.1.2	Volume compression with respect to Pressure for Mn_2PtC	30
Fig 4.1.3	Volume compression with respect to Pressure for Rh_2MnZn	31
Fig 4.1.4	Volume compression with respect to Pressure for Rh_2FeZn	33
Fig 4.1.5	Volume compression with respect to Pressure for Co_2NbB	34
Fig 4.1.6	Volume compression with respect to Pressure for Co_2TaB	36
Fig 4.2.1	Volume compression with respect to Pressure for FeCrTiSb	40
Fig 4.2.2	Volume compression with respect to Pressure for FeCrTiSn	42
Fig 4.3.1	Variation compression of volume of graphite w.r.t the Pressure	47
Fig 4.3.2	Variation compression of volume of Al_2O_3 w.r.t the Pressure	48
Fig 4.3.3	Variation compression of volume of SWCNT's w.r.t the Pressure	49
Fig 4.3.4	Variation compression of volume of Nano-Ni w.r.t the Pressure	50
Fig 4.3.5	Variation compression of volume of Nano-ε-Fe w.r.t the Pressure	51
Fig 4.4.1	Volume compression with respect to pressure for Aluminium	54
Fig 4.4.2	Volume compression with respect to Pressure for Copper	55
Fig 4.4.3	Volume compression with respect to pressure for lead	56
Fig 4.4.4	Volume compression with respect to pressure for Nickel	58
Fig 4.4.5	Volume compression with respect to pressure for Zinc	59

Fig 4.5.1	Volume thermal compression of C60 fullerenes at different temperatures	61

Contents

S. No.	Contents	Page No.
	Acknowledgement	V
	Abstract	vi-vii
	List of Tables	Ix-x
	List of Figures	x-xi
	Contents	xi-xii
CHAPTER 1: Introduction		1-12
1.1	Nanomaterials	1-6
1.2	Heusler compounds	6-7
1.2.1	Rh_2MnZn and Rh_2FeZn Heusler Compounds	8
1.2.2	Mn_2CoCr and Mn_2PtCo Heusler Compounds	8
1.2.3	Co_2TaB and Co_2NbB Heusler Compounds	9
1.3	Equation of State Approach	9-10
1.3.1	Murnaghan equation of state	10
1.3.2	Kohliya and Chandra equation of state	10
1.3.3	Shankers equation of state	10-11
1.3.4	Tait Equation of State	11
1.3.5	Modified Suzuki equation of State	11-12
CHAPTER 2: Literature Review		13-19
2.1	Literature Review	13-19
CHAPTER 3: Method of Analysis		20-23
3.1	Method of Analysis	20-23
CHAPTER 4: Results and Discussions		23-48
4.1	**Investigation of Compression Behavior of Heusler Compounds Using Various Equations of State**	24-36

	✓ Introduction	24-25
	✓ Method of Analysis	25-26
	✓ Results and Discussion	26-36
	✓ Conclusion	36
4.2	**Study of the Compression Behaviour of FeCrTiSn and FeCrTiSb Using Various Equation of States**	37-42
	✓ Introduction	37-38
	✓ Methods of Analysis	38-39
	✓ Results and Discussion	39-42
	✓ Conclusion	42
4.3	**Investigation of Physical Properties of Nano Materials at High Pressure**	43-51
	✓ Introduction	43-44
	✓ Methods of Analysis	44-45
	✓ Results and Discussion	45-51
	✓ Conclusion	51
4.4	**Investigation of compressive behaviour of bulk inorganic materials (Al, Cu, Pb, Ni, and Zn) under high pressure**	52-61
	✓ Introduction	52-59
	✓ Comparative behaviour of bulk and nanomaterials	59-61
4.5	**Thermal Compression Behaviour of (C60) Fullerene under High Temperature**	61-63
CHAPTER 5: Conclusion		64-66
References		67-99

Chapter-1: Introduction

1.1 Nanomaterials: Materials with at least one dimension in the range of approximately 1-100 nm, possessing dimension-dependent characteristics are classified as nanomaterials [1-3]. Nanocrystalline materials exhibit different properties than bulk materials, which may be related to their high surface-to-volume ratio [2, 4-6]. Due to their size- and shape-dependent physical and chemical characteristics, nanomaterials have become one of the most significant material classes with a broad range of potential uses in the scientific and technical fields [2-4, 7-9]. Nanotechnology is widely used in the medical field as nanomedicine which incorporates diagnosis, imaging, and treatment of a variety of diseases, as well as ailments related to the cardiovascular, and central nervous systems [3-5]. It has emerged as a result of the growing use of nanotechnology products in healthcare because of their strong antimicrobial qualities and potential uses in antibacterial coatings, wound dressings, and even targeted drug delivery [2-8]. It has been also witnessed that zinc oxide (ZnO) and copper oxide (CuO) nanoparticles-based nanotechnology have attracted a lot of attention in the medical field. On the other side the understudy bulk materials like Aluminium (Al), copper (Cu), nickel (Ni), lead (Pb), and zinc (Zn) also play a substantial role in medicine; contributing to a variety of technologies and therapies [6-9]. These metals improve patient outcomes and quality of life by advancing medical treatments and healthcare innovations [7-10]. Manufacturing nanomaterials involves various methods, broadly categorized into top-down and bottom-up approaches [10-12]. The top-down method includes techniques like mechanical milling, lithography, and etching, where bulk materials are broken down into nanoscale particles [11-14]. On the other hand, bottom-up methods involve assembling nanomaterials from atomic or molecular components through processes like chemical vapour deposition, sol-gel synthesis, and self-assembly [14-16]. Each technique offers unique advantages in terms of control over size, shape, and composition, allowing for tailored properties for specific applications in fields such as medicine, electronics, and energy storage [17-20]. Applying high pressure is a crucial technique for inducing changes in the size, shape, and structure of nanomaterials [8-10, 21]. This method allows the manipulation of their physical and chemical properties, enabling the creation of novel materials with enhanced or unique functionalities [14-19]. High-pressure investigations are essential because they provide insights into the behavior of nanomaterials under extreme conditions, revealing phase transitions, structural deformations, and other critical phenomena [21-22]. These studies are vital for advancing applications in areas such as material science, nanotechnology, and high-performance engineering. [15-18-23]**.** The properties of

nanocrystalline materials can be significantly varied by the application of temperature. Thermal treatments can alter the size, shape, and crystalline structure of these materials, impacting their mechanical, electrical, and optical properties [8-11]. For instance, heating can promote grain growth, reduce defects, and induce phase transformations, while controlled cooling can refine grain size and enhance stability [23-24]. These temperature-induced modifications are essential for tailoring nanomaterials for specific applications, such as improving the efficiency of catalysts, enhancing the performance of electronic devices, and optimizing the strength and durability of structural materials [25-26]. The present study covers the theoretical investigation of mechanical properties, including bulk modulus, compression, and thermal expansion of several nanomaterials, such as γ-Al_2O_3, n-εFe, Sn-Ni, and single wall carbon nanotubes (SWCNT).

Carbon atoms rolled up from graphene sheets to form hollow, tube-shaped nanostructures known as carbon nanotubes (CNTs) [27-28]. Carbon is a substance that is present in millions of molecules, and these molecules have a wide range of unique qualities, ranging from solids like diamonds, the hardest material in nature, to gases like propane [27]. Carbon atoms can create bonds with a wide range of atoms through a process known as covalent bonding. There is no other element in the periodic table that links to itself as firmly and in as many ways as the carbon atom [28-29]. Each carbon atom may make these covalent bonds with four other atoms. Depending on how many layers they include, CNTs can be classified as single-walled (SWCNTs) or multi-walled (MWCNTs). SWCNTs are approximately 100,000 times smaller than a human hair, with a diameter of 0.5–2.0 nanometers [27-30]. There are two naturally occurring crystalline forms of pure carbon: diamond and graphite. In case of a diamond, four bonds are oriented towards the corners of a regular tetrahedron due to sp3 hybridization. One reason for the hardness of the diamond is its regular and rigid 3D network. In graphite, each atom is uniformly bonded to three carbons (at a 120° angle) in the xy plane as a result of sp^2 hybridization, generating the hexagonal (honeycomb) lattice of a graphite sheet, and there is a weak π bond along the z-axis. The nanotubes are considered as nearly one-dimensional nanostructures due to their large aspect ratio (length-to-diameter ratio) [31]. Pure SWCNT is composed of carbon atoms arranged in hexagonal rings of the benzene type, which resemble a rolled-up tubular shell of graphene sheet as shown in figure 1.1.

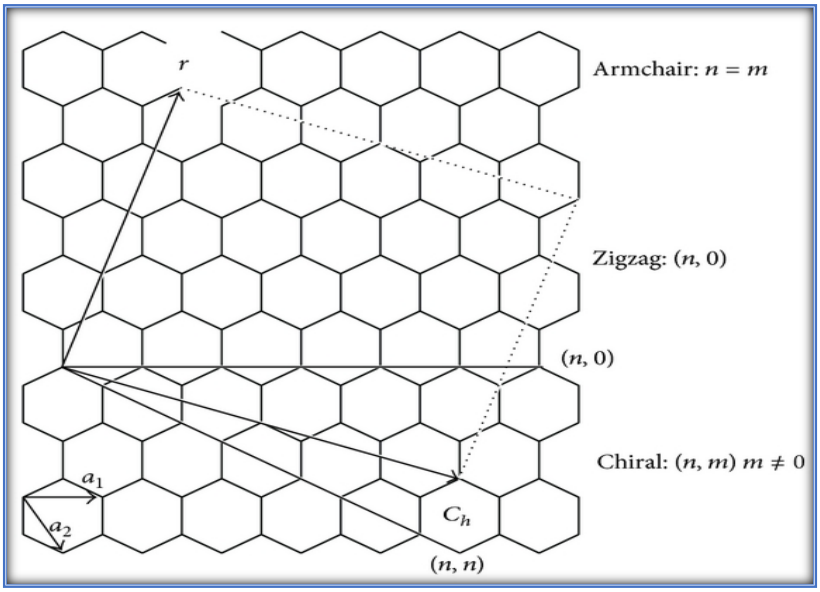


Fig.1.1: Structure of pure single walled carbon nanotubes (SWCNT) [32]

SWCNTs typically comprise only 10 atoms around the circumference, with a tube thickness of only one atom [32, 33]. MWCNT is an array of graphene sheets wrapped into concentric cylinders. Each nanotube is a single molecule with diameters as small as 0.7 nm and length upto tens of micrometers which contains millions of atoms [32, 34]. Typically, the outer diameter of a MWCNT nanostructure is less than 15 nm. When the outside diameter of a MWCNT nanostructure is greater than 15 nm, it is referred to as a carbon nanofiber [32-33, 35]. Besides the above two types, CNTs are classified into other three types, depending upon how the graphite is rolled up during the fabrication process viz. zigzag carbon nanotubes, armchair carbon nanotubes and chiral carbon nanotubes Fig 1.2 [32, 36]. The number of unit vectors along the two directions in the honeycomb crystal lattice of graphene is designated by the pair of indices, n and m, which together are referred as the chiral vector. If n=0, zigzag carbon nanotubes can be produced, and if n=m, armchair carbon nanotubes; all other configurations are referred to as chiral [32, 37-38].

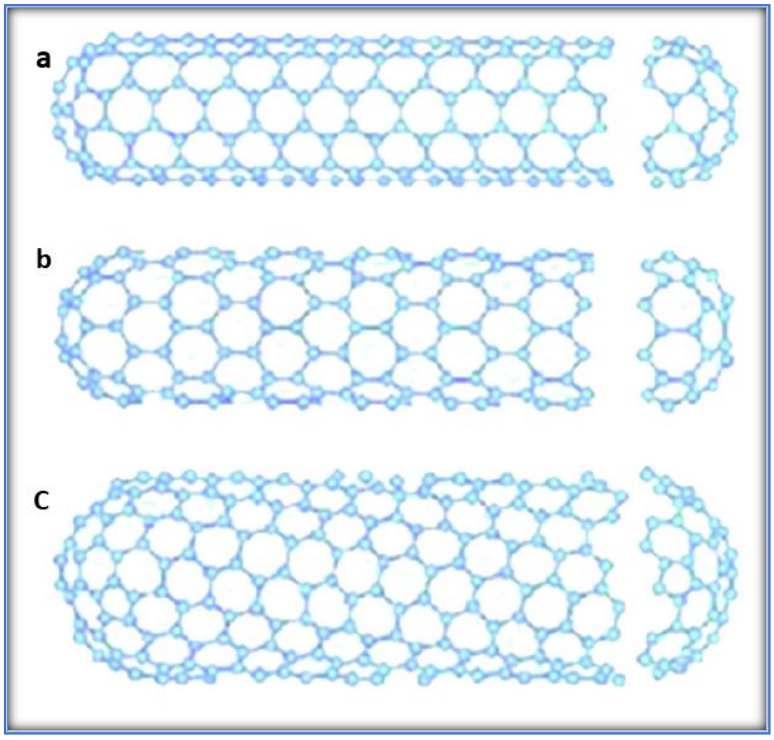


Fig 1.2: The types of CNTs, (a): armchair nanotube (b): zigzag nanotube (c): chiral nanotubes [32]

The unique molecule known as carbon-60, or fullerene, is composed of 60 carbon atoms grouped in a spherical form that resembles a Soccer ball fig 1.3, which comprise many forms for the geometric shapes of carbon molecules [39-45]. Which include various carbon molecules with distinct geometric shapes. It belongs to a class of carbon allotropes called fullerenes. Fullerenes exists in discrete molecular form and consists of a hollow spherical cluster of sixty carbon atoms (figure1.3); a single molecule is denoted by C_{60}.Each molecule is composed of groups of carbon atoms that are bonded to one another to form to both hexagon and pentagon geometrical configurations [46-47]. One such molecule is found to consist of 20 hexagons and 12 pentagons, which are arrayed such that no two pentagons share a common side; the molecular surface thus exhibits the symmetry of soccer ball [38-42]. The material composed of C_{60} molecules that contain sixty carbon atoms in a network of sp^2 bonding which forms a spherical structure, is known Buckminster fullerene [48-50].The strength of a chemical bond can often be inferred from its bond length. In sp^3- bonded diamond, the C-C bond length is 1.54 Å, while in sp^2-bonded graphite the in plane C-C bond length is 1.42 Å. In a C_{60} fullerene molecule, there are two bond lengths; these are 1.46 Å and 1.40 Å. This suggests that an isolated C_{60} molecule might be quite "stiff" (Bulk modulus 491GPa) [51-53]. It is a good metal in the form of graphite, a wide gap super hard semiconductor in the form of diamond .C_{60} is

the most stable of the fullerenes with the greatest symmetry. Because of the simplicity of C_{60} relative to other fullerenes, it has been widely discussed. Carbon-60 fullerenes are fascinating molecules with a unique structure and diverse potential applications in fields ranging from materials science to medicine and electronics [54-58]. Studies suggest that because of its 491GPa bulk modulus, an isolated C_{60} molecule is fairly stiff [58-60].

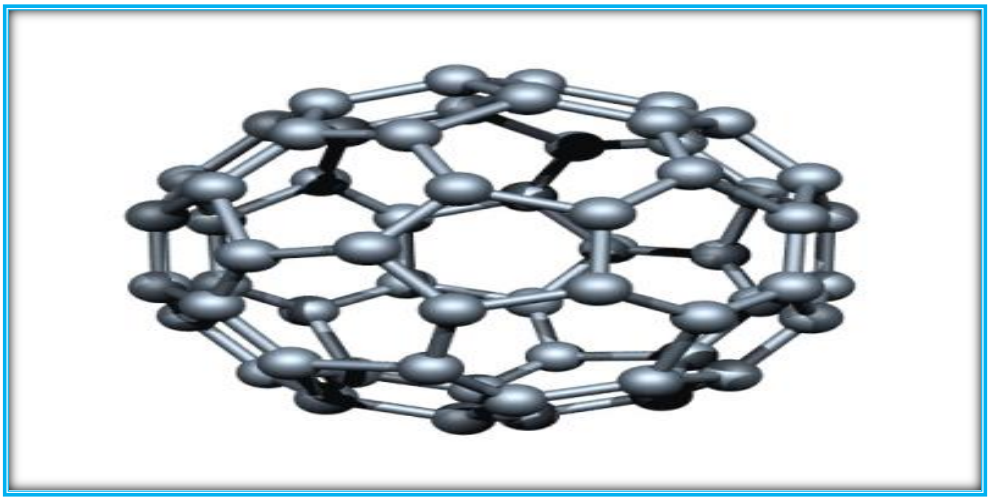


Figure 1.3 Structure of fullerene C_{60} [58]

Numerous theoretical and practical studies have been carried out with nanocrystalline iron (n-Fe) [61]. The small grain size of n-Fe has improved properties such as electrical, magnetic, thermal surface passivation and mechanical properties such as phonon density-of-states, hardness and ductility [62]. Nanocrystalline materials, characterized as materials with dimensions less than 100 nm, exhibit improved and novel applications in various fields such as engineering, chemistry and physics owing to the high-volume fraction of grain boundaries, which act as barriers to dislocation motion, thereby influencing magnetic domain structures and increasing strength [61, 63]. Nanocrystalline nickel is a specialized form of nickel exhibiting incredibly small grain size, typically ranging from 1 to 100 nanometers [64-65]. Due to Hall-Petch relationship, where the number of grain boundaries significantly increases as the grain size decreases, this material is known for its enhanced properties such as hardness, mechanical strength, corrosion and resistance to wear in comparison to its conventional coarse-grained counterparts [66]. Because of its ability to withstand greater pressures and retain structural integrity in harsh environments, n-Ni is a highly desirable material for use in aerospace, high-performance engineering, and military components [64-66]. Furthermore, n-Ni exhibits superior magnetic and electrical conductivity, which make its significant use in advanced electronic equipment's and magnetic storage media. Even with these encouraging

benefits, research is still being done to address issues like grain development at high temperatures and production costs in order to maximise the material's stability and economic viability for broad commercial application. Alumina, also referred to as aluminium oxide (Al_2O_3), is a crystalline material renowned for exceptional properties such as thermal stability, electrical insulation and hardness, which make it a potential material for industrial and technological importance [67]. Alumina is a naturally occurring oxide that can be found in the Earth's crust in a variety of mineral forms such as bauxite, corundum and sapphire [67]. The exceptional resistance to thermal shock and high melting point makes it invaluable across various applications in the field of materials science and engineering fields such as it is utilised in crucibles, furnace linings and kilns [68]. Moreover, it is a suitable candidate for abrasive applications, such as sandblasting, cutting and grinding due to its exceptional hardness and it serves as an insulating layer in integrated circuits and a substrate for semiconductor devices due it's to remarkable electrical insulating properties [68-69]

1.2 Heusler compounds: Heusler compounds, discovered by German chemist and mining engineer Friedrich Heusler in 1903, are a class of magnetic intermetallic materials which are characterized by their face-centered cubic crystal structure and have the general composition XYZ or X_2YZ, in which Z is a p-block element and X and Y are transition metals [70, 71]. Renowned for their tunable and adjustable physical characteristics, Heusler compounds find applications in spintronics, advanced electronic device and magnetic sensors [70, 74]. Heusler compounds are valuable in a wide range of advanced technological applications due to their versatile and tenable properties, which are made possible by their unique composition and structure [72-75]. These compounds have attracted significant attention for their ability to enable a wide range of functionalities in half-metallicity, magnetism, and superconductivity [73, 75-76]. Their most prominent applications are in the realm of spintronics, where they serve as key materials for magnetic tunnel junctions, spin valves and spin injectors [72, 74]. Their high spin polarization and half-metallicity are critical for enhancing the efficiency of spintronic devices, which aim to exploit electron spin rather than charge for data storage and transfer, leading to faster and more energy-efficient technologies [18-19, 75]. Additionally, Heusler compounds are employed in magnetic sensors and actuators, where their robust magnetic properties and high Curie temperatures ensure reliable performance in harsh environments, such as in automotive and aerospace industries [38, 76-77]. Beyond magnetism, Heusler compounds exhibit intriguing thermoelectric properties, making them suitable for energy harvesting applications [13, 18-19]. Their ability to convert waste heat into electrical energy can significantly improve the efficiency of power generation systems. Furthermore, certain

Heusler alloys have been identified as topological insulators, materials that conduct electricity on their surface while remaining insulating in their bulk. This unique feature holds promise for quantum computing and advanced electronic devices, where controlled surface states can be harnessed for robust and low-power consumption electronics [13, 74]. In the realm of superconductivity, Heusler compounds are also being explored for their potential to exhibit high-temperature superconducting phases, which could revolutionize power transmission and magnetic levitation technologies [76-80]. Their tunable electronic structure allows for the fine-tuning of superconducting properties, making them ideal candidates for next-generation superconductors [80]. Additionally, Heusler compounds' adaptability extends to their mechanical properties, where they are investigated for use in smart materials and shape memory alloys, contributing to innovations in robotics and biomedical devices. Overall, the diverse applications of Heusler compounds, ranging from spintronics and magnetic sensing to energy conversion and advanced computing, underscore their importance in driving forward the frontier of material science and technology [73-75, 77]. Their unique combination of magnetic, electronic, and structural properties continues to inspire new research and development, paving the way for future technological breakthroughs [73-78]. The following section deals with the properties of Rh and Mn and Co -based Heusler compounds.

1.2.1 Rh_2MnZn and Rh_2FeZn Heusler Compounds:

Rh_2MnZn and Rh_2FeZn are intermetallic compounds that belong to the Heusler alloy family, renowned for their distinctive magnetic and electronic properties [79-80]. Both compounds typically crystallize in the cubic L_{21} Heusler structure, characterized by a face-cantered cubic (FCC) arrangement. In the Rh_2MnZn compound, rhodium (Rh) atoms are positioned at (0, 0, 0) and (1/2,1/2,1/2), manganese (Mn) atoms at (1/4,1/4,1/4), and zinc (Zn) atoms at (3/4,3/4,3/4) within the cubic lattice. The mechanical properties of Rh_2MnZn can be fine-tuned through alloying and thermal treatment processes, enhancing its potential for various technological applications. Similarly, in the Rh_2FeZn compound, rhodium atoms occupy the (0,0,0) and (1/2, 1/2,1/2) positions, iron (Fe) atoms are located at (1/4,1/4,1/4), and zinc atoms at (3/4,3/4,3/4) within the cubic lattice. This highly symmetric and ordered atomic arrangement endows Rh_2FeZn with unique physical properties, making it a valuable material for diverse technological uses. Despite the similarities between Rh_2MnZn and Rh_2FeZn, they exhibit differences in their magnetic properties and potential applications due to variations in their composition [79-80].

1.2.2 Mn_2CoCr and Mn_2PtCo Heusler Compounds:

Mn_2CoCr and Mn_2PtCo are notable members of the Heusler alloy family, crystallizing in a cubic structure and exhibiting fascinating properties with potential applications in fields such as spintronics, magnetism, and thermoelectricity [81-82]. In Mn_2PtCo, manganese (Mn) atoms are situated at the (0, 0, 0) and (1/4,1/4,1/4) positions, platinum (Pt) atoms occupy the (1/2,1/2,1/2) position, and cobalt (Co) atoms are located at (3/4,3/4,3/4) within the cubic lattice. This symmetric and orderly atomic arrangement confers distinctive physical properties to Mn_2PtCo, making it valuable for various technological applications [82]. Notably, Mn_2PtCo is thermally stable, maintaining its structural and magnetic properties at high temperatures, which is essential for applications involving elevated temperatures [82-83]. Similarly, in Mn_2CoCr, manganese atoms are at the (0, 0 ,0) and (1/4,1/4,1/4) positions, cobalt atoms at (1/2,1/2,1/2), and chromium (Cr) atoms at (3/4,3/4,3/4) within the cubic lattice. This ordered and symmetric atomic structure endows Mn_2CoCr with unique physical properties, making it a valuable material for various technological uses [65-67]. Mn_2CoCr, like other Heusler alloys, shows promise in thermoelectric applications, where it can be optimized for energy conversion efficiency [84].

1.2.3 Co_2TaB and Co_2NbB Heusler Compounds:

Cobalt-based borides, members of the Heusler alloy family, such as Co_2TaB and Co_2NbB, have garnered significant interest due to their potential applications across various domains, including high-temperature structural materials, robust coatings, and superconductors [85-86]. Both Co_2TaB and Co_2NbB adopt a hexagonal crystal structure system, typically crystallizing in the AlB_2-type structure. This structural configuration is characterized by alternating layers of metal atoms (cobalt and tantalum or niobium) and boron atoms. In Co_2TaB, cobalt (Co) atoms occupy two distinct positions: Co1 at (0, 0, 0) and Co2 at (1/4, 1/4, 1/4), while tantalum (Ta) atoms are positioned at (1/2, 1/2, 1/2), and boron (B) atoms reside at (3/4, 3/4, 3/4) [50]. Such precise atomic arrangements confer upon Co_2TaB a robust and symmetrical crystal lattice. Similarly, in Co_2NbB, cobalt (Co) atoms occupy two non-equivalent positions within the unit cell: Co1 at (0, 0, 0) and Co2 at (1/4, 1/4, 1/4). Niobium (Nb) atoms are situated at (1/2, 1/2, 1/2), and boron (B) atoms are positioned at (3/4, 3/4, 3/4) [86]. This atomic arrangement results in a highly symmetric and stable crystal structure. The coordination environment in Co_2NbB is characterized by cobalt atoms being surrounded by niobium and

boron atoms, creating a balanced and symmetric arrangement that significantly influences the compound's electronic and magnetic properties [85-87].

1.3 Equation of State Approach: Equation of state (EOS) is a thermodynamic expression that relates pressure, volume and temperature. In thermodynamics, this equation provides us useful information about the relationship between thermodynamic state variables viz. pressure, volume and temperature for both systems of a pure component and also for multicomponent mixture [88-91]. Various equations of state were proposed to study the volume thermal compression in nano-crystalline as well as bulk materials under different thermodynamic variables viz. temperature, pressure and volume. As a result, equations of state can be used to describe the properties of bulk and nanomaterials. [91-94]. So, we can say equation of state is a basic characteristic of a matter which makes possible the application of all the general principles of thermodynamics, and reflects atomic structure, chemical bonding and stability of material [92-96]. The equations of state are useful in describing the stability of solid material by changing various parameters like pressure, volume, entropy and temperature [92-94]. The pressure volume-temperature relationship, often known as the *equation of state*, is one of the primary outcomes of high-pressure research. Below are several forms of equations of state which have been presented for better representation of PVT relationship for both bulk and nanomaterials [93-94, 97].

Various equations of state viz. Tait's equation of state, Murnaghan's equation of state, Kholiya and Chandra Equation of State, Shanker's equation of state are used to describes the mechanical properties mainly compression, thermal expansion, bulk modulus of different nano and bulk materials and the comparative analysis of their results by using equation of states [75-77, 80-81]. The studies based on EOS are extensively important not only in physics but also in chemistry and geophysics. Theoretical investigations of EOS at high pressure and high temperature are fundamentally important as they allow extrapolation as well as interpolation into zones where experimental data is not sufficient [96-98].

1.3.1 Murnaghan's equation of state: This is one of the many state equations, which have been used to express the behaviour of matter under conditions of high pressure. This equation is extracted under specific suppositions and includes two accommodated variables, the modulus of incompressibility B_o and its first order pressure derivatives $B_o^{/}$. Mathematically this equation is expressed as (Eq. 1) [99-102],

$$P(V) = B_o/B_o^{/}[(V/V_o)^{-Bo/} - 1] \quad (1)$$

Where, P(V) is pressure as a function of volume, V is volume of the material, V_0 is reference volume, typically the volume at ambient pressure, P_0 is reference pressure, often taken as ambient pressure. $B_0$is Bulk modulus at the reference volume V_0. B_0' is pressure derivative of the bulk modulus, which indicates how the bulk modulus changes with pressure.

1.3.2 Kohliya and Chandra equation of state: This equation of state (Eq. 2) is mathematical relationship of pressure and volume used in the study of high-pressure physics. It describes the volumetric change under the effect of high pressure for various materials. This equation act as a useful tool to predict the materials behaviour under extreme conditions of pressure by involving only two valuable input parameters that is bulk modulus and its first derivative. This is important technique in various fields including material science [94, 103-104].

$$P = \frac{B_0}{2}\left[(B_0' - 3) - 2(B_0' - 2)\left(\frac{V}{V_0}\right)^{-1} + (B_0' - 1)\left(\frac{V}{V_0}\right)^{-2}\right] \quad (2)$$

Where P represents pressure, B_0 bulk modulus and B_0' its first derivative.

1.3.3 Shankers equation of state: Shanker's equation of state (Eq.3) is a semi-empirical model that provides the reasonably accurate description of pressure- volume relationship for wide range of material under high pressure conditions by involving only two valued input parameters that is bulk B_0 and its first derivativeB_0'. This equation has been found very expedient in the study of condensed materials physics, where description of material behaviour under extreme conditions is important in various applications in material physics [98, 103-104].

$$P = B_0\left[\left(1 - \frac{V}{V_0}\right) + \left(B_0' + \frac{1}{2}\right)\left(1 - \left(\frac{V}{V_0}\right)^2\right)\right] \quad (3)$$

Where P represents the pressure, B_0 bulk modulus and B_0' its first derivative.

1.3.4 Tait Equation of State: This equation (Eq. 4) is of great assistance in nonlinear compression and pressure correlations for a wide range of materials. It has been found that this equation taking the outcome of the thermal coefficient of volume thermal extension (α) and bulk modulus (B) to stay steady under the impact of pressure and is given by [105-106],

$$B(P) = B_0 \frac{V}{V_0} \exp\left\{\left(1 - \frac{V}{V_0}\right)(B0 + 1)\right\} \quad (4)$$

Where B_0 is bulk modulus and B_0' is its first order pressure derivative, $\left(\frac{V}{V_0}\right)$ is volume expansion.

1.3.5 Modified Suzuki equation of State: Modified Suzuki equation as derived by Goyal and Gupta is mathematically and thermodynamically equation, this equation is very useful to predict compression values at high temperature, as this equation is mostly used in nonlinear compression and pressure correlations for a wide range of materials After several modifications the equation reads as

$$\frac{V}{V_0} = \left[1 - \frac{1 - [1 - 2\alpha_0\{T - T_0\}\{B_0 - 1\}]^{1/2}}{B_0 - 1}\right] \quad (5)$$

Where α_0 thermal expansion coefficient, T_0 is room temperature and T is some elevated temperature.

For calculation, just two input parameters are required: the bulk modulus and its initial pressure derivatives [90-93, 105-106]. After reviewing the literature, it has been observed that pressure affects the compression of bulk as well as nanomaterials. The structure effect is much more prominent for higher pressure and decreases for decreasing pressure. All equations of state for extreme compression of solids are constrained by the initial density along with ambient measurement of the bulk modulus B_o and pressure derivative of bulk modulus B_o' [95, 107-108].

In 1996, Munish Kumar utilized the Murnaghan and Birch equations of state to investigate the impact of high pressure on various types of solids, including ionic, metallic, covalent, and rare gases. Additionally, he introduced a straightforward and practical method for determining the bulk modulus as a function of pressure [109]. In 2022, Al Faris and colleagues conducted theoretical calculations to study the effects of high pressure on the thermodynamic properties of GaN at room temperature, up to 40 GPa [110]. Their calculations were based on the Birch-Murnaghan and modified Lennard-Jones equations of state, incorporating the Grüneisen approximation theory. From these equations, they derived a formulation for the bulk modulus, which predicted an increasing trend. The high bulk modulus value of GaN resulted in a minimal change in volume (less than 15%) even under extreme pressures up to 45 GPa [110]. In 2023, Neda Nazemi and collaborators explored the structural, electronic, and magnetic characteristics of Heusler compounds O_2BaX (X = Na, K, Rb, and Cs) [111]. Their study employed first-principles calculations and density functional theory utilizing the full-potential linearized augmented plane wave method. Findings indicated that the lowest energy state for all four compounds was the $AlCu_2Mn$-type structure in a

ferromagnetic configuration. They predicted that O_2BaX (X = Na, K, Rb, and Cs) compounds exhibit ferromagnetic half-metal behavior in both the $AlCu_2Mn$-type and $CuHg_2Ti$-type phases [111]. A. M. Al-Sheikh in 2011, studied the effect of high pressure on nano-Ge parameters by calculating the compressed volume V/V_o, Bulk modulus BT, Energy Gap Eg, under extreme pressure [112]. All equations used for this study namely Brich-Muranghan, Vinet, ML-J, Thomson and Madan showed compatibility with the experimental result. B.Archana et al., in 2012, worked on size- dependent equation of state for nanomaterials. In this study the isothermal compression of Ni and ε-Fe has been computed for different particle sizes. A change in pressure curve was obtained by increasing the particle size. The results have been contrasted with the accessible data. A decent consensus among theory and experiment reveals the authenticity of technique has been proposed [113].

This research examined the compressive behavior of several Co, Rh, and Mn-based Heusler compounds, including Co_2TaB, Co_2NbB, Rh_2MnZn, Rh_2FeZn, Mn_2PtCo, and Mn_2CoCr. The study employed various equations of state, such as the Tait equation, Murnaghan equation, Shanker's equation, and Kholiya and Chandra equation, to analyze computed values of bulk modulus and the relative volume change (V/V_0) as a function of pressure at a constant temperature. Additionally, the compression behavior of Heusler compounds FeCrTiSn and FeCrTiSb has been thoroughly investigated. We have also investigated the compression behaviour of materials like single-walled carbon nanotubes (SWCNTs), graphite, aluminium oxide (Al_2O_3), nano-ε-Fe and nano-Ni by employing different equations of state. The effect of temperature on volume expansion (V/V_0) for C_{60} has also been investigated.

Chapter -2

Literature Review

2.1 Literature Review

The utilization of equations of state (EOS) stands as a fundamental and pervasive aspect of modern physics. In the realm of thermodynamics, EOS plays a pivotal role in describing the behavior of matter under varying conditions of pressure, temperature, and volume. These equations provide valuable insights into the properties of gases, liquids, and solids, enabling researchers to predict and understand phase transitions, critical points, and other thermodynamic phenomena. Furthermore, in astrophysics and cosmology, EOS are indispensable tools for modelling the properties of celestial objects and the evolution of the universe itself. The versatility and applicability of EOS extend beyond the confines of classical thermodynamics, finding applications in condensed matter physics, fluid dynamics, and even high-energy particle physics. This literature review chapter explores the historical development, key theoretical foundations, and contemporary advancements in the use of equations of state across various subfields of physics, shedding light on the profound impact they have had on our understanding of the physical world.

K. Sushil et al., 2004, while working on examination of finite-pressure equation of state for solids under high pressures, reformulated equation of state for solids based on Lagrangian and Eulerian strain following the method developed by Stacey. The results are obtained for pressure (P), isothermal bulk modulus (K_T) and its pressure derivative for Ne, Ar, Cu, LiH and MgO solids for a wide range of compression (V/V_o) down to 0.5 [114].

Kumar & Kumar, 2008, explored nanomaterials under high pressure and successfully implemented use of equation of state. They found that the relation obtained in the present work gave the result which is in satisfying concurrence with the examined data as compared with the earlier data [115].

R. Kumar and Munish Kumar in 2013, studied nanomaterials at high pressure and temperature. The effect of temperature (under constant pressure) and the effect of pressure (under constant pressure) have been explored in this research, and the approach to the system under combined effect of pressure and temperature for various nano systems has been elaborated. The results indicate a better agreement between theory and experimental data, demonstrating the validity of the current procedure [116].

Uma D Sharma et al., 2011, demonstrated examination of equation of state for nanomaterials. In this study they proposed the equation of state for 20 different nanomaterials. This equation of state was used to concentrate on the impact of temperature on pressure of Ni (20mm). It was detected that there is a little shift in isotherm due to rise in the temperature. The result so obtained was found in better consensus with the available experimental data [117].

B.Archana et al., in 2012, worked on size- dependent equation of state for nanomaterials. In this study it was found that the isothermal compression of Ni and ε-Fe has been computed for different particle sizes. A change in pressure curve was obtained by increasing the particle size. The results have been contrasted with the accessible data. A decent consensus among theory and experiment reveals the authenticity of technique proposed in the present paper [118].

Bhatt C. Jeewan et al. in 2013, investigated high pressure equations of state for nanomaterialssuch as n-Rb_3C_{60}, n-CdSe (rocket phase), n-TiO_2 (anatase and rutilr phase), Fe-filled nanotube, and -Fe_2O_3 in order to determine the pressure-volume relationship for nanomaterials. The empirical equations of state results are found to be in good agreement with the available experimental data [119].

S. Madan et al., in 2013, have studied nanomaterials under high pressure. In their study various conceivable types of equations of state are deliberated upon with their relationship with the help of just two variables namely bulk modulus and its first derivatives. To analyse the impact of pressure on them, the calculation was done on various nano-materials. The theoretical investigations are in consistent with the experimentally reported results and the other theoretical models for given nanomaterials [120].

Singh and Singh in 2015, reported the thermal expansion coefficient of nanomaterials increases with decreasing particle size while examining the effect of size and temperature on the thermal expansion. Different nanomaterials of various sizes were examined under varying temperatures, and it has been observed that V/Vo increases with the increasingtemperature [121].

V. A. Greshnyakovet al., in 2014, worked on comparative analysis of different techniques for calculating the bulk modulus of solid bodies. A new technique for calculating the bulk modulus was proposed which was especially adapted for the theoretical calculation of the elastic properties of crystals. The new technique makes it possible to calculate the values of bulk moduli at high pressures with greater accuracy [122].

Chandra and Kholiya in 2016, have employed equation of motion (model) to investigate the compressional behaviour of nanomaterials under pressure such as C_uO, TiO_2, α -Fe_2O_3, n-Zn_O, n-CeO_2, n-PbS etc. The idea is based on the fact that under pressure, the product of the thermal expansion coefficient (α) and the bulk modulus (B_T), remains constant. The model utilised in this study is unique in that it requires just one main variable, the bulk modulus at zero pressure [123].

S. Mahipalin 2016, examined the temperature effect in the temperature range of 300K-700K on the isothermal bulk modulus of nanomaterials. It has been observed that the relative isothermal bulk thermal bulk modulus of nanomaterials such as fullerene (C60), 20nm-Ni and 15nm (80Ni+20Fe) decreases with increasing temperature [124].

G. Monika et al. in 2019, investigated the effect of shape, size, and temperature on the flexibility of nanomaterials through Young's modulus and thermal expansivity. It has been observed that the Young's modulus decreases as particle size decreases, whereas thermal expansivity increases as size of nanomaterials decreases [125].

C. Hinna et al., in 2014, have explored subordinate equation of state to examine the properties of nanomaterials just as bulk materials under various states of size, shape, pressure and temperature with the application to bulk materials and a combined formulation has been introduced to comprehend the properties of nanomaterials as well as bulk materials. After using the model, the outcome was observed to be in reasonable agreement with the experimental results [126]

A.M Alsheikh et al., in 2020, studied theoretical behaviour of both bulk as well as nanomaterials under high pressure. In this study it was found that the results which were obtained after using the various equations of state for evaluation of disparity of V/V_o against huge pressure in both the bulk as well as nano-forms for Ni, Ag and Cu are in better consensus with the experimentally observed data [127].

G.I Abdulwahab et al., in 2021, have employed various equation of states to analyse the thermo-flexible properties of nanomaterial such as Nano-TiO_2 under enormous pressure. The outcome of V/V_o variation calculation under immense pressure, using all the four EOSs it has been detected that there is excellent coincidence with the experimental data. This leads to the conclusion that the equation of states Brich Murnaghan, modified Lennard- Jones Tait) applicable to the bulk materials, may also be applied to nanomaterials for evaluation. [128].

L. Katherine et al., in 2018, have worked on crystalline solids using equation of state under change in volume, pressure, volume, temperature and entropy. Several metrics were employed throughout this study for evaluating the quantity of fit for eight distinct equations of state including 87 elements and more than 100 compounds that have been reported in the literature. But in this study, they failed to predict exact equation of state [129].

K. Dharmendra et al., in 2021, confirmed that the generalized Rydberg equation of state with $K_{\infty}{}^{/}$=5/3, while studying the first order pressure derivative of bulk modulus at very high pressure. Where, $K_{\infty}{}^{/}$ represents the infinite pressure value of first derivatives of bulk modulus. Iron was examined at 300K and it has been concluded that the Stacey reciprocal K/-EOS and the EOS are compatible to each other. The obtained were consistent with the Stacey reciprocal $k^{/}$-EOS of the lower mantle and outer core of the earth up to a pressure of 330GPa (nearly) [130].

A.M. Al-Sheikh in 2011, studied the effect of high pressure on nano-Ge parameters by calculating the compressed volume $V/V_{o,}$ Bulk modulus BT, Energy Gap Eg, under extreme pressure. All equations used for this study namely Brich-Muranghan, Vinet, ML-J, Thomson and Madan showed compatibility with the experimental result [131].

G. Monika et al., in 2019, calculated the impact of shape, size and temperature- dependent elastic properties of nano-materials. In this work, the Guisbers Model is combined with an isobaric tait equation of state, and the resulting model is used to examine the effects of temperature, size, and shape on Young's modulus and thermal expansion in nanomaterials. It has been found on comparing the computed result with the simulated and experimental result that Young's modulus showed decreasing nature on decreasing the particle size of nanomaterials, while as the thermal expansivity gets increased. [132].

G.Rohit et al., in 2021, worked on second order pressure derivatives of bulk modulus, in this study they calculated the extreme-pressure compression behaviour of some nano-oxides materials like titanium oxide, iron oxide magnesium oxide and copper oxide by using several equations of state. The calculated values then compared with the already knowing experimental values and found both the results agreed each other after comparison [133].

M. Moued., in 2019, employed local spin density approximation as executed in Wien 2k to determine various properties such as the electronic structure, elastic and magnetic properties of full Heusler Alloy. It has been observed that the band structure of this material is of a metallic character for both spin orientations because the energy level near to the Fermi is primarily

occupied by Ir-d and Fe-d-electrons. In this study the researcher accorded more attention in calculating the elastic constant, where he derived shear and bulk modules with employing Voigt-Reuss-Hill approach. Moreover, the compound under consideration satisfies the Born'scriteria which confirms its mechanical stability and the origin of magnetism in this alloy of Heusler is expected to be the outcome of the transition metal Fe [134].

Y.J.Sara et al., in 2022, investigated the structural behaviour of some full Heusler compounds viz. Co_2CrAl and Cr_2MnSb in terms of electronic, elastic and magnetic properties by using an Ab Initio Study. In this study the researchers were basically investigated the electronic, elastic and magnetic properties of inverse and conventional Heusler compounds (Co_2CrAl and Cr_2MnSb). The half metallic nature of both the conventional Heusler Co_2CrAl and inverse Heusler compound Cr2MnSb was observed which leads its significant character for spintronic applications. Also, using PBE-GGA method, the directband gap of 0.8eV and 0.9eV of tetragonal Heusler Co2CrAl and Cr_2MnSb, respectively was observed. Since the tetragonal and conventional Heusler compounds had small total magnetic moments, indicating that they were ferromagnetic and mechanically stable [135].

Y.K. Dinesh et al., in 2020, examined of semi- Heusler Alloys such as MnNbZ and FeNbZ where (Z= As, Sb) by employing density functional theory (DFT). Various properties such as structural, elastic, electronic and magnetic properties have been studies in detail. It has been found the magnetic phase and hence the structural stability of the alloys were considered wherein the ferromagnetic state is found to be stable. Moreover, it has been concluded that various parameters are thermodynamically and mechanically stable such as cohesive energy, formation energy and independent elastic constant C_{ij}. In addition to this, from Slater-Pauling rule for semi-Heusler, it has been confirmed that the calculated value of total magnetic moment for half-metallic compounds was 1.00 μ_B[136].

S.M Reham., in 2017, explored first principle density function theory (DFT) and successfully examined structural, electronic and elastic properties of topological Half-Heusler compounds such as LaPbBi under high pressure. The researcher calculated density of states (DOS), energy gap, the lattice constant, bulk modulus, band structure and also used the generalized gradient (GGA) approximation to calculate its first order pressure derivative of bulk modulus. By employing the above-mentioned approximation to LaPbBi compound, the calculated lattice constant and energy gap are estimated to be 6.98 Å and 0.315, respectively, which were observed in good agreement with the experimental results. Also, the calculated values of the

bulk modulus and its first order pressure derivatives were found to be 72.25 Gpa and 4.4, respectively [137].

A. Metin in 2022, employed density function theory to examine various properties of half Heusler alloy such as xKxMgN with x= 0, 0.25, 0.75,1. From the structural properties, it has been observed that the lattice parameter of cubic $Li_{1-x}K_xMgN$ vary from 4.97 Å to 5.91 Å. Also, from the density of states, it has been investigated that the nitrogen atoms have a very leading effect near the valance band maximum and the conduction band minimum. Moreover, it has been observed from electric gap calculation that the direct band gap of alloy under discussion differs from 1.39eV to 3.07eV and concluded that $Li_{1-x}K_xMgN$ is a good candidate for visible and near IR optoelectronics applications owing to its appreciable band gap range. It has been concluded from the results achieved from structure and electronic calculations allows growing the alloy on various common substrates such as Si, Ga, As, Ge, INP for optoelectronic application's [138].

M. Khalfa et al., in 2015, have studied full Heusler compounds such as Fe_2VX (X=Al,Ga) using FP-LAPW + lo method within CGA and investigated various properties such as mechanical, electronic and thermodynamic, etc. From the calculated electronic properties, the researcher concluded that Fe_2VAl and Fe_2VGa are semimetals and observed that computed structural parameters and the previously available experimental data agreed fairly well. Finally, for both the compounds, Fe_2VAl and Fe_2VGa, the discussion regarding to various studies including Debye temperature with pressure and temperature, thermal expansion heat capacity, the thermal properties, in which the variations of the volume, and bulk modulus were thoroughly detailed [139].

M. Sanjay et al., in 2015, have explored the equation of state to investigate the mechanical properties of various nanomaterials. The researchers have calculated various parameters such as compression, isothermal bulk modulus and relative isothermal expansion coefficient, respectively for various nanomaterials such as 67nm and 37nm γ-Al_2O_3, nanocrystalline Ni, 3C-SiC, Nano ε-Fe. It is very much predicted from the results that the relative compression obtained from Tiat equation of state are consistent with the available experimental data. Moreover, the 37nm γ-Al_2O_3 is found to be more compressible at high pressure as compared to the 67nm nanocrystalline γ-Al_2O_3. Finally, it is observed that usual Tiat's equation of state gives the very satisfactory results in calculating the compression behaviour under the effect of high pressure of nanomaterials [140].

P.K. Singh, in 2011, have studied the effect of pressure on the bulk modulus for solids based on the first principal results determined from the augmented plane wave method for metals, non- metals and diatomic solids. It is observed that for the study of higher derivatives of bulk modulus and thermoelastic characteristics, the K-primed equations of state for various solids are more important than traditional pressure-volume relationships. In conclusion, the results obtained in the form of the reciprocal K-primed quadratic equation are consistent with first principal results obtained from the plane wave method for various solids [141].

S.D.Uma et al., in 2011, established simple model to investigate the effect of pressure and temperature on C_{60} fluorite solid. The researcher has presented a simple and straight forward method based on the theory of EOS to investigate the properties of C_{60} under varying conditions of pressure and temperature. The used equations are Murnaghan, Brich-Murnaghan, Vinet, and the theory of EOS as reported by Kumar are critically analysed by study the compression behaviour of C_{60} data in the light of experimental data. The investigation has been done under varying the temperature from room temperature to 2000k, and pressure from room pressure to 200kbar.The results were found in good agreement with the available experimental results [142].

S. Madan et al., in 2013, studied the volume expansion of various nanomaterials viz. CDSe94.2nm), Fe-Cu (14nm) Ni (20nm), γ-Al2O (67nm), γ—Al2O3 (37nm) and developed a theory to investigate the effect of pressure on volume expansion by employing various equations of state. For this study the researcher involves only two input parameter that is the pressure and first order pressure derivatives. The results obtained in this investigation were found in good agreement with the already available experimental values [143].

Chapter 3: Method of Analysis

3.1 Method of Analysis

In this study, various equations of states (EOS) were used for determining the compression behavior as a function of pressure at constant temperature. Bulk modulus measures the resistance of a material to change in volume when subjected to an external pressure and is determined by the ratio of the infinitesimal change in pressure to the corresponding fractional change in volume. The equation of state used for the determining the effect of pressure and temperature becomes important to understand their behavior for various thermodynamic variables because of their tremendous application features.

The equation of state established by Sharma and Kumar [117] reads:

$$\mathrm{P} = a_0 + a_1\left(1-\frac{V}{V_0}\right) + a_2\left(1-\frac{V}{V_0}\right)^2 + a_3\left(1-\frac{V}{V_0}\right)^3 \qquad (3.1)$$

Where a_0, a_1, a_2 and a_3 are the sized dependent parameters, which may be determined from bulk modulus and first / second order pressure derivatives of the bulk modulus. Also, in equation 3.1, there are no higher powers terms since such terms will comprise higher-order pressure derivatives of the bulk modulus. The Bulk Modulus B, is given as

$$B = -V\left(\frac{\partial P}{\partial V}\right)_T \qquad (3.2)$$

According to the definition of bulk modulus, equation (2) is written as

$$\mathrm{B} = \frac{V}{V_0}\left[a_1 + 2a_2\left(1-\frac{V}{V_0}\right) + 3a_3\left(1-\frac{V}{V_0}\right)^2\right] \qquad (3.3)$$

Likewise, the bulk modulus of the first-order pressure derivatives is given by

$$B' = \left(\frac{\partial B}{\partial P}\right)_T = -\frac{V}{B}\left(\frac{\partial B}{\partial V}\right)_T \qquad (3.4)$$

Above equation for the first order pressure derivatives of the bulk modulus can be written as

$$B' = -\frac{1}{B}\frac{V}{V_0}\left[a_1 + 2a_2\left(1-\frac{V}{V_0}\right) + 3a_3\left(1-\frac{V}{V_0}\right)^2 - \frac{V}{V_0}\left(2a_2 + 6a_3\left(1-\frac{V}{V_0}\right)\right)\right] \qquad (3.5)$$

Applying Boundary condition in equation 3.3 &3.5 that is $B = B_0$ at $V = V_0$, we get

$$a_0 = 0$$

$$a_1 = B_0$$

$$a_2 = B_0 \frac{(B_0' + 1)}{2}$$

Thus equation 3.1 takes the form

$$\mathrm{P} = B_0 \left(1 - \frac{V}{V_0}\right) + B_0 \frac{(B_0'+1)}{2} \left(1 - \frac{V}{V_0}\right)^2 \qquad (3.6)$$

After simplifying, we get

$$\mathrm{P} = \mathrm{B}_0 \left[\left(1 - \frac{\mathrm{V}}{\mathrm{V}_0}\right) + \left(\frac{\mathrm{B}_0'+1}{2}\right)\left(1 - \left(\frac{\mathrm{V}}{\mathrm{V}_0}\right)^2\right)\right] \qquad (3.7)$$

Eq. (3.7) is basically an isothermal equation of state which is used to study the high compression behavior involves two input parameters, the bulk modulus and the first order pressure derivatives of bulk modulus. This equation is known as Shankers equation of state [136-138, 145-148].

Tait equation of state generally fits best for the compression behaviour of the chosen material had given by P.G. Tait in 1888, which was the non-linear relation of compression with pressure for liquids. After many modifications the new modified form of equation of state is introduced known as Usual Tait equation (UTE) is in the following form for different solids.

$$\frac{\mathrm{V}}{\mathrm{V}_0} = \left[\, 1 - \frac{1}{\mathrm{B}_0+1} \ln\left\{1 + \left(\frac{\mathrm{B}_0+1}{\mathrm{B}_0}\right)\mathrm{P}\right\}\right] \qquad (3.8)$$

Using this realistic approach, we can calculate the relative volume compression V/V_0 for different solids. Also, the expression for isothermal bulk modulus $B(P)$by using relation can be written as:

$$\mathrm{B} = \mathrm{B}_0 \frac{\mathrm{V}}{\mathrm{V}_0}\left\{1 + \left(\frac{\mathrm{B}_0+1}{\mathrm{B}_0}\right)\mathrm{P}\right\} \qquad (3.9)$$

$$\Rightarrow 1 + \left(\frac{\mathrm{B}_0+1}{\mathrm{B}_0}\right)\mathrm{P} = \exp\left\{\left(1 - \frac{\mathrm{V}}{\mathrm{V}_0}\right)(\mathrm{B}_0 + 1)\right\} \qquad (3.10)$$

From above equations, we get

$$\mathrm{B(P)} = \mathrm{B}_0 \frac{\mathrm{V}}{\mathrm{V}_0} \exp\left\{\left(1 - \frac{\mathrm{V}}{\mathrm{V}_0}\right)(\mathrm{B}_0 + 1)\right\} \qquad (3.11)$$

This is the Tiat's equation for isothermal bulk modulus.

Consider the product of the thermal coefficient of volume thermal expansion (α) and bulk modulus (B_T) to remain constant under the effect of pressure i.e.

αB = constant (3.12)

Differentiation of equation (2.12) with respect to volume at constant temperature gives

$$\alpha\left(\frac{dB}{dV}\right)_T + B\left(\frac{d\alpha}{dV}\right)_T = 0 \quad (3.13)$$

Which yields,

$$\delta_T = \frac{V}{\alpha}\left(\frac{d\alpha}{dV}\right)_T = -\frac{V}{K}\left(\frac{dB}{dV}\right)_T \quad (3.14)$$

Where $\delta_T$is Anderson-Gruneisen parameter at constant temperature

$$\frac{dB}{B} = -\delta_T \frac{dV}{V} \quad (3.15)$$

Integrating equation (3.15) with $B=B_0$, when $V=V_0$. Assuming that δ_T is independent of V, we get

$$\frac{B}{B_0} = \left(\frac{V}{V_0}\right)^{-\delta_T} \quad (3.16)$$

Since, $B = -V\left(\frac{dP}{dV}\right)_T$ then equation (3 .16) becomes

$$\frac{V}{K_0}\left(\frac{dP}{dV}\right) = \left(\frac{V}{V_0}\right)^{-\delta_T} \quad (3.17)$$

$$\frac{dV}{V^{\delta T+1}} = -\frac{1}{B_0 V_0^{\delta_T}} dP \quad (3.18)$$

The integration of equation (3.18) gives us the following relation

$$\mathrm{P} = \frac{\mathrm{B}_0}{\mathrm{B}_0'}\left[\exp\left\{-\mathrm{B}_0' \ln\left(\frac{\mathrm{V}}{\mathrm{V}_0}\right)\right\} - 1\right] \quad (3.19)$$

Equation (3.19) is the same relation as given by Murnaghan [136-138, 145-146] known as Murnaghan equation of state.

Similarly, Kohliya and Chandra [154-156, 162-166] equation of state is given the relation

$$P = \frac{B_0}{2}\left[(B_0' - 3) - 2(B_0' - 2)\left(\frac{V}{V_0}\right)^{-1} + (B_0' - 1)\left(\frac{V}{V_0}\right)^{-2}\right] \quad (3.20)$$

We have investigated the thermal compression behaviour of C_{60}(fullerene) under high temperature at constant pressure by using modified Suzuki equation of state and is given by the equation as:

$$\frac{V}{V_0} = \left[1 - \frac{1 - [1 - 2\alpha_0\{T - T_0\}\{B_0 - 1\}]^{1/2}}{B_0 - 1}\right] \quad (3.21)$$

Where α_0 thermal expansion coefficient, T_0 is room temperature and T is some elevated temperature.

Chapter-4: Results and Discussions

4.1: Investigation of Compression Behavior of Heusler Compounds Using Various Equations of State

Introduction

Intermetallic Heusler compounds have attracted significant attention in recent years due to their unique physical, electrical, and magnetic properties. Understanding the compression behavior of these compounds is crucial for predicting their mechanical properties and for potential applications in fields such as energy storage, thermos-electrics, and spintronics. In this context, several studies have investigated the compression behavior of different Heusler compounds using various equations of state (EOS) models. In recent days, various multi component mixture compounds like Mn_2CoCr, Mn_2PtCo, Rh_2MnZn, and Rh_2FeZn are gaining more attention due to their extraordinary properties like compressible and structural properties by changing the pressure, volume and temperature [149-155]. These Heusler compounds are known for their exciting magnetic, electronic, and thermoelectric properties, making them capable materials for various technological applications [155-161]. Heusler compounds have various potential applications due to their unique combination of physical and chemical properties. Some of the major technological applications of such compounds namely Mn_2CoCr, Mn_2PtCo, Rh_2MnZn, Rh_2FeZn, Co_2NbB and Co_2TaB include:

i. *Magnetic materials:* Heusler compounds reveal high magnetic properties, making them suitable for use in various magnetic applications, such as magnetic storage devices and magnetic sensors.
ii. *Hard Materials:* Heusler compounds exhibit high hardness and wear resistance, making them appropriate for used as hard materials in wear- resistant coatings,
iii. *Energy Storage devices:* All under study Heusler compounds exhibit good electrochemical performance, making them potential materials for use in energy storage devices such as batteries.
iv. *Spintronics:* These materials have been studied for its potential in spintronics, a field that uses the spin of electron in solid-state system.

It is worth to mention that these compounds have a distinctive crystal structure, with alternating layers of transition metal and main group elements, and exhibit a range of magnetic and electronic phases. Because of high thermal stability, these compounds are applicable for high-temperature applications.

Equation of state is a relationship that describes the state of a system in terms of its variables, such as temperature, pressure, volume, and density [162-165]. It is used to predict the behavior of a substance under different conditions viz. pressure, volume and temperature for both systems of a pure component and also for multicomponent mixture. The equations of state are useful in describing the stability of solid material by changing various parameters like pressure volume entropy and temperature [166-167]. So, the equation of state is a basic characteristic of a matter which makes possible the application of all the general principles of thermodynamics, and reflects atomic structure, chemical bonding and stability of material [168-170].

In this paper, we have studied the compression behavior of some Co, Rh, Mn based Heusler compounds in terms of calculated values of relative change in volume (V/V_0) and bulk modulus as a function of pressure at constant temperature by using some theoretical models, known as equations of state.

Methods of Analysis:

In this study, various equations of state (EOS)0 have been used to determine the compression behavior of Heusler compounds based on Co, Rh, and Mn. This was done by calculating the relative change in volume (V/Vo) and bulk modulus as a function of pressure at a constant temperature. Bulk modulus measures the resistance of a material to change in volume when subjected to an external pressure and is determined by the ratio of the infinitesimal change in pressure to the corresponding fractional change in volume. In the present study we have used Tait equation state, Murnaghan EOS, Kohliya and Chandra and Shankers equation of state, to determine the pressure dependence of volume compression and bulk modulus of some Heusler compounds namely Mn_2CoCr, Mn_2PtCo, Rh_2MnZn, Rh_2FeZn, Co_2NbB and Co_2TaB.

Tait equation of state generally fits best for the compression behavior of the chosen material had given by P.G. Tait in 1888, which was the non-linear relation of compression with pressure for liquids. After many modifications the new modified form of equation of state is introduced known as Usual Tait equation (UTE) is in the following form for different solids.

$$\frac{V}{V_0} = \left[1 - \frac{1}{B_0 + 1} \ln\left\{1 + \left(\frac{B_0 + 1}{B_0}\right) P\right\}\right]$$

Using this realistic approach, we can calculate the relative compression V/V_0 for different solids.

Also, the expression for isothermal bulk modulus $B(P)$by using relation can be written as:

$$B = B_0 \frac{V}{V_0}\left\{1 + \left(\frac{B_0 + 1}{B_0}\right)P\right\}$$

$$\text{Or} \qquad 1 + \left(\frac{B_0+1}{B_0}\right)P = \exp\left\{\left(1 - \frac{V}{V_0}\right)(B_0 + 1)\right\}$$

From above equations, we get

$$B(P) = B_0 \frac{V}{V_0} \exp\left\{\left(1 - \frac{V}{V_0}\right)(B_0 + 1)\right\} (4.1.1)$$

Which is the Tiat equation for isothermal bulk modulus.

Other equations of states, Murnaghan equation of state, Kholiya and Chandra equation of state and Shankers equation of state are given by the following relations:

Murnaghan EOS [171-173, 180-181] is given by the relation

$$P = \frac{B_0}{B_0'}\left[\exp\left\{-B_0' \ln\left(\frac{V}{V_0}\right)\right\} - 1\right] \qquad (4.1.2)$$

Kohliya and Chandra [171-173, 179-182] equation of state is given the relation

$$P = \frac{B_0}{2}\left[(B_0' - 3) - 2(B_0' - 2)\left(\frac{V}{V_0}\right)^{-1} + (B_0' - 1)\left(\frac{V}{V_0}\right)^{-2}\right] \qquad (4.1.3)$$

Shankers equation of state [171-173, 174-182] is given by the equation

$$P = B_0\left[\left(1 - \frac{V}{V_0}\right) + \left(B_0' + \frac{1}{2}\right)\left(1 - \left(\frac{V}{V_0}\right)^2\right)\right] \qquad (4.1.4)$$

Result and Discussion:

Heusler compounds are famous for their applications such as magnetic storage devices. It becomes important to understand their behavior under various thermodynamic variables. In this study we have calculated the thermodynamic variable like bulk modulus and its first pressure derivatives by using various equations of states. The input data of Co, Rh, Mn based Heusler compounds required for the present work to calculate the volume compression of six full Heusler compounds are given in Table 4.1.1.

Table 4.1.1: Input data of Co, Rh, Mn based Heusler compounds

Compounds	B_0 (GPa)	B_0'(GPa)
Mn_2CoCr	171	5.91
Mn_2PtCo	185.6	4.1
Rh_2MnZn	183.2	5.5
Rh_2FeZn	196.9	4.72
Co_2NbB	244.35	3.76
Co_2TaB	241.80	4

Table 3.2 shows the compression behavior of Mn_2CoCr at different pressures (in GPa) as predicted by different equations of state: Tait, Murnaghan, Kholiya and Chandra, and Shankers. The V/V_0 values in the table represent the volume of the material at each pressure relative to its initial volume (V_0).

The Tait equation of state predicts that the material's volume decreases gradually with increasing pressure, with a V/V_0 value of 0.9228 at 16 GPa. The Murnaghan equation of state also predicts a similar trend, but with a slightly higher V/V_0 value of 0.9251 at 16 GPa. The Kholiya and Chandra equation of state predicts a more rapid decrease in volume, with a V/V_0 value of 0.9272 at 16 GPa. The Shankers equation of state predicts the most rapid decrease in volume, with a V/V_0 value of 0.9283 at 16 GPa (Fig. 4.1.1). Overall, the table shows that as the pressure increases, the volume of Mn_2CoCr decreases, which is expected for most materials. However, the exact rate of compression varies depending on the equation of state used to model the behavior.

The comparative analysis of different equations of state (EOS)—Tait, Murnaghan, Kholiya and Chandra, and Shanker—reveals that all models predict a consistent decrease in relative volume (V/V_0) with increasing pressure, reflecting the expected compression behavior of solids. Among them, the Tait EOS shows the most significant volume reduction, indicating a lower compressibility and thus a higher bulk modulus, while the Shanker EOS predicts the least volume reduction, corresponding to higher compressibility and a lower bulk modulus. This variation highlights that compressibility is inversely related to the bulk modulus and is sensitive to the form of the EOS used. The choice of an appropriate EOS is therefore crucial in accurately

describing the pressure-volume relationship of materials, especially in high-pressure physics and materials science applications where precise mechanical behavior is critical.

Table 4.1.2: Compression behaviour of Mn_2CoCr predicted by various EOS

Pressure (GPa)	Tait Equation of State V/V_0	Murnaghan Equation of State V/V_0	Kholiya and Chandra Equation of State V/V_0	Shankers Equation of State V/V_0
0	1	1	1	1
2	0.99	0.991	0.992	0.9921
4	0.98	0.981	0.982	0.983
6	0.97	0.972	0.9739	0.975
8	0.96	0.961	0.9631	0.9661
10	0.95	0.952	0.954	0.955
12	0.94	0.942	0.9437	0.9438
14	0.931	0.932	0.935	0.936
16	0.9228	0.9251	0.9272	0.9283

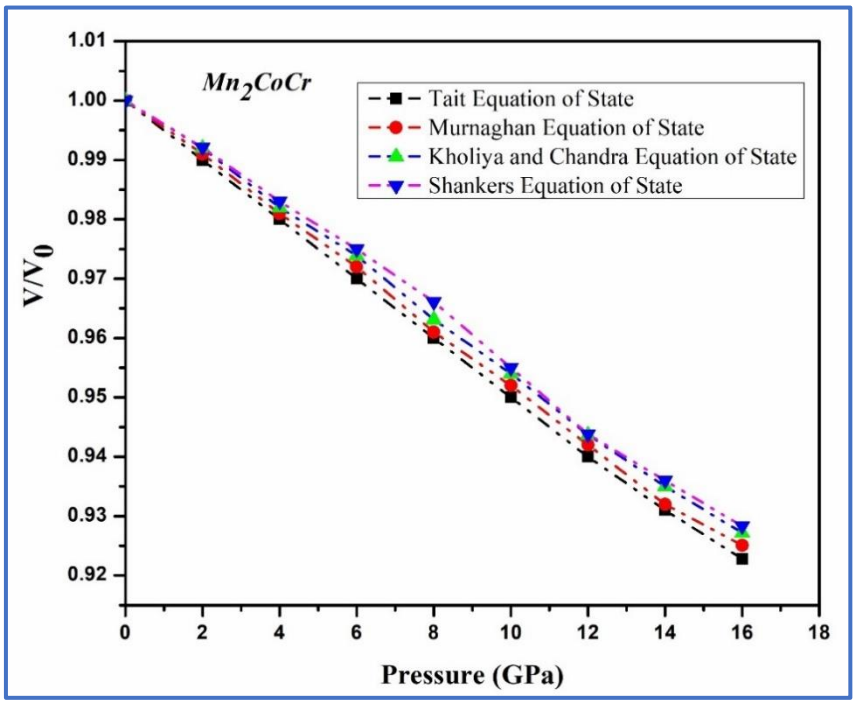


Fig 4.1.1: Volume compression with respect to Pressure for Mn_2CoCr

Table 4.1.3 shows the compression behavior of Mn_2PtCo at different pressures (in GPa) as predicted by different equations of state: Tait, Murnaghan, Kholiya and Chandra, and Shankers (shown in Fig 4.1.2). The V/V_0 values in the table represent the volume of the material at each pressure relative to its initial volume (V_0). The table shows that as the pressure increases, the volume of Mn_2PtCo decreases, which is consistent with the behavior of most materials under compression. The Tait equation of state predicts a gradual decrease in volume, with a V/V_0 value of 0.9209 at 16 GPa. The Murnaghan equation of state also predicts a gradual decrease in volume, with a slightly higher V/V_0 value of 0.9239 at 16 GPa. The Kholiya and Chandra equation of state predicts a slightly more rapid decrease in volume, with a V/V0 value of 0.925 at 16 GPa. The Shankers equation of state predicts the most rapid decrease in volume, with a V/V_0 value of 0.9258 at 16 GPa.

Table 4.1.3: Compression behaviour of Mn_2PtCo predicted by various EOS

Pressure (GPa)	Tait Equation of State V/V_0	Murnaghan Equation of State V/V_0	Kholiya and Chandra Equation of State V/V_0	Shankers Equation of State V/V_0
0	1	1	1	1
2	0.99	0.992	0.9923	0.9933
4	0.98	0.9815	0.9821	0.9841
6	0.97	0.971	0.9732	0.974
8	0.96	0.961	0.9625	0.9642
10	0.95	0.9513	0.9521	0.9544
12	0.94	0.942	0.9431	0.9415
14	0.93	0.9315	0.9325	0.9331
16	0.9209	0.9239	0.925	0.9258

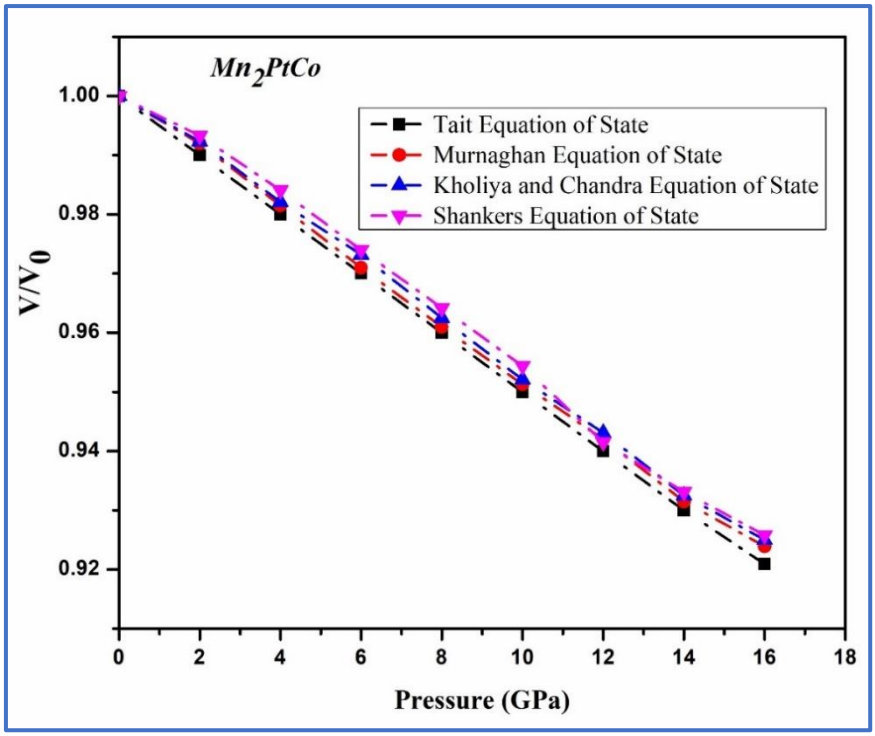


Fig 4.1.2: Volume compression with respect to Pressure for Mn_2PtCo

Table 4.1.4 presents the compression behavior of Rh_2MnZn at different pressures (in GPa) as predicted by different equations of state: Tait, Murnaghan, Kholiya and Chandra, and Shankers (shown in Fig 4.1.3). The table indicates that as the pressure increases, the volume of Rh_2MnZn decreases, which is consistent with the behavior of most materials under compression. The Tait equation of state predicts a gradual decrease in volume, with a V/V_0 value of 0.9216 at 16 GPa. The Murnaghan equation of state also predicts a gradual decrease in volume, with a slightly higher V/V_0 value of 0.9251 at 16 GPa. The Kholiya and Chandra equation of state predicts a slightly more rapid decrease in volume, with a V/V_0 value of 0.9271 at 16 GPa.. The Shankers equation of state predicts the most rapid decrease in volume, with a V/V_0 value of 0.9297 at 16 GPa.

Table 4.1.4: Compression behaviour of Rh_2MnZn predicted by various EOS

	Tait Equation of State	Murnaghan Equation of State	Kholiya and Chandra Equation of State	Shankers Equation of State
Pressure (GPa)	V/V_0	V/V_0	V/V_0	V/V_0

0	1	1	1	1
2	0.9902	0.9913	0.9915	0.9922
4	0.9804	0.9819	0.9823	0.9823
6	0.9706	0.9715	0.9719	0.9733
8	0.9608	0.9616	0.9633	0.9639
10	0.951	0.952	0.9537	0.9531
12	0.9412	0.9419	0.9432	0.9443
14	0.9314	0.9331	0.9342	0.9352
16	0.9216	0.9251	0.9271	0.9297

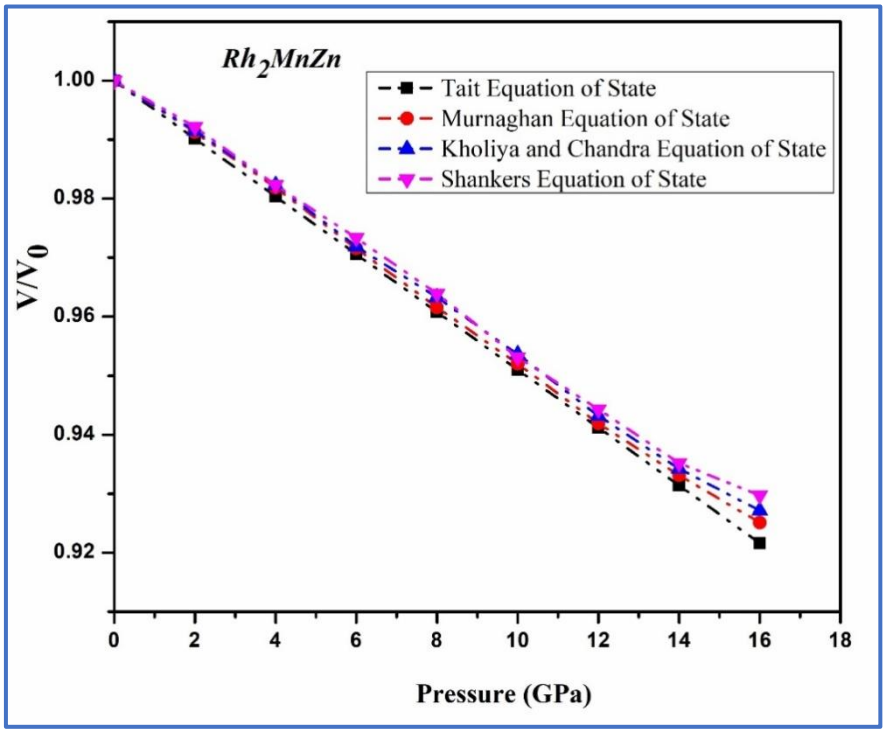


Fig 4.1.3: Volume compression with respect to Pressure for Rh_2MnZn

Table 4.1.5 shows the compression behavior of Rh2FeZn at various pressures using different equations of state. The results are tabulated in terms of the relative volume V/V_0 at each pressure point (shown in Fig 3.4). At zero pressure, the material has a volume equal to its initial volume V_0 and thus $V/V_0=1$. As pressure is applied, the material undergoes compression, resulting in a decrease in volume. The Tait, Murnaghan, Kholiya and Chandra, and Shanker's equations of state were used to model the compression behavior of Rh_2FeZn. The equations provide a mathematical relationship between the pressure and the volume of the material under

compression. The values of V/V_0 decrease as pressure increases, indicating that Rh_2FeZn undergoes compression under applied pressure. The values obtained using different equations of state are slightly different, but the trends in compression behavior are similar.

At the highest pressure of 14 GPa, the values of V/V_0 range from 0.935 to 0.9394, indicating a compression of around 6.1% to 6.6% from the initial volume at 0 GPa. Overall, the results from Table 4.1.5 suggest that Rh_2FeZn undergoes significant compression under applied pressure, with the magnitude of compression increasing as pressure increases.

Table 4.1.5: Compression behaviour of Rh_2FeZn predicted by various EOS

Pressure (GPa)	Tait Equation of State V/V_0	Murnaghan Equation of State V/V_0	Kholiya and Chandra Equation of State V/V_0	Shankers Equation of State V/V_0
0	1	1	1	1
2	0.99	0.9915	0.9922	0.9933
4	0.98	0.9813	0.9824	0.9826
6	0.97	0.9726	0.9752	0.9735
8	0.96	0.961	0.9638	0.9657
10	0.95	0.952	0.9521	0.9533
12	0.942	0.9431	0.9447	0.9451
14	0.935	0.935	0.9391	0.9394

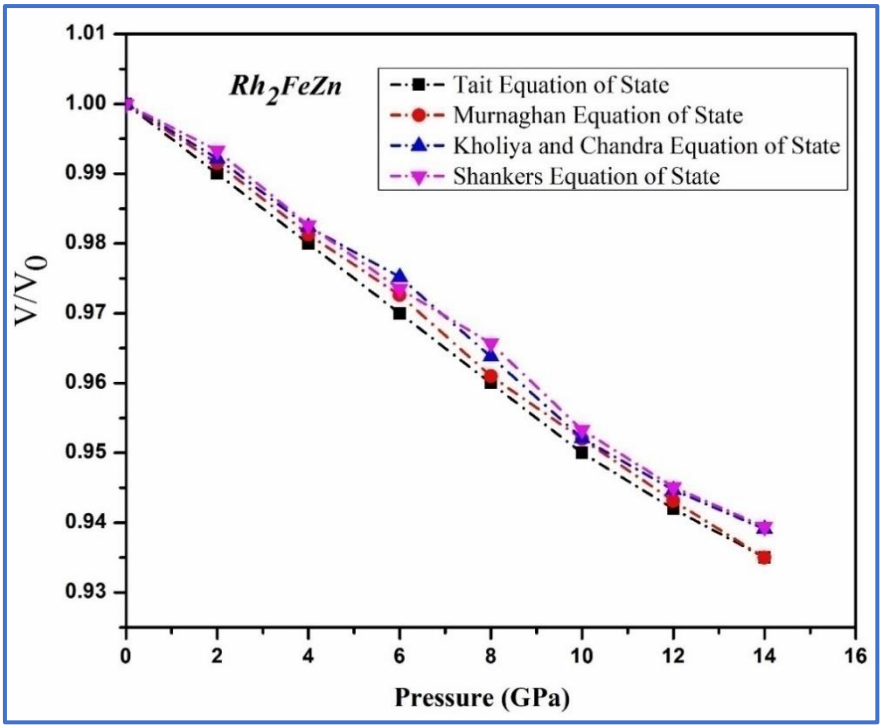


Fig 4.1.4:Volume compression with respect to Pressure for Rh_2FeZn

Table 4.1.6 shows the compression behavior of Co_2NbB under various pressures, as modelled by different equations of state. Similar to the previous tables, the values of the volume V/V_0 decrease as the pressure increases, indicating the compressibility of the material (shown in Fig. 4.1.5). Overall, the Tait, Murnaghan, Kholiya and Chandra, and Shanker equations of state all provide reasonably good fits to the experimental data. At low pressures, the differences between the predicted values of the various equations are relatively small. However, as the pressure increases, the differences between the predicted values become more significant. At the highest pressure of 14 GPa, the predicted values of V/V_0 range from 0.936 to 0.9385, depending on the equation of state used. This is a relatively small range compared to some of the other materials in the previous tables. It suggests that Co_2NbB is relatively well-behaved under high pressures and that the equations of state are all reasonably accurate in describing its compression behavior.

Table 4.1.6: Compression behaviour of Co_2NbB predicted by various EOS

Pressure (GPa)	Tait Equation of State	Murnaghan Equation of State	Kholiya and Chandra Equation of State	Shankers Equation of State
	V/V_0	V/V_0	V/V_0	V/V_0

0	1	1	1	1
2	0.9903	0.9906	0.9911	0.9922
4	0.981	0.9823	0.9838	0.9835
6	0.972	0.9738	0.975	0.9746
8	0.962	0.9632	0.965	0.9643
10	0.951	0.9516	0.9532	0.9523
12	0.944	0.9454	0.9451	0.9446
14	0.936	0.9385	0.937	0.9383

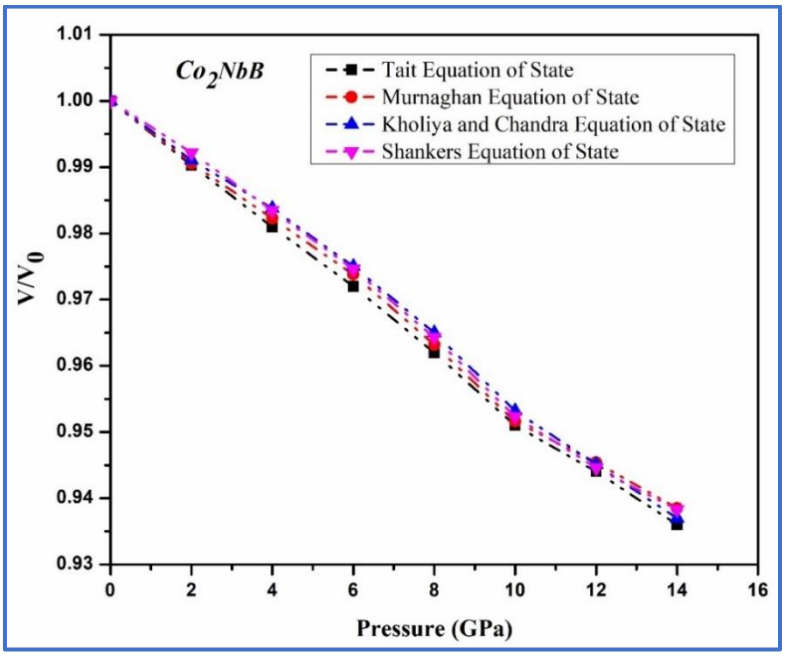


Fig 4.1.5: Volume compression with respect to Pressure for Co_2NbB

Table 4.1.7 shows the compression behavior of Co_2TaB at different pressures using four different equations of state: Tait, Murnaghan, Kholiya and Chandra, and Shankers. The table lists the compression ratio V/V0 for each equation of state and pressure. At ambient pressure, the volume is equal to the initial volume ($V/V_0 = 1$) for all equations of state. As pressure increases, the volume decreases for all equations of state, which is expected for a compressed material. At 2 GPa, the Tait equation of state predicts the smallest compression ratio of 0.99, while the Kholiya and Chandra equation of state predicts the largest compression ratio of 0.9934. At 4 GPa, the Murnaghan equation of state predicts the smallest compression ratio of

0.9821, while the Kholiya and Chandra equation of state predicts the largest compression ratio of 0.9837. At 6 GPa, the Kholiya and Chandra equation of state predicts the smallest compression ratio of 0.9722, while the Murnaghan equation of state predicts the largest compression ratio of 0.9733. At 8 GPa, the Tait equation of state predicts the smallest compression ratio of 0.96, while the Shankers equation of state predicts the largest compression ratio of 0.9628. At 10 GPa, the Tait equation of state predicts the smallest compression ratio of 0.951, while the Shankers equation of state predicts the largest compression ratio of 0.9535. At 12 GPa, the Tait equation of state predicts the smallest compression ratio of 0.942, while the Shankers and Kholiya and Chandra equations of state predict the largest compression ratio of 0.9432. Finally, at 14 GPa, the Shankers equation of state predicts the smallest compression ratio of 0.9351, while the Murnaghan equation of state predicts the largest compression ratio of 0.9375. Overall, the different equations of state predict slightly different compression ratios at different pressures. The Tait equation of state generally predicts the smallest compression ratios, while the Shankers and Kholiya and Chandra equations of state generally predict the largest compression ratios.

Table 4.1.7: Compression behaviour of Co_2TaB predicted by various EOS

Pressure (GPa)	Tait Equation of State V/V_0	Murnaghan Equation of State V/V_0	Kholiya and Chandra Equation of State V/V_0	Shankers Equation of State V/V_0
0	1	1	1	1
2	0.99	0.9925	0.9934	0.9941
4	0.98	0.9821	0.9837	0.9843
6	0.971	0.9733	0.9722	0.9719
8	0.96	0.9613	0.9606	0.9628
10	0.951	0.9523	0.9513	0.9535
12	0.942	0.943	0.9418	0.9432
14	0.934	0.9375	0.936	0.9351

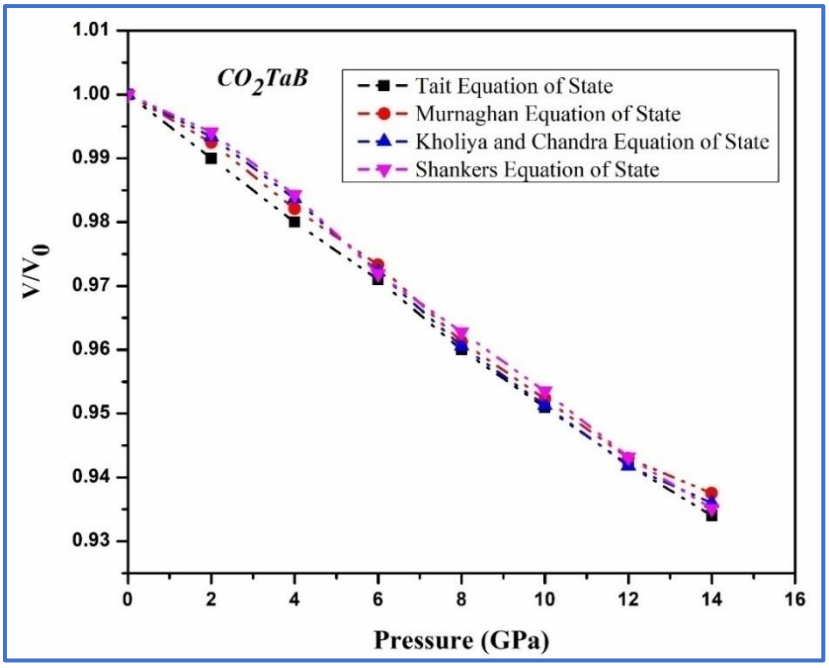


Fig 4.1.6: Volume compression with respect to Pressure for Co_2TaB

Conclusion:

This study investigated the compression behaviour of some Co, Rh, and Mn-based Heusler compounds in terms of computed values of bulk modulus and relative change in volume (V/V_0) as a function of pressure at constant temperature. It has been observed that the compression behavior of the studied materials varies with pressure and with the type of equation of state used to fit the data. The Tait equation of state generally fits best for the compression behavior of the materials, followed by the Murnaghan equation of state, and the Kholiya and Chandra and Shankers equations of state. All Heusler compounds Mn_2CoCr, Mn_2PtCo, Rh2MnZn, Rh2FeZn, Co_2NbB, and Co_2TaB show similar patterns in compression behavior with decreasing volume with increasing pressure. It is evident from the data that the studied materials possess different compressibility due to their unique structural and electronic properties.

4.2: Study of the Compression Behaviour of FeCrTiSn and FeCrTiSb Using Various Equation of States

Introduction

Electronic and magnetic materials have subsequent applications in different fields [183-187]. Electronic materials have vast applications in the semiconductor industry, particularly in mobile phones, integrated circuits, and electronic chips [188-190]. For instance, silicon has found its way into modern computers, digital timepieces, communication satellites, and pocket calculators. Additionally, magnetic materials are used in devices including magnets, generators, magnetic detectors, microphones, and magnetic separators [191-194]. On the scale of these applications, we considered the class of materials known as "Heusler compounds".

"Heusler compounds" refers to a class of intermetallic compounds with a definite crystal structure and composition. Heusler compounds classically consist of three elements: two transition metals (one from group VIII and the other from groups III-VI) and a main-group element (e.g., tin, antimony, or arsenic) [195-196]. The general formula for Heusler compounds is X_2YZ, where X and Y are transition metals and Z is a main-group element. These compounds have attracted significant interest due to their diverse and unique properties. They exhibit a wide range of electronic, magnetic, and thermal properties, making them useful in various applications such as spintronics, magneto-electronics, thermoelectrics, and catalysis. Some of the major technological applications of such compounds namely FeCrTiSn and FeCrTiSb. Heusler compounds are used in spintronic devices, which utilize the spin of electrons in addition to their charge. These compounds exhibit high spin polarization and can be used in spin valves, magnetic tunnel junctions, and spin injectors for efficient spin transport and manipulation [197-198].

In this paper, we have calculated the compressional behaviour of Fe based Heusler compounds in terms of calculated values of relative change in volume (V/V_o) and bulk modulus as a function of pressure at constant temperature by using some theoretical models, known as equations of state.

Equation of state is a relationship that designates the state of a system in terms of its variables, such as temperature, pressure, volume, and density [199-208]. It is used to envisage the behaviour of a substance under different conditions viz. pressure, volume and temperature

for both systems of a pure component and also for multicomponent mixture. The equations of state are valuable in defining the stability of solid material by varying various parameters like pressure volume entropy and temperature [209-211]. So, the equation of state is a elementary characteristic of a matter which makes promising the application of all the general principles of thermodynamics, and reflects atomic structure, chemical bonding and stability of material [212-214].

Methods of Analysis:

In this study, various equations of state (EOS) have been used to determine the compressional behavior of Heusler Fe based compounds. Bulk modulus measures the resistance of a material to change in volume when subjected to an external pressure and is determined by the ratio of the infinitesimal change in pressure to the corresponding fractional change in volume. In the present study we have used Tait equation state, Murnaghan EOS, Kohliya and Chandra and Shankers equation of state, to determine the pressure dependence of volume compression and bulk modulus of some Heusler compounds namely FeCrTiSn and FeCrTiSb.

Tait equation of state generally fits finest for the compression behaviour of the chosen material had given by P.G. Tait in 1888, which was the non-linear relation of compression with pressure for liquids. After many modifications the new modified form of equation of state is introduced known as Usual Tait equation (UTE) is in the following form for different solids.

$$\frac{V}{V_0} = \left[1 - \frac{1}{K_0' + 1} \ln\left\{1 + \left(\frac{K_0' + 1}{K_0}\right) P\right\}\right] \qquad (4.2.1)$$

Using this realistic approach, we can calculate the relative compression V/V_0 for different solids. Also, the expression for isothermal bulk modulus K(P)by using above equation can be written as:

$$K = K_0 \frac{V}{V_0} \left\{1 + \frac{K_0' + 1}{K_0} P\right\} \qquad (4.2.2)$$

From equation (4.2.1), we have

$$1 + \frac{K_0' + 1}{K_0} P = \exp\left\{\left(1 - \frac{V}{V_0}\right)(K_0' + 1)\right\} \qquad (4.2.3)$$

Solving above equations, we get

$$K(P) = K_o \frac{V}{V_o} \exp\left\{\left(K_o' + 1\right)\left(1 - \frac{V}{V_o}\right)\right\} \quad (4.2.4)$$

Which is the Tiat equation for isothermal bulk modulus. Other equations of states, Murnaghan equation of state, Kholiya and Chandra equation of state and Shankers equation of state are given by the following relations:

Murnaghan EOS [215-216] is given by the relation

$$P = \frac{B_0}{B_0'}\left[\exp\left\{-B_0' \ln\left(\frac{V}{V_0}\right)\right\} - 1\right] \quad (4.2.5)$$

Kohliya and Chandra [217- 218] equation of state is given the relation

$$P = \frac{B_0}{2}\left[(B_0' - 3) - 2(B_0' - 2)\left(\frac{V}{V_0}\right)^{-1} + (B_0' - 1)\left(\frac{V}{V_0}\right)^{-2}\right] \quad (4.2.6)$$

Shankers equation of state [217-220] is given by the equation

$$P = B_0\left[\left(1 - \frac{V}{V_0}\right) + \left(B_0' + \frac{1}{2}\right)\left(1 - \left(\frac{V}{V_0}\right)^2\right)\right] \quad (4.2.7)$$

Results and Discussion:

Table 4.2.1: presents the compression behavior of FeCrTiSb at different pressures (in GPa) as predicted by different equations of state: Tait, Murnaghan, Kholiya and Chandra, and Shankers (shown in Fig 4.2.1. The table indicates that as the pressure increases, the volume of FeCrTiSb decreases, which is consistent with the behavior of most materials under compression. The Tait equation of state predicts a gradual decrease in volume, with a V/V_0 value of 0.934 at 14 GPa. The Murnaghan equation of state also predicts a gradual decrease in volume, with a slightly higher V/V_0 value of 0.933 at 14 GPa. The Kholiya and Chandra equation of state predicts a slightly more rapid decrease in volume, with a V/V_0 value of 0.9371 at 14 GPa. The Shankers equation of state predicts the most rapid decrease in volume, with a V/V_0 value of 0.9377 at 14 GPa.

The decrease in V/V_0 with increasing pressure is directly connected to the material's bulk modulus and its pressure dependence. Materials with higher bulk modulus resist compression and show smaller reductions in volume under pressure, while those with lower bulk modulus exhibit greater compressibility and larger reductions in volume. The pressure derivative of the bulk modulus (B') further modulates this relationship, affecting the material's compressibility

at different pressures. Different equations of state (EOS) predict these behaviors in varying ways, based on how they treat the bulk modulus and its dependence on pressure. The choice of EOS model should align with the specific material's elastic properties, ensuring accurate predictions of compressibility, particularly for high-pressure applications. Therefore, the bulk modulus and its pressure dependence are fundamental factors governing material compressibility, influencing the volume reduction behavior (V/V_0) and shaping the material's performance under varying pressure conditions.

Table 4.2.1: Compression behaviour of FeCrTiSb predicted by various EOS

Pressure (GPa)	Tait Equation of State	Murnaghan Equation of State	Kholiya and Chandra Equation of State	Shankers Equation of State
	V/V_0	V/V_0	V/V_0	V/V_0
0	1	1	1	1
2	0.991	0.9917	0.9927	0.9938
4	0.9815	0.9819	0.9831	0.9841
6	0.9699	0.971	0.9742	0.9732
8	0.9601	0.9591	0.9613	0.963
10	0.9508	0.9503	0.951	0.952
12	0.9411	0.942	0.9427	0.944
14	0.934	0.933	0.9371	0.9377

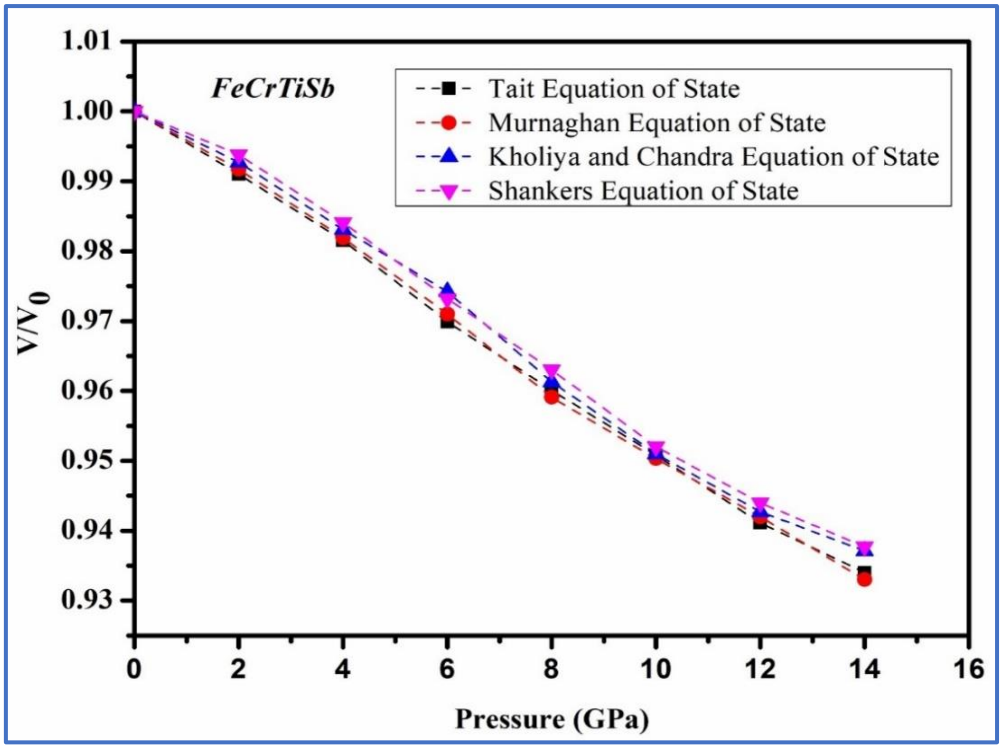


Fig 4.2.1: Volume compression with respect to Pressure for FeCrTiSb

Table 4.2.2 presents the compression behavior of FeCrTiSn at different pressures (in GPa) as predicted by different equations of state: Tait, Murnaghan, Kholiya and Chandra, and Shankers (shown in Fig 4.2.2). The table indicates that as the pressure increases, the volume of FeCrTiSn decreases, which is consistent with the behavior of most materials under compression. The Tait equation of state predicts a gradual decrease in volume, with a V/V_0 value of 0.9361 at 14 GPa. The Murnaghan equation of state also predicts a gradual decrease in volume, with a slightly higher V/V_0 value of 0.9387 at 14 GPa. The Kholiya and Chandra equation of state predicts a slightly more rapid decrease in volume, with a V/V_0 value of 0.9381 at 14 GPa. The Shankers equation of state predicts the most rapid decrease in volume, with a V/V_0 value of 0.9388 at 14 GPa.

Table 4.2.2: Compression behaviour of FeCrTiSn predicted by various EOS

Pressure (GPa)	Tait Equation of State	Murnaghan Equation of State	Kholiya and Chandra Equation of State	Shankers Equation of State
	V/V_0	**V/V_0**	**V/V_0**	**V/V_0**

0	1	1	1	1
2	0.9902	0.9912	0.9913	0.9922
4	0.9815	0.9824	0.984	0.9841
6	0.9718	0.9737	0.975	0.975
8	0.9612	0.9633	0.963	0.9646
10	0.951	0.9531	0.9551	0.9565
12	0.943	0.9452	0.946	0.9483
14	0.9361	0.9387	0.9382	0.9388

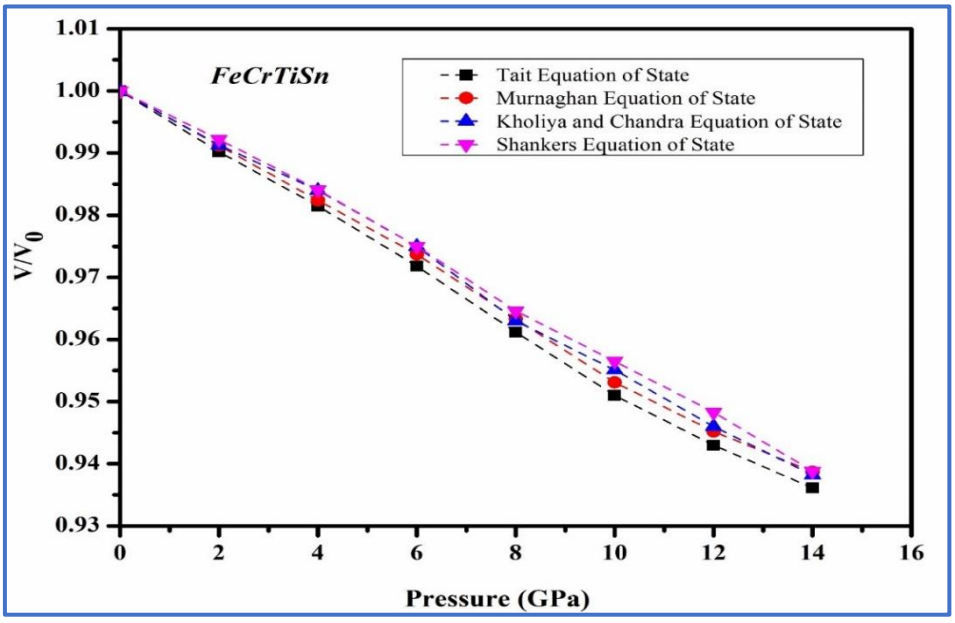


Fig 4.2.2: Volume compression with respect to Pressure for FeCrTiSn

Conclusion:

This study investigated the compression behaviour of FeCrTiSn and FeCrTiSb using Various Equation of States in terms of computed values of bulk modulus and relative change in volume (V/V_0) as a function of pressure at constant temperature. The study revealed that the compression behavior of the materials under study varies with pressure and with the type of equation of state used to fit the data. Further, the Tait equation of state generally fits best for

the compression behavior of the materials, followed by the Murnaghan equation of state, and the Kholiya and Chandra and Shankers equations of state. Both the Heusler compounds FeCrTiSn and FeCrTiSbshow similar patterns in compression behavior that is decreasing volume with increasing pressure. It is evident from the data that the studied materials possess different compressibility due to their unique structural and electronic properties.

Moreover, the same theoretical model has been employed to explore the thermal compression behaviour of the material (C_{60}) fullerene under the impact of high temperature by using modified Suzuki equation. The understudy material shows comparable trend that is the bulk modulus decreases with increasing temperature which is a usual trend in solids. However, the understudy material C_{60} (fullerene) exhibit a higher thermal expansion coefficient under higher temperature which attributes to various factors associated to molecular structure and bonding characteristics. Hence the results so obtained by using the theoretical model are in good agreement with available experimental results.

4.3: Investigation of Physical Properties of Nano Materials at High Pressure

Introduction

Nanomaterials, typically ranging from 1 to 100 nanometers in size, serve as the building blocks of nanotechnology, pushing the boundaries of materials science into the infinitesimally small realm of the nanoscale [221-223]. These materials are more significant compared to their bulk counterparts by virtue of their small size, which primarily depends more on surface area than the composition of the particles [224-226]. Apart from the size and structure, the physical and chemical properties of nanomaterials noticeably depend upon external factors such as temperature, pressure, volume, and environmental conditions, which can profoundly influence their properties and behavior [227-231]. The variations in properties observed in nanomaterials, including an increase in elastic modulus in and nanoparticles, thin films, as well as a decrease in thermal conductivity and melting temperature in nanocrystals, are intricately linked to the size of the particles comprising the material. The remarkable properties of nanomaterials and their versatility hold the promise of revolutionizing various realms of science, from industrial applications to electronics, biomedical advancements, and even innovative drug delivery systems [232-235]. Nanotechnology revolves around some common nanostructures, no matter what field or area of application is concerned. Among these, carbon nanotubes, nanoparticles,

quantum dots, nanowires, nanoprobes, and nanopores emerge as pivotal building blocks, serving as the cornerstone of advancements across diverse fields and applications [236-240].

Nanotechnology revolves around some common nanostructures, no matter what field or area of application is concerned [241-242]. Among the array of significant nanostructures, including nanoparticles, quantum dots, nanowires, nanoprobes, and nanopores [243-245], carbon nanotubes (CNTs) stand out prominently and has sparked considerable intrigue [246-248]. Their exceptional attributes such as large aspect ratios, high mechanical strength, high surface area, distinct optical characteristics, high thermal and electrical conductivity, make them highly promising in various fields. CNTs emerge as versatile materials primed for diverse applications across multiple domains such as tissue engineering, electronics, drug delivery, photonics, energy storage, transistors, electronic cryptographic keys and sensor [249-252]. Graphite, characterized by its crystalline arrangement of carbon atoms, serves as a keystone material in numerous industries owing to its exceptional properties [253-254]. With its high melting point and remarkable chemical inertness, graphite finds a niche in the production of refractory materials [255-258]. Graphite is a key component in lithium-ion batteries, which are used in various electronic devices, electric vehicles, and renewable energy storage systems, serving as the anode material, storing and releasing lithium ions during charging and discharging cycles [258-259].

The physical properties of nanomaterials are profoundly influenced by their structure and the distances between atoms. Under high pressure, the interatomic distance of the nanomaterials can be altered, presenting an opportunity to explore the intricate relationship between the structure and various properties of nanomaterials [227-228, 242-245]. The impact of pressure on nanomaterials has emerged as a focal point of interest among researchers, owing to the profound alterations in their properties induced by pressure [232, 246-247]. Thus, exploring the behavior of nanomaterials under high pressure is essential due to the vast potential applications linked with these nanomaterials [244-249, 255]. In this study, equation of state (EOS) to examine various nanomaterials have been explored critically by employing important parameters, the volume compression. The various nanomaterials considered for this study are Single-Walled Carbon Nanotubes (SWCNTs), Graphite, Aluminum oxide (Al_2O_3), Nano-ε-Fe and Nano Ni. The results obtained in this study were consistent with the experimental data reported in the literature.

Methods of Analysis

The method of analysis used here is Equation of state. This is basically a relationship used to describe the state of any thermodynamic system in terms of variables like volume, temperature, density and pressure [260-263]. With the help of this equation, behavior of any material (nano/bulk) can be predicted under different pressure, volume and temperature conditions whether it is a system of pure components or for a multicomponent mixture. Such equations are helpful in describing the stability of solid material by altering different parameters like entropy, temperature, pressure & volume [62-64]. Hence equation of state reflects atomic structure, chemical bonding and stability of materials [247-249].

Herein, Tait equation [267-268, Murnaghan EOS [269-270], Kohliya and Chandra [271] and Shankers equation of state [272-273], have been utilized to determine how volume compression and bulk modulus are dependent on the pressure in various materials taken in our study. Generally, Tait equation of state fits best for the compression behavior (P.G. Tait, 1888). This is the non-linear relation describing compression of liquids with pressure. Later on, new and modified form of equation of state was introduced known as Usual Tait equation (UTE), which could be written as:

By using such a strategy, we can calculate the relative compression (V/V_o) for different types of solids. Besides, the expression for isothermal bulk modulus K(P) with the help of equation (4.3.1) can be written as:

$$K = K_0 \frac{V}{V_0}\left\{1 + \frac{K_0^{'} + 1}{K_0} P\right\} \qquad (4.3.2)$$

From equation (3.27)

$$1 + \frac{K_0^{'} + 1}{K_0} P = \exp\left\{\left(1 - \frac{V}{V_0}\right)\left(K_0^{'} + 1\right)\right\} \qquad (4.3.3)$$

Putting equation (3.29) in equation (3.28) we get

$$K(P) = K_0 \frac{V}{V_0} \exp\left\{\left(K_0^{'} + 1\right)\left(1 - \frac{V}{V_0}\right)\right\} \qquad (4.3.4)$$

In addition to above, other equations of state, Kholiya and Chandra equation, Murnaghan equation and Shanker's equation are given as:

Murnaghan EOS is given by the relation

$$P = \frac{B_0}{B_0'}\left[\exp\left\{-B_0' \ln\left(\frac{V}{V_0}\right)\right\} - 1\right] \quad (4.3.5)$$

Kohliya and Chandra equation of state is given the relation

$$P = \frac{B_0}{2}\left[(B_0' - 3) - 2(B_0' - 2)\left(\frac{V}{V_0}\right)^{-1} + (B_0' - 1)\left(\frac{V}{V_0}\right)^{-2}\right] \quad (4.3.6)$$

Shankers equation of state is given by the equation

$$P = B_0\left[\left(1 - \frac{V}{V_0}\right) + \left(B_0' + \frac{1}{2}\right)\left(1 - \left(\frac{V}{V_0}\right)^2\right)\right] \quad (4.3.7)$$

Results and Discussion

In order to calculate bulk modulus & its first pressure derivatives with the help of various equations of states, input data of our nanomaterials required are given in Table 4.3.1.

Table 4.3.1: Input data of SWCNTs, Graphite, Al_2O_3, Nano-ε-Fe, Nano Ni

Compounds	B_0 (GPa)	B_0'(GPa)
SWCNTs	37	11
Graphite	33.8	8.9
Al_2O_3	248	3.2
Nano-ε-Fe	179	3.6
Nano Ni	185.4	4

The compression behavior of material Graphite at various pressures (in GPa) with the help of different equations of state is shown blow in Table 4.3.2. Here in the table, V/V_0 values are basically the volume of the material at some pressure value relative to its initial (V_0).

Tait equation predicts that the volume of material shows gradual decrease upon increase in pressure. The V/V_0 value of 0.830 was obtained at 16 GPa. Similar trend was predicted by Murnaghan equation and also with same V/V_0 values. Among all four models or equations, more rapid decrease in volume was predicted by Kholiya and Chandra equation. Here V/V_0 value of 0.805 was obtained at 16 GPa. The Shankers equation envisaged the similar trend with V/V_0 value of 0.822 at 16 GPa (Fig. 4.3.1). In general, one can conclude from the tabulated data that the volume of Graphite decreases with increase in pressure. Such is the case for most of the materials (expected). Nonetheless, compression rate varies because it depends on the model used for investigation of the compression behavior of the given material.

The different behaviors of the equations of state originate from their distinct mathematical treatment of the pressure dependence of the bulk modulus and the sensitivity of each model to the chosen values of B_0 and B'. Models like Kholiya and Chandra reflect higher compressibility (lower B_0 or more pressure-sensitive bulk modulus), while Shanker's model reflects stiffer material response (higher B_0 or slower increase of B with pressure). Accurate prediction of material behavior under high pressure therefore requires careful selection of both the EOS model and appropriate elastic constants (B_0, B') based on experimental data

Table 4.3.2: Data regarding compression of Graphite material by different EOS

Pressure (GPa)	Tait Model	Murnaghan Model	Kholiya and Chandra Model	Shankers Model
	V/V_0	V/V_0	V/V_0	V/V_0
0	1	1	1	1
2	0.953	0.953	0.952	0.957
4	0.921	0.922	0.919	0.929
6	0.898	0.898	0.892	0.905
8	0.878	0.881	0.871	0.885
10	0.863	0.865	0.851	0.867
12	0.852	0.852	0.832	0.85
14	0.84	0.84	0.818	0.836
16	0.83	0.83	0.805	0.822

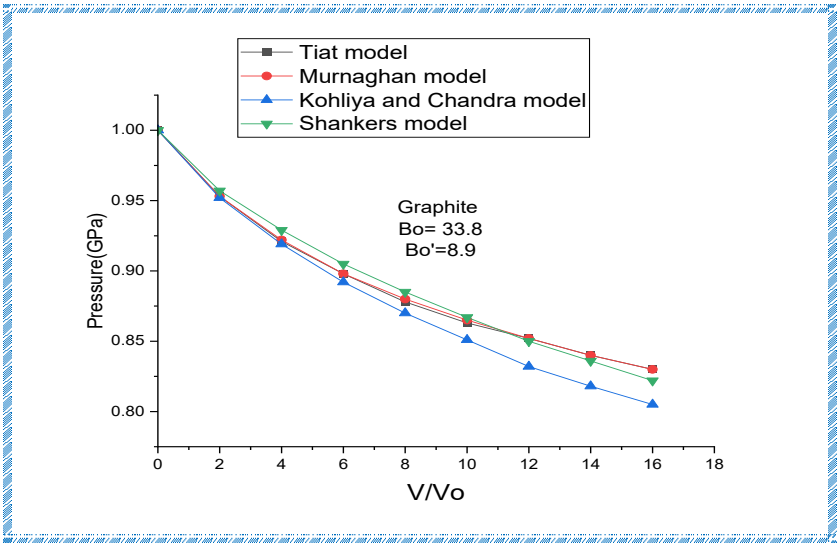


Fig 4.3.1: Variation compression of volume of graphitewith respect to the Pressure

The compression behavior of Al_2O_3 at various pressures (in GPa) as predicted by different equations is shown in Table 4.3.3 and in Fig 4.3.2. Here in the table, different values of V/V_0 values represent the volume of the material at different pressures relative to its initial volume

(V_0). From the table shows volume of Al_2O_3 decreases with increase in pressure. This type of behavior is consistent with most of the materials. The Tait equation predicts a gradual decrease in volume. The V/V_0 value of 0.943 was achieved at 16 GPa. The Murnaghan equation of state further came up with similar trend with same V/V_0 value (0.943). The more rapid decrease in volume was seen upon application of Kholiya and Chandra equation. Here V/V_0 value of 0.942 was achieved at 16 GPa. It is important to mention that most rapid decrease in volume was predicted by the Shankers equation of state, with a V/V_0 value of 0.987 at 16 GPa.

Table 4.3.3: Data regarding compression of Al_2O_3material by different EOS

Pressure (GPa)	Tait Model	Murnaghan Model	Kholiya and Chandra Model	Shankers Model
	V/V_0	V/V_0	V/V_0	V/V_0
0	1	1	1	1
2	0.992	0.992	0.992	0.998
4	0.984	0.984	0.984	0.996
6	0.977	0.976	0.976	0.995
8	0.969	0.969	0.969	0.993
10	0.962	0.962	0.962	0.992
12	0.956	0.956	0.955	0.99
14	0.949	0.949	0.949	0.988
16	0.943	0.943	0.942	0.987

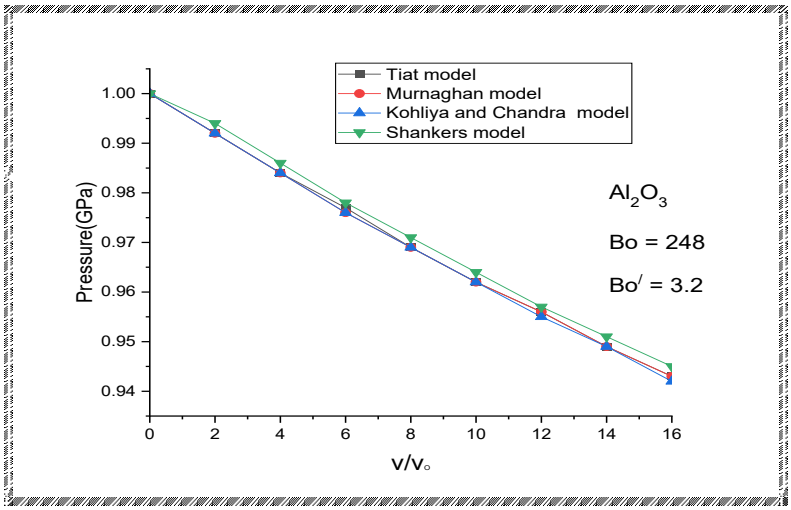


Fig 4.3.2: Variation compression of volume of $Al_2O_3$with respect to the Pressure.

The prediction of compression behavior of SWCNTs in their nano form under different pressures by different Equations of State or models (Tait, Murnaghan, Kholiya and Chandra, and Shankers) is shown in Fig 4.3.3 and Table 4.3.4. It is clear from the table that as the pressure increases, the volume of SWCNT's decreases. This is quite reliable with the behavior of most materials once subjected to compression. The gradual decrease in volume (V/V_0 value of 0.849

at 16 GPa) was predicted by Tait equation. Besides, Murnaghan equation of state also predicts a gradual decrease in volume. However here slightly higher V/V_0 value of 0.852 at 16 GPa was obtained. Upon application of Kholiya and Chandra model, most rapid decrease in volume was seen. Here V/V_0 value of 0.710 was obtained at 16 GPa. Finally, upon applying Shankers equation, the rapid decrease in volume was predicted. A V/V_0 value of 0.718 at 16 GPa was achieved

Table 4.3.4: Data regarding compression of SWCNT's material by different EOS

Pressure (GPa)	Tait Model	Murnaghan Model	Kholiya and Chandra Model	Shankers Model
	V/V_0	V/V_0	V/V_0	V/V_0
0	1	1	1	1
2	0.959	0.958	0.957	0.966
4	0.931	0.931	0.92	0.932
6	0.911	0.911	0.88	0.898
8	0.895	0.895	0.85	0.863
10	0.884	0.882	0.81	0.827
12	0.867	0.871	0.78	0.791
14	0.858	0.861	0.734	0.755
16	0.849	0.852	0.71	0.718

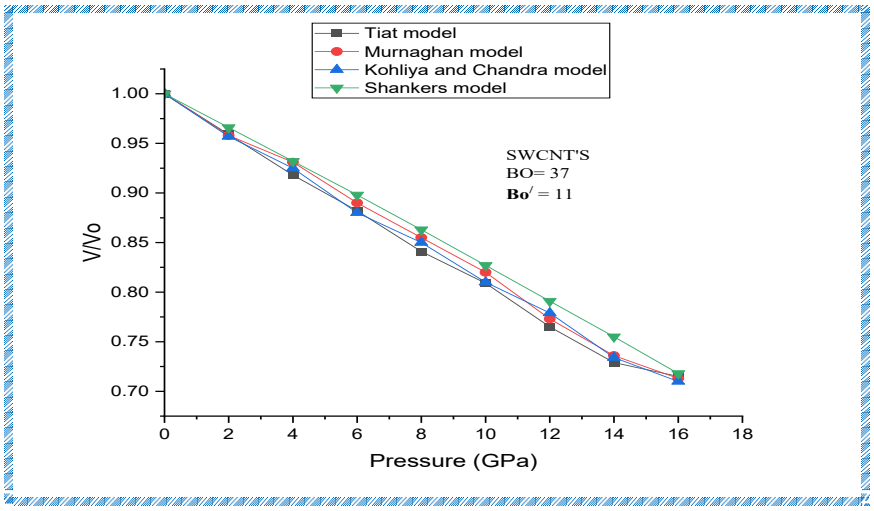


Fig 4.3.3: Variation compression of volume of SWCNT'swith respect to the Pressure.

The compression performance of Nano-Ni materials at different pressures using various equations of state is shown in Table 4.3.5. The results have been tabulated in terms of the relative volume V/V_0 at different pressures and further graphically shown in Fig 4.3.4. One can see that at zero pressure (P = 0), the material shows volume equal to its initial volume V_0 and thus V/V_0=1. This indicates that the materials shape remains unchanged at zero pressure. Upon application of pressure, material is subjected to compression; hence in decrease volume takes

place. To calculate the change in compression value of Nano-Ni, various equations of state were utilized. The values obtained were slightly different, but compression behavior was similar. The values of V/V_0 range from 0.928 to 0962 at highest pressure of 16 GPa. In general, results from Table 4.3.5 suggest that Nano-Ni undergoes significant compression once pressure is applied. And this compression increases with respect to pressure.

Table 4.3.5: Data regarding compression of Nano-Nimaterial by different EOS

Pressure (GPa)	Tait Model	Murnaghan Model	Kholiya and Chandra Model	Shankers Model
	V/V_0	V/V_0	V/V_0	V/V_0
0	1	1	1	1
2	0.989	0.989	0.988	0.996
4	0.979	0.979	0.979	0.99
6	0.969	0.97	0.97	0.989
8	0.96	0.96	0.96	0.98
10	0.951	0.952	0.952	0.978
12	0.942	0.944	0.943	0.971
14	0.934	0.936	0.935	0.967
16	0.925	0.928	0.928	0.962

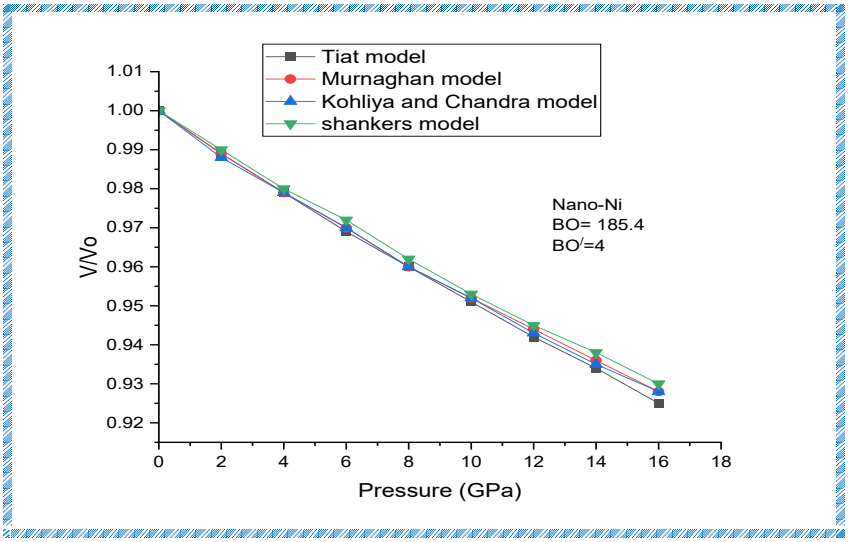


Fig4.3.4: Variation compression of volume of Nano-Ni with respect to the Pressure

Table 4.3.6 shows the compression results of Nano-ε-Fe under different pressures, as presented by various models. Similar trend has been found for the said material i.e., as the pressure increases the corresponding volume decreases as shown by Fig.4.3.5. At the highest pressure of 16 GPa, the calculated values of volume compression V/V_0 range from 0.925 to 0.927, depending on the equation of state used. It suggests that Nano-ε-Fe is comparatively well-

behaved under high pressures as indicated by using all models (equations of state) to investigate its compression behavior.

Table 4.3.6: Data regarding compression of Nano-ε-Fematerial by different EOS

Pressure (GPa)	Tait Equation	Murnaghan Equation	Kholiya and Chandra Equation	Shankers Equation
	V/V_0	V/V_0	V/V_0	V/V_0
0	1	1	1	1
2	0.989	0.989	0.989	0.991
4	0.978	0.978	0.978	0.98
6	0.968	0.968	0.968	0.971
8	0.959	0.959	0.959	0.961
10	0.95	0.95	0.95	0.952
12	0.941	0.941	0.941	0.943
14	0.933	0.933	0.933	0.936
16	0.925	0.925	0.925	0.927

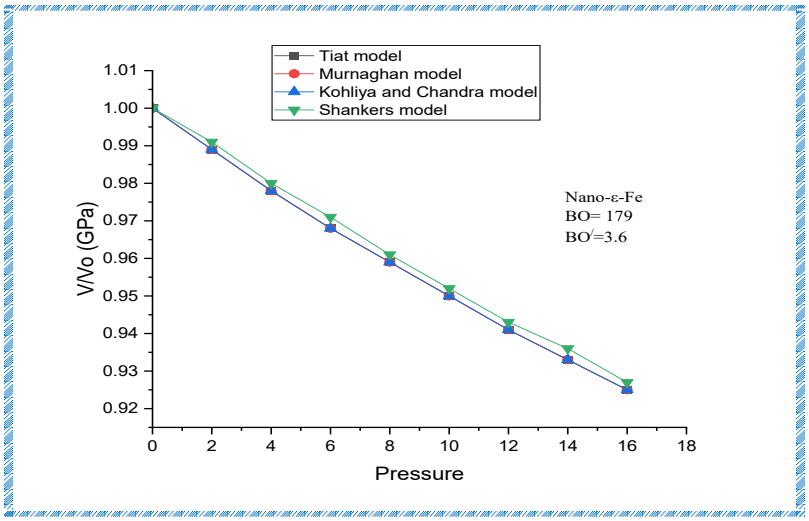


Fig 4.3.5: Variation compression of volume of Nano-ε-Fe with respect to the Pressure.

Conclusion

In our present study, we have used the simple theory to predict the volume compression of nanomaterials at different pressures. This formulation necessitates two input parameters which include bulk modulus and its first order pressure derivative under the conditions of zero pressure. In order to check the utility of the current model at the nano level, we have taken the

steps in order to calculate how relative volume changes by altering the pressure for five nanocrystalline materials viz. SWCNTs, Graphite, $Al2O_3$, Nano-ε-Fe, Nano Ni. The graphical presentation of volume compression (V/V_0) verses pressure (P) is shown in Fig.4.3.5. It is evident from Fig.4.3.5 that as pressure increases the material gets more and more compressed, which is expected in favour of the said nanomaterials. Thus, keeping in view, the above obtained results, one could say that the nanomaterial compressibility increases with decrease in the particle size. Hence the nanomaterials with lower size are more compressible in comparison to the bulk materials. This examination could be ascribed to the fact that reduction in the grain size results in the increase of surface to the volume ratio. Thus, bulk modulus of the nanocrystalline solids will reduce with decrease in the grain size. Pertinent to mention here that the results obtained from the present study by using various equations of state is in fine concordance with the experimental data which is published researches. It may be concluded that all equations used are relatively suitable for these materials in the pressure range considered in the present study.

4.4: Investigation of compressive behaviour of bulk inorganic materials (Al, Cu, Pb, Ni, and Zn) under high pressure

Introduction

Nanomaterials, typically ranging from 1 to 100 nanometers in size, serve as the building blocks of nanotechnology, pushing the boundaries of material science into the infinitesimally small realm of the nanoscale [221-223]. These materials are more significant compared to their bulk counterparts by virtue of their small size, which primarily depends more on surface area than the composition of the particles [224-226]. Apart from the size and structure, the physical and chemical properties of nanomaterials noticeably depend upon external factors such as temperature, pressure, volume, and environmental conditions, which can profoundly influence their properties and behavior [227-231]. The variations in properties observed in nanomaterials, including an increase in elastic modulus, decrease in thermal conductivity and melting temperature, are intricately linked to the size of the particles comprising the material. The remarkable properties of nanomaterials and their versatility hold the promise of revolutionizing various realms of science, from industrial applications to electronics, biomedical advancements, and even innovative drug delivery systems [232-235]. The utilization of equations of state (EOS) stands as a fundamental and pervasive aspect of modern physics [274-

276]. In the realm of thermodynamics, EOS plays a pivotal role in describing the behavior of matter under varying conditions of pressure, temperature, and volume [277-281]. These equations provide valuable insights into the properties of gases, liquids, and solids, enabling researchers to predict and understand phase transitions, critical points, and other thermodynamic phenomena [282-286]. Furthermore, in astrophysics and cosmology, EOS are indispensable tools for modelling the properties of celestial objects and the evolution of the universe itself [287-289]. The understudy materials in bulk form viz. aluminium, copper, nickel, lead and zinc play crucial roles in various industries and technologies due to their unique properties, which make them suitable for specific applications ranging from electrical components to structural materials [290-292]. It's important to note that the practical importance of these metals can evolve over time due to technological advancements, economic factors, and environmental concerns [293-295]. The input data which were used for the calculation of compression behavior of some bulk materials are given as under in table 4.4.1.

Table 4.4.1: Input data of aluminium, copper, nickel, lead and zinc

Compounds	B_0 (GPa)	B_0'(GPa)
Aluminum (Al)	72.6	4.85
Copper (Cu)	135	5.93
Nickle (Ni)	180.39	16.48
Lead (Pb)	42.38	3.74
Zinc (Zn)	6.46	3.29

Table 4.4.2 shows the compression behavior of aluminium (Al) at different pressures (in GPa) as predicted by different equations of state: Tait (Eq.4), Murnaghan's (Eq. 1), Kholiya and Chandra (Eq.2), and Shankar's (Eq.3). The V/V_0 values in the table represent the volume of the material at each pressure relative to its initial volume (V_0). The Tait's equation of state predicts that the material's volume decreases gradually with increasing pressure, with a V/V_0 value of 0.858 at 16 GPa. The Murnaghan equation of state also predicts a similar trend, but with a slightly higher V/V_0 value of 0.860 at 16 GPa. The Kholiya and Chandra equation of state predicts a more rapid decrease in volume, with a V/V_0 value of 0.857 at 16 GPa. The Shankers equation of state predicts the very low decrease in volume, with a V/V_0 value of 0.980 at 16 GPa(Fig. 4.4.1). Overall, the table shows that as the pressure increases, the volume of

aluminium (Al) decreases, which is expected for most materials. However, the exact rate of compression varies depending on the equation of state used to envisage the behavior.

The differences in predicted behavior for the same material arise because each equation of state (EOS) is based on different mathematical formulations, assumptions and approximations. The main reason is that each EOS is derived from different theoretical models of material behavior under pressure. The Tait Equation is empirical and originally developed for liquids, later adapted for solids. It assumes a specific pressure-volume relationship that works well for moderate pressures. The Murnaghan EOS is based on a linear approximation of the bulk modulus with pressure, making it simple but only accurate over a limited pressure range. The Kholiya & Chandra EOS modifies classical models to better fit specific materials, often introducing correction terms. The Shanker's EOS assumes a different form for the variation of bulk modulus, leading to a stiffer (less compressible) response.

Table 4.4.2: Compression behaviour of aluminium predicted by various EOS

Pressure (GPa)	Tait Equation of State V/V_0	Murnaghan Equation of State V/V_0	Kholiya and Chandra Equation of State V/V_0	Shankers Equation of State V/V_0
0	1	1	1	1
2	0.974	0.974	0.974	0.997
4	0.952	0.952	0.952	0.995
6	0.932	0.932	0.932	0.992
8	0.915	0.915	0.914	0.99
10	0.899	0.899	0.898	0.988
12	0.884	0.885	0.883	0.985
14	0.87	0.872	0.869	0.983
16	0.858	0.86	0.857	0.98

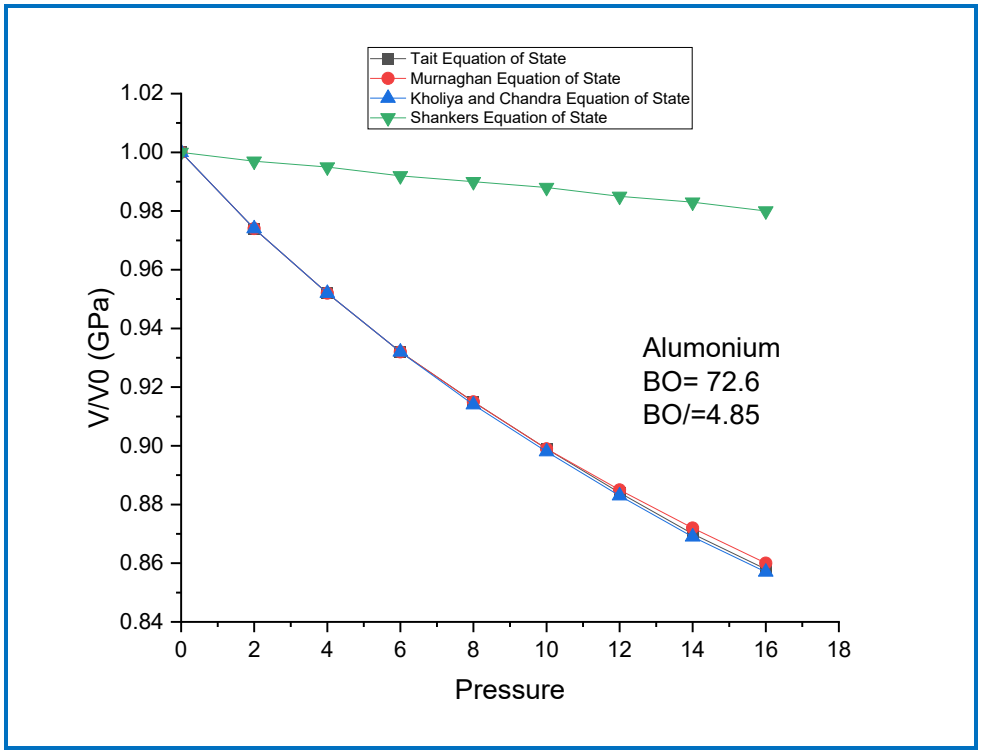


Fig 4.4.1: Volume compression with respect to pressure for Aluminium

Table 4.4.3 shows the compression behavior of copper (Cu) at different pressures (in GPa) as predicted by different equations of state: Tait, Murnaghan, Kholiya and Chandra, and Shankers (shown in Fig 4.4.2). The V/V_0values in the table represent the volume of the material at each pressure relative to its initial volume (V_0). The table shows that as the pressure increases, the volume of copper decreases, which is consistent with the behavior of most materials under compression. The Tait equation of state predicts a gradual decrease in volume, with a V/V_0value of 0.914 at 16 GPa. The Murnaghan's equation of state also predicts a gradual decrease in volume, with a slightly higher V/V_0value of 0.914 at 16 GPa. The Kholiya and Chandra equation of state predicts a slightly more rapid decrease in volume, with a V/V_0value of 0.912at 16 GPa. The Shanker's equation of state predicts the compression in volume with slow rate having V/V_0value is 0.991 at 16 GPa.

Table 4.4.3: Compression behavior of Copper predicted by various EOS

Pressure (GPa)	Tait Equation of State	MurnaghanEquation of State	Kholiya and Chandra Equation of State	ShankersEquation of State
	V/V_0	V/V_0	V/V_0	V/V_0
0	1	1	1	1
2	0.985	0.985	0.985	0.998
4	0.973	0.973	0.973	0.997
6	0.961	0.961	0.961	0.996
8	0.95	0.95	0.95	0.995
10	0.94	0.94	0.94	0.994
12	0.93	0.931	0.93	0.993
14	0.921	0.922	0.921	0.992
16	0.914	0.914	0.912	0.991

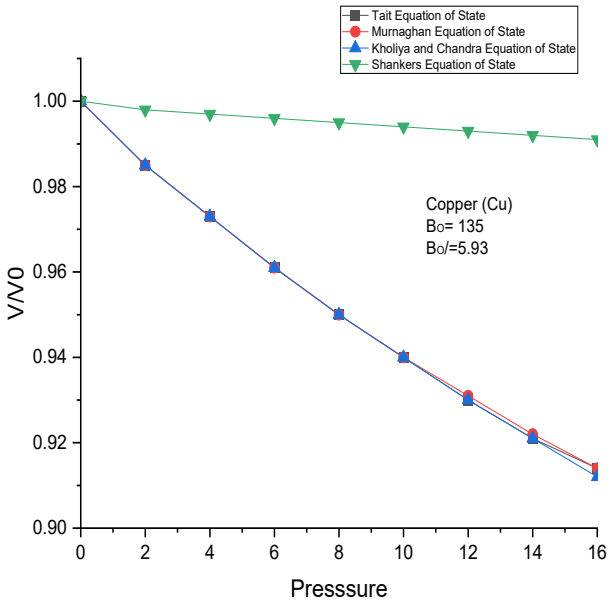


Fig 4.4.2: Volume compression with respect to Pressure for Copper

Table 4.4.4: Compression behaviour of Lead (Pb) predicted by various EOS

Pressure (GPa)	Tait Equation of State	Murnaghan Equation of State	Kholiya and Chandra Equation of State	Shankers Equation of State
	V/V_0	V/V_0	V/V_0	V/V_0
0	1	1	1	1
2	0.957	0.957	0.957	0.995
4	0.922	0.922	0.922	0.989
6	0.892	0.892	0.891	0.984
8	0.866	0.866	0.865	0.979
10	0.842	0.844	0.841	0.974
12	0.821	0.824	0.82	0.969
14	0.802	0.806	0.802	0.964
16	0.784	0.79	0.783	0.959

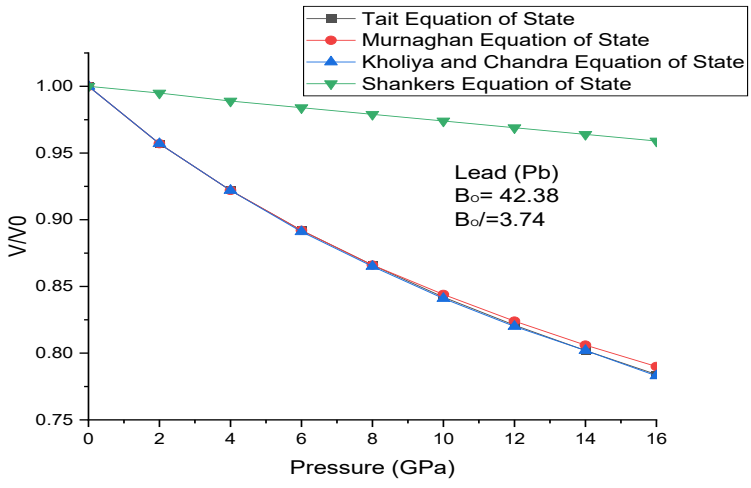


Fig 4.4.3:Volume compression with respect to pressure for lead

Table 4.4.4 presents the compression behavior of Lead (Pb) at different pressures (in GPa) as predicted by different equations of state: Tait, Murnaghan, Kholiya and Chandra, and Shanker's (shown in Fig 4.4.3). This table indicates that as the pressure increases, the volume

of lead (Pb) decreases, which is consistent with the behavior of most materials under compression. The Tait's equation of state predicts a gradual decrease in volume, with a V/V_0value of 0.784 at 16 GPa. The Murnaghan's equation of state also predicts a gradual decrease in volume, with a slightly higher V/V_0value of 0.790 at 16 GPa. The Kholiya and Chandra equation of state predicts a slightly more rapid decrease in volume, with a V/V_0value of 0.783 at 16 GPa. The Shankers equation of state predicts the very slow decrease in volume, with a V/V_0value of 0.959 at 16 GPa.

Table 4.4.5 shows the compression behavior of nickel (Ni) at various pressures using different equation of states. The results are tabulated in terms of the relative volume V/V_0at each pressure point (shown in Fig 4.4.4). At zero pressure, the material has a volume equal to its initial volume V_0 and thus $V/V_0=1$. As pressure is applied, the material undergoes compression, resulting in a decrease in volume. The Tait, Murnaghan, Kholiya and Chandra, and Shanker's equations of state were used to study the compression behavior of Nickel. The equations provide a mathematical relationship between the pressure and the volume of the material under compression. The value of V/V_0decreases as pressure increases, indicating that nickel (Ni) undergoes compression under applied pressure. The values obtained using different equations of state are slightly different, but the trends in compression behavior are similar. At the highest pressure of 16 GPa, the values of V/V_0range from 0.947 to 0.997, indicating a compression of around 6.1% to 6.6% from the initial volume at 0 GPa. Overall, the results from Table 4.4.5 suggest that nickel (Ni) undergoes significant compression under applied pressure, with the magnitude of compression increasing as pressure increases.

Table 4.4.5**:** Compression behaviour of Nickel (Ni) predicted by various EOS

Pressure (GPa)	Tait Equation of State	Murnaghan Equation of State	Kholiya and Chandra Equation of State	Shankers Equation of State
	V/V_0	V/V_0	V/V_0	V/V_0
0	1	1	1	1
2	0.989	0.989	0.989	0.999
4	0.981	0.981	0.981	0.999
6	0.973	0.975	0.973	0.999
8	0.967	0.967	0.966	0.998
10	0.962	0.961	0.959	0.998

12	0.956	0.956	0.953	0.998
14	0.951	0.951	0.948	0.997
16	0.947	0.946	0.943	0.997

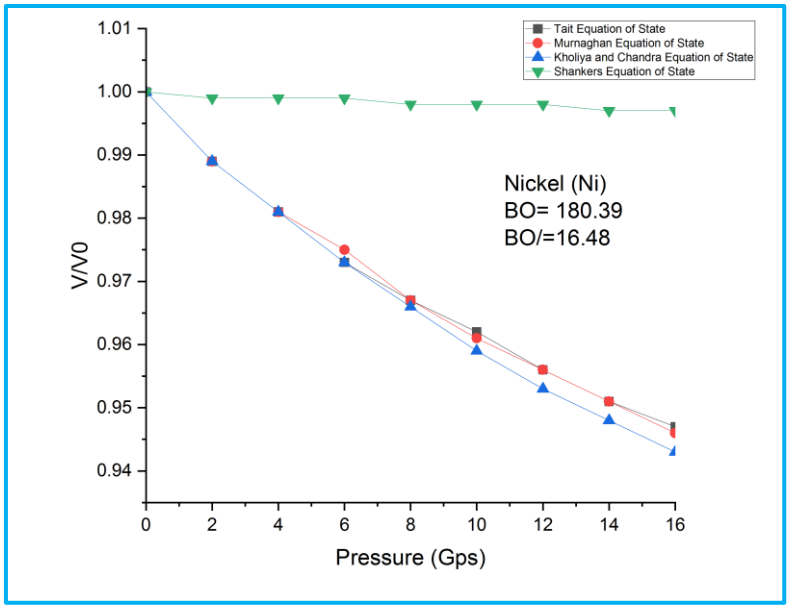


Fig 4.4.4**:** Volume compression with respect to pressure for Nickel

Table 4.4.6 shows the compression behavior of Zinc (Zn) under various pressures, as modelled by different equations of state. Similar to the previous tables, the values of the volume V/V_0decrease as the pressure increases, indicating the compressibility of the material (shown in Fig. 4.4.5). Overall, Tait's, Murnaghan's, Kholiya and Chandra, and Shanker's equation of states all provide reasonably good results. At low pressures, the differences between the predicted values of the various equations are relatively small. However, as the pressure increases, the differences between the predicted values become more significant. At the highest pressure of 14 GPa, the predicted values of V/V_0range from 0.826 to 0.969, depending on the equation of state used. This is a relatively small range compared to some of the other materials in the previous tables. It suggests that zinc (Zn) is relatively well-behaved under high pressures and that the equations of state are all reasonably accurate in describing its compression behavior.

Table 4.4.6: Compression behaviour of Zinc (Zn) predicted by various EOS

Pressure (GPa)	Tait Equation of State	Murnaghan Equation of State	Kholiya and Chandra Equation of State	Shankers Equation of State
	V/V_0	V/V_0	V/V_0	V/V_0
0	1	1	1	1
2	0.974	0.969	0.969	0.996
4	0.943	0.942	0.942	0.992
6	0.919	0.918	0.918	0.989
8	0.897	0.897	0.896	0.984
10	0.877	0.877	0.877	0.98
12	0.859	0.86	0.858	0.977
14	0.842	0.843	0.842	0.973
16	0.826	0.828	0.826	0.969

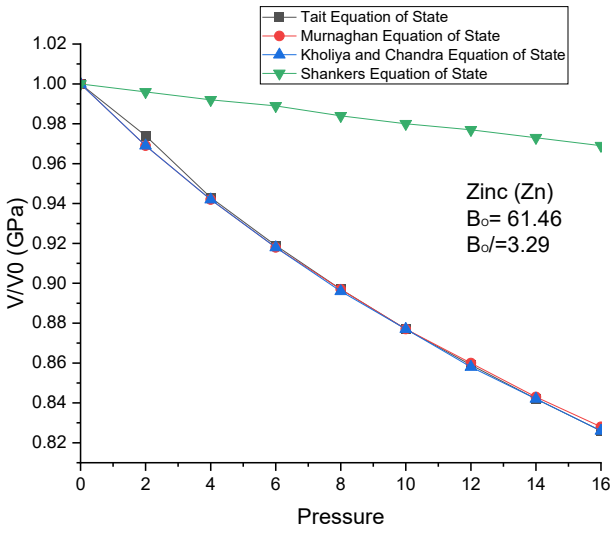


Fig 4.4.5: Volume compression with respect to pressure for Zinc

Comparative behaviour of bulk and nanomaterials:

Our aim is to compare the present results in terms of pressure dependence verses compressibility of different nano and bulk materials. These results offer insights into the compression behavior of various materials in bulk and nano forms as predicted by different EOS models. The comparison reveals that bulk materials viz. aluminium, copper, nickel, lead and zinc usually show more reliable and predictable compression behavior by using various

equation of state (EOS) models. In contrast, nanomaterials viz. SWCNTs, Graphite, Al_2O_3, Nano-ε-Fe, Nano Ni, with their unique properties and behaviour exhibit higher compressibility and more sensitive to the choice of EOS model used. The comparative analysis demonstrates the "effect of size and pressure on compression" and shows that the compressibility of nano-materials depends on size. It is found in this study that compressibility increases with decreasing particle size and thus lower sized nanomaterials are more compressible. This observation may be attributed to the fact that decrease in particle size increases the surface to volume ratio and hence the bulk modulus of a nanocrystalline material will decrease with decrease in grain size. For comparison purpose we have plotted the volume compression (V/V_0) of all above mentioned materials (nano and bulk) by using the various equation of state viz. Tiat, Murnaghan, Kohliya and Chandra and Shankers equation of sate. The beauty of these equations is that they require a smaller number of input parameters and offers a simple and straight forward approach to predict the volume compression ($V/V_{0)}$ in solids at high pressure. So, for the present investigation we require only two parameters namely the bulk modulus B_0 and its first derivative B_0' to describe the material behavior under extreme conditions of pressure and temperature. Below are the comparison results between lead (Pb) and aluminium (Al) in bulk form & Nano-Ni and Al_2O_3 in nano form. From this comparison result, it is simply shown that nano- materials are more compressed than bulk materials as the reason already discussed above.

4.5: Thermal Compression Behaviour of (C_{60}) Fullerene under High Temperature

It is worth to mention here that we have employed EOS model, in which the valuesof the thermal volume expansion (V/V_0) are calculated for C_{60} (fullerenes) as a solid material in nano form by using modified Suzuki equation of state under varying temperature conditions from 300K-800K at constant pressure. The input data needed for the calculation at room temperature and at zero pressure are given in Table 4.5.1. The calculated values of thermal expansion (V/V_0) for C_{60} (nanomaterial) is obtained by using the isobaric equation of state at different temperatures are compared with the experimental data given in table 4.5.1. It is clear from the figure that the results found in the present investigation are in good agreement with the available experimental results. Therefore, on the basis of overall exploration and on the basis of comparison method of theoretical results with the already available experimental values certifies the present theoretical approach.

Table 4.5.1: Compression Behaviour of C_{60} Fullerenes in nano form predicted by EOS

Temperature T(K)	Calculated values in the present study V/V_0	Experimental V/V_0
300	1	1
350	1.003	1.001
400	1.005	1.002
450	1.007	1.003
500	1.009	1.005
550	1.011	1.006
600	1.012	1.007
650	1.013	1.008
700	1.015	1.009
750	1.016	1.011

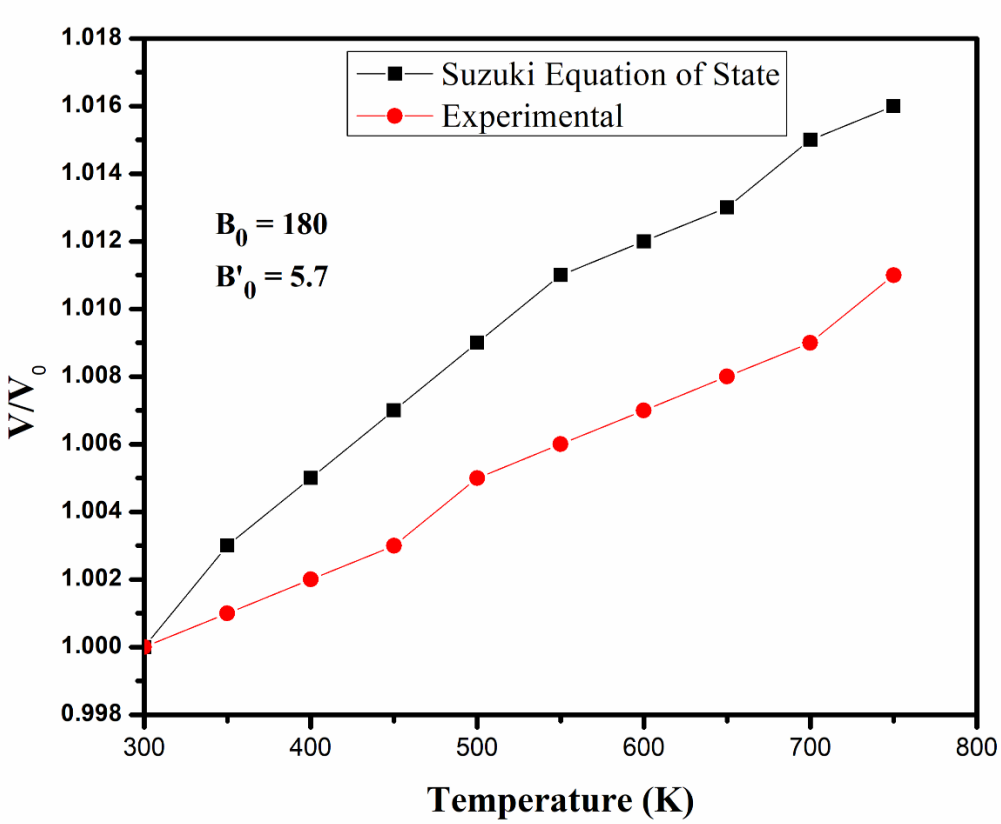


Fig.4.5.1: Volume thermal compression of C_{60} fullerenes at different temperatures

The calculated values of the thermal expansion ($\mathbf{V/V_0}$) obtained by using the modified Suzuki equation of state at different temperatures are compared with the experimental data shown in Fig 4.5.1. It is very much clear from the same fig. that the results found in the present study shows similar trend as the understudy material (C_{60}) shows experimentally under high temperature.

It is pertinent to mention here that the result obtained in the present study from the modified Suzuki equation of state (which is mathematically and thermodynamically consistent) predicts values at high temperature successfully. Hence the calculated values of the C_{60} (Fullerene) validate the quasi- harmonic approximation.

Chapter-5

Conclusion

This study investigated the compression behaviour of some Co, Rh, and Mn-based Heusler compounds in terms of computed values of bulk modulus and relative change in volume (V/V_0) as a function of pressure at constant temperature. The key observations are summarized below

- The compression behaviour of the studied materials varies with pressure and with the type of equation of state used to fit the data.
- The Tait equation of state generally fits best for the compression behaviour of the materials, followed by the Murnaghan equation of state, and the Kholiya and Chandra and Shankers equations of state.
- All Heusler compounds Mn_2CoCr, Mn_2PtCo, Rh_2MnZn, Rh_2FeZn, Co_2NbB, Co_2TaB, FeCrTiSn and FeCrTiSb show similar patterns in compression behaviour with decreasing volume with increasing pressure.
- It is evident from the data that the studied materials possess different compressibility due to their unique structural and electronic properties.

Moreover, we used the simple theory to predict the volume compression of nanomaterials at different pressures. This formulation necessitates two input parameters which include bulk modulus and its first order pressure derivative under the conditions of zero pressure. In order to check the utility of the current model at the nano level, we have taken the steps in order to calculate how relative volume changes by altering the pressure for five nanocrystalline materials viz. SWCNTs, Graphite, Al_2O_3, Nano-ε-Fe, Nano Ni. It has been observed that:

- The graphical presentation of volume compression (V/V_0) verses pressure (P) indicates that as pressure increases the material gets more and more compressed, which is expected in favour of the said nanomaterials.
- Thus, keeping in view, the above obtained results, one could say that the nanomaterial compressibility increases with decrease in the particle size. Hence the nanomaterials with lower size are more compressible in comparison to the bulk materials. This examination could be ascribed to the fact that reduction in the grain size results in the increase of surface to the volume ratio.

- The bulk modulus of the nanocrystalline solids will reduce with decrease in the grain size. It may be concluded that all equations used are relatively suitable for these materials in the pressure range considered in the present study.

Furthermore, we have investigated the compression behaviour of some bulk materials viz. aluminium, copper, nickel, lead and zinc at different pressures. The main aim of this approach is to calculate how relative volume changes ($V/V_{0)}$ by way of volume compression with varying the pressure of study materials by using equation of states at constant temperature. It has been observed that:

- The graphical representation of the said materials depicts that the value of V/V_0 decreases as the pressure increases indicates compressibility of material, which is consistent with the behaviour of most materials under compression, this process may lead to phase transition of the materials.
- The decrease in V/V_0 with increasing pressure is directly connected to the bulk modulus of the material and its pressure dependence.
- Materials with higher bulk modulus resist compression and show smaller reductions in volume under pressure, while those with lower bulk modulus exhibit greater compressibility and larger reductions in volume.
- The pressure derivative of the bulk modulus (B') further modulates this relationship, affecting the material's compressibility at different pressures.
- Different equations of state (EOS) predict these behaviours in varying ways, based on how they treat the bulk modulus and its dependence on pressure.
- The choice of EOS model should align with the specific material's elastic properties, ensuring accurate predictions of compressibility, particularly for high-pressure applications.
- The bulk modulus and its pressure dependence are fundamental factors governing material compressibility, influencing the volume reduction behaviour (V/V_0) and shaping the material's performance under varying pressure conditions.
- On comparison the results of the above investigation of both (nano & bulk) forms of materials, it reveals that bulk materials usually show more consistent and expected compression behaviour by using various equation of states (EOS).

- In contrast, nanomaterials with their exceptional properties reveal higher compressibility and more responsive by using the equation of states (model).
- The comparative study clearly depict that the compressibility of nano-materials depends on size, as compressibility increases with decreasing particle size, thus lower sized nanomaterials are more compressible than bulk materials.
- This investigation may be credited to the fact that decrease in particle size increases the surface to volume ratio and thus the bulk modulus of a nanocrystalline material will decrease with decrease in grain size.
- Furthermore, we have investigated the thermal volume expansion (V/V_0) behaviour of fullerene (C_{60}) by using modified Suzuki equation at different temperatures over the temperature range 300K-800K under zero pressure condition.
- The calculated values of thermal volume expansion (V/V_0) are compared with the available experimental data; it is evident from the graphical representation that there is close agreement of our theoretical results with the available experimental values.
- Under this investigation, it has been revealed that thermal volume expansion coefficient (α_0) of fullerene (C_{60}) increases with increase in temperature, which is the common trend of each material under high temperature investigation. So this close agreement validates our present theoretical approach.

References

[1] Patel, J. K., Patel, A., & Bhatia, D. (2021). Introduction to nanomaterials and nanotechnology. In *Emerging technologies for nanoparticle manufacturing* (pp. 3-23). Cham: Springer International Publishing.

[2] Sindhu, R. K., Chitkara, M., & Sandhu, I. S. (2021). *Nanotechnology: principles and applications*. CRC Press.

[3] Arora, N., Joshi, D. P., & Pachauri, U. (2018). Effect of size and dimension dependent specific heat on thermal conductivity of nanostructured semiconductors. *Materials Chemistry and Physics*, *217*, 235-241.

[4] Suryanarayana, C. (2002). The structure and properties of nanocrystalline materials: issues and concerns. *Jom*, *54*, 24-27.

[5] Gusev, A. I., & Rempel′, A. A. (2004). *Nanocrystalline materials*. Cambridge Int Science Publishing.

[6] Gleiter, H. (1991). Nanocrystalline materials. In *Advanced Structural and Functional Materials: Proceedings of an International Seminar Organized by Deutsche ForschungsanstaltfürLuft-und Raumfahrt (DLR), Köln, June 1991* (pp. 1-37). Springer Berlin Heidelberg.

[7] Goyal, M., & Singh, M. (2020). Size and shape dependence of optical properties of nanostructures. *Applied Physics A*, *126*, 1-8.

[8] Adekoya, J. A., Ogunniran, K. O., Siyanbola, T. O., Dare, E. O., &Revaprasadu, N. (2018). Band structure, morphology, functionality, and size-dependent properties of metal nanoparticles. *Noble and Precious Metals-Properties, Nanoscale Effects and Applications*, 15-42.

[9] Kulanthaivel, S., & Mishra, P. (2021). Shape-and Size-Dependent Antibacterial Activity of Nanomaterials. *Microbial Interactions at Nanobiotechnology Interfaces: Molecular Mechanisms and Applications*, 1-52.

[10] Biswas, A., Bayer, I. S., Biris, A. S., Wang, T., Dervishi, E., &Faupel, F. (2012). Advances in top–down and bottom–up surface nanofabrication: Techniques, applications & future prospects. *Advances in colloid and interface science*, *170*(1-2), 2-27.

[11] Majumder, D. D., Banerjee, R., Ulrichs, C. H., Mewis, I., & Goswami, A. (2007). Nano-materials: Science of bottom-up and top-down. *IETE technical review*, *24*(1), 9-25.

[12] Thiruvengadathan, R., Korampally, V., Ghosh, A., Chanda, N., Gangopadhyay, K., &Gangopadhyay, S. (2013). Nanomaterial processing using self-assembly-bottom-up chemical and biological approaches. *Reports on Progress in Physics*, *76*(6), 066501.

[13] Chen, F., Yan, T. H., Bashir, S., & Liu, J. L. (2022). Synthesis of nanomaterials using top-down methods. *Advanced Nanomaterials and Their Applications in Renewable Energy*, 37-60.

[14] Majumder, D. D., Banerjee, R., Ulrichs, C. H., Mewis, I., & Goswami, A. (2007). Nano-materials: Science of bottom-up and top-down. *IETE technical review*, *24*(1), 9-25.

[15] Arole, V. M., &Munde, S. V. (2014). Fabrication of nanomaterials by top-down and bottom-up approaches-an overview. J. Mater. Sci, 1, 89-93.

[16] Wang, J., Qi, Y., Zhi, Z., Guo, J., Li, M., & Zhang, Y. (2007). A self-assembly mechanism for sol–gel derived ZnO thin films. *Smart Materials and Structures*, *16*(6), 2673.

[17] Hoeven, J. E. V. D., Shneidman, A. V., Nicolas, N. J., & Aizenberg, J. (2022). Evaporation-induced self-assembly of metal oxide inverse opals: From synthesis to applications. *Accounts of Chemical Research*, *55*(13), 1809-1820.

[18] Pomerantseva, E., Bonaccorso, F., Feng, X., Cui, Y., &Gogotsi, Y. (2019). Energy storage: The future enabled by nanomaterials. *Science*, *366*(6468), eaan8285.

[19] Zhou, L., Zhuang, Z., Zhao, H., Lin, M., Zhao, D., & Mai, L. (2017). Intricate hollow structures: controlled synthesis and applications in energy storage and conversion. *Advanced materials*, *29*(20), 1602914.

[20] Wang, X., Feng, J. I., Bai, Y., Zhang, Q., & Yin, Y. (2016). Synthesis, properties, and applications of hollow micro-/nanostructures. *Chemical reviews*, *116*(18), 10983-11060.

[21] Bai, F., Bian, K., Huang, X., Wang, Z., & Fan, H. (2019). Pressure induced nanoparticle phase behavior, property, and applications. *Chemical reviews*, *119*(12), 7673-7717.

[22] Machon, D., Pischedda, V., Le Floch, S., & San-Miguel, A. (2018). Perspective: High pressure transformations in nanomaterials and opportunities in material design. *Journal of Applied Physics*, *124*(16).

[23] Joshi, M., & Bhattacharyya, A. (2011). Nanotechnology–a new route to high-performance functional textiles. *Textile progress*, *43*(3), 155-233.

[24] Nasiri, Z., Ghaemifar, S., Naghizadeh, M., &Mirzadeh, H. (2021). Thermal mechanisms of grain refinement in steels: a review. *Metals and Materials International*, *27*, 2078-2094.

[25] Anandhakumar, S., Sasidharan, M., Tsao, C. W., &Raichur, A. M. (2014). Tailor-made hollow silver nanoparticle cages assembled with silver nanoparticles: An

efficient catalyst for epoxidation. *ACS Applied Materials & Interfaces*, *6*(5), 3275-3281.

[26] Anandhakumar, S., Sasidharan, M., Tsao, C. W., &Raichur, A. M. (2014). Tailor-made hollow silver nanoparticle cages assembled with silver nanoparticles: An efficient catalyst for epoxidation. *ACS Applied Materials & Interfaces*, *6*(5), 3275-3281.

[27] Varshney, K. (2014). Carbon nanotubes: a review on synthesis, properties and applications. *International journal of engineering research and general science*, *2*(4), 660-677.

[28] Khanna, S. (2019). Carbon Nanotubes: Properties and Applications. In *Carbon Nanotubes and Nanoparticles* (pp. 195-216). Apple Academic Press.

[29] Zhou, W., Bai, X., Wang, E., &Xie, S. (2009). Synthesis, structure, and properties of single-walled carbon nanotubes. *Advanced Materials*, *21*(45), 4565-4583.

[30] Mousa, M. S. (2018, February). Comparison between single-walled CNT, multi-walled CNT, and carbon nanotube-fiberpyrograf III. In *IOP Conference Series: Materials Science and Engineering* (Vol. 305, p. 012025). IOP Publishing.

[31] Weber, J., Singhal, R., Zekri, S., & Kumar, A. (2008). One-dimensional nanostructures: fabrication, characterisation and applications. *International Materials Reviews*, *53*(4), 235-255.

[32] Saifuddin, N., Raziah, A. Z., &Junizah, A. R. (2013). Carbon nanotubes: a review on structure and their interaction with proteins. *Journal of Chemistry*, *2013*.

[33] White, C. T., &Mintmire, J. W. (2005). Fundamental properties of single-wall carbon nanotubes. *The Journal of Physical Chemistry B*, *109*(1), 52-65.

[34] Malik, S. R., Maqbool, M. A., Hussain, S., & Irfan, H. (2008). Carbon nanotubes: description, properties and applications. *J. Pak. Mater. Soc*, *2*(1), 21-26.

[35] Parveen, S., Rana, S., &Fangueiro, R. (2013). A review on nanomaterial dispersion, microstructure, and mechanical properties of carbon nanotube and nanofiber reinforced cementitious composites. *Journal of Nanomaterials*, *2013*, 80-80.

[36] Kumar, A., Khan, S., Husain, S., & Husain, M. (2018). Carbon based Nanomaterials: Synthesis and Applications (A Review).

[37] Dumlich, H. (2013). *A path to monochiral ensembles of carbon nanotubes and their properties* (Doctoral dissertation).

[38] Jamal, G. R. A. (2022). Chirality dependent empirical modeling of optical transitions and bandgapsin carbon nanotubes and graphene nanoribbons.

[39] Madankar, R. S., Bhilkar, P. R., Tiple, A. D., Nagmote, M. S., Potbhare, A. K., Sharma, R., ... & Chaudhary, R. G. (2024). Role of carbonaceous fullerene materials in crop improvement and targeted pesticide management. In *Carbon-Based Nanomaterials in Biosystems* (pp. 223-242). Academic Press. Hedberg, K., Hedberg, L., Bethune, D. S., Brown, C. A., Dorn, H. C., Johnson, R. D., & De Vries, M. (1991). Bond lengths in free molecules of buckminsterfullerene, C60, from gas-phase electron diffraction. *Science*, *254*(5030), 410-412.

[40] Baati, T. About C60 Carbon Discovery of the 60 Carbon.

[41] Sabry, F. (2022). Fullerene: Building nano-sized machines which can be inserted into the human body to detect and repair diseased cells for cancer and AIDS (Vol. 7). One Billion Knowledgeable.

[42] Pavlovic, M., & Pavlovic, M. (2015). Nanotechnology: Novel Emerging Concepts. Bioengineering: A Conceptual Approach, 245-265.

[43] Flood, D. J., & Barron, A. R. (2013). Carbon Nanotubes.

[44] Sederberg, D., Bryan, L., & Giordano, N. (2009, June). Allotropes of carbon. In NCLT-National Center for Learning and Teaching in Nanoscale Science and Engineering.

[45] Abu Bakar, H. H. (1993). Icosahedral symmetry and its application to possible models of the fullerene molecule C60 (Doctoral dissertation, City, University of London).

[46] Yadav, B. C., & Kumar, R. (2008). Structure, properties and applications of fullerenes. International Journal of Nanotechnology and Applications, 2(1), 15-24.

[47] Kroto, H. W., Allaf, A. W., & Balm, S. P. (1991). C60: Buckminsterfullerene. Chemical Reviews, 91(6), 1213-1235.

[48] Kroto, H. W. (1992). C60: Buckminsterfullerene, the celestial sphere that fell to earth. AngewandteChemie International Edition in English, 31(2), 111-129.

[49] Moore, J. H., & Spencer, N. D. (2020). C1. 2 Fullerenes. Encyclopedia of Chemical Physics and Physical Chemistry-3 Volume Set, 2093-2117.

[50] Heiney, P. A. (1992). Structure, dynamics and ordering transition of solid C60. Journal of Physics and Chemistry of Solids, 53(11), 1333-1352.

[51] Root, S. E., Savagatrup, S., Printz, A. D., Rodriquez, D., &Lipomi, D. J. (2017). Mechanical properties of organic semiconductors for stretchable, highly flexible, and mechanically robust electronics. Chemical reviews, 117(9), 6467-6499.

[52] Thakur, V. K., & Thakur, M. K. (2018). Chemical functionalization of carbon nanomaterials (pp. 5-13). Warentown (NJ: CRC Press.

[53] Sabry, F. (2022). Fullerene: Building nano-sized machines which can be inserted into the human body to detect and repair diseased cells for cancer and AIDS (Vol. 7). One Billion Knowledgeable.

[54] Talbot, C. (1999). Fullerene and nanotube chemistry: an update. School science review, 81, 37-48.

[55] Alegaonkar, A. P., &Alegaonkar, P. S. (2023). Nanocarbons: Preparation, Assessments, and Applications. CRC Press.

[56] Jennepalli, S. (2015). Synthesis of [60] fullerenyl amino acid derivatives for medicinal chemistry and material science applications.

[57] Stout, D. A., Durmus, N. G., & Webster, T. J. (2013). Synthesis of carbon based nanomaterials for tissue engineering applications. In Nanomaterials in tissue engineering (pp. 119-157). Woodhead Publishing.

[58] Argentine, S. M. (1995). *Spectroscopic studies of carbon (60) and carbon (70)*. University of Michigan.

[59] Schwerdtfeger, P., Wirz, L. N., & Avery, J. (2015). The topology of fullerenes. *Wiley Interdisciplinary Reviews: Computational Molecular Science*, *5*(1), 96-145.

[60] Pérez-Terrazas, J. E., Romero, A. H., &Terrones, M. (2008). Effects of novel and stable intermolecular connections in the mechanical and electronic properties of C60 polymerized structures. *Chemical Physics Letters*, *458*(1-3), 128-133.

[61] Moszyński, D., Kiełbasa, K., &Arabczyk, W. (2013). Influence of crystallites' size on iron nitriding and reduction of iron nitrides in nanocrystalline Fe–N system. *Materials Chemistry and Physics*, *141*(2-3), 674-679.

[62] Suryanarayana, C. J. I. M. R. (1995). Nanocrystalline materials. *International materials reviews*, *40*(2), 41-64.

[63] Meyers, M. A., Mishra, A., & Benson, D. J. (2006). Mechanical properties of nanocrystalline materials. *Progress in materials science*, *51*(4), 427-556.

[64] Siow, K. S., Tay, A. A. O., &Oruganti, P. (2004). Mechanical properties of nanocrystalline copper and nickel. *Materials science and technology*, *20*(3), 285-294.

[65] Natter, H., Schmelzer, M., &Hempelmann, R. (1998). Nanocrystalline nickel and nickel-copper alloys: Synthesis, characterization, and thermal stability. *Journal of Materials research*, *13*(5), 1186-1197.

[66] Lehto, P., Remes, H., Saukkonen, T., Hänninen, H., & Romanoff, J. (2014). Influence of grain size distribution on the Hall–Petch relationship of welded structural steel. *Materials Science and Engineering: A*, *592*, 28-39.

[67] Davis, K. (2010). Material Review: Alumina (Al 2 O 3). *School of Doctoral Studies European Union Journal*, (2).

[68] Sassa, V. S., &Gorshenkov, A. N. (1977). A high-alumina lining for crucible-type induction furnaces. *Refractories*, *18*(3), 151-154.

[69] Chen, L., Neudeck, P. G., Spry, D. J., Beheim, G. M., & Hunter, G. W. (2021). A 96% alumina based packaging system for 500° C test of SiC integrated circuits. *Additional Papers and Presentations*, *2021*(HiTEC), 000069-000075.

[70] Jiang, S., & Yang, K. (2021). Review of high-throughput computational design of Heusler alloys. *Journal of Alloys and Compounds*, *867*, 158854.

[71] Oliynyk, A. O., Antono, E., Sparks, T. D., Ghadbeigi, L., Gaultois, M. W., Meredig, B., & Mar, A. (2016). High-throughput machine-learning-driven synthesis of full-Heusler compounds. *Chemistry of Materials*, *28*(20), 7324-7331.

[72] Elphick, K., Frost, W., Samiepour, M., Kubota, T., Takanashi, K., Sukegawa, H., ... &Hirohata, A. (2021). Heusler alloys for spintronic devices: review on recent development and future perspectives. *Science and technology of advanced materials*, *22*(1), 235-271.

[73] Graf, T., Winterlik, J., Müchler, L., Fecher, G. H., Felser, C., & Parkin, S. S. (2013). Magnetic heusler compounds. In *Handbook of magnetic materials* (Vol. 21, pp. 1-75). Elsevier.

[74] Ouardi, S. (2012). Electronic structure and physical properties of Heusler compounds for thermoelectric and spintronic applications.

[75] Jourdan, M., Minár, J., Braun, J., Kronenberg, A., Chadov, S., Balke, B., ... &Kläui, M. (2014). Direct observation of half-metallicity in the Heusler compound Co2MnSi. *Nature communications*, *5*(1), 3974.

[76] Xiao, H., Hu, T., Liu, W., Zhu, Y. L., Li, P. G., Mu, G., ... & Mao, Z. Q. (2018). Superconductivity in the half-Heusler compound TbPdBi. *Physical Review B*, *97*(22), 224511.

[77] Wang, H., Bai, S., Chen, L., Cuenat, A., Joshi, G., Kleinke, H., ... & Tseng, Y. C. (2015). International round-robin study of the thermoelectric transport properties of an n-Type half-heusler compound from 300 K to 773 K. *Journal of Electronic Materials*, *44*, 4482-4491.

[78] Srivastava, V., & Bhatti, K. P. (2012). Ferromagnetic shape memory Heusler alloys. *Solid State Phenomena*, *189*, 189-208.

[79] Kaur, N., & Srivastava, V. (2022, May). First-principles calculations on mechanical properties of Rh2MnZn Heusler alloy. In *Journal of Physics: Conference Series* (Vol. 2267, No. 1, p. 012038). IOP Publishing.

[80] Kaur, N., & Srivastava, V. (2018). Review on Electronic and Magnetic properties of Fe–based full-Heusler compounds.

[81] Srivastava, V., Kaur, N., Khenata, R., & Dar, S. A. (2020). Investigation of the electronic, magnetic, elastic, thermodynamic and thermoelectric properties of

Mn2CoCr Heusler compound: A DFT-based simulation. *Journal of Magnetism and Magnetic Materials*, *513*, 167107

[82] Kaur, N., Srivastava, V., & Dar, S. A. (2022). GGA based study on electronic structure and thermoelectric properties of Mn2PtCo full-Heusler compound. *Indian Journal of Physics*, *96*(1), 71-77.

[83] Srivastava, V., Kaur, N., Wang, X., Mushtaq, M., & Dar, S. A. (2021). First-principles study on structural, electronic, magnetic, elastic, mechanical and thermodynamic properties of Mn2PtCo Heusler alloy. *International Journal of Energy Research*, *45*(7), 11305-11319.

[84] Srivastava, V., Kaur, N., & Dar, S. A. (2020, May). FP-LAPW calculations on electronic and thermoelectric properties of Mn2CoCr Heusler compound. In *Journal of Physics: Conference Series* (Vol. 1531, No. 1, p. 012031). IOP Publishing.

[85] Kaur, N., Sharma, R., Al-Douri, Y., Srivastava, V., & Abd El-Rehim, A. F. (2023). Thermodynamic, thermoelectric and optoelectronic performances of Co2MB (M= Nb, Ta) full-heusler compounds for solar cell and UV absorber applications. *Materials Science in Semiconductor Processing*, *165*, 107676.

[86] Ahmed, A., Said, H., Tarik, O., Bouhalouane, A., &Kadda, A. (2015). Ab initio study of Co2ZrGe and Co2NbB Full Heusler compounds. *International Journal of Physical and Mathematical Sciences*, *9*(4), 349-357.

[87] Lopes, M. V., de Souza, E. C., Santos, J. G., de Araujo, J. M., Lima, L., de Oliveira, A. B., ... & Correa, M. A. (2020). Modulating the spin Seebeck effect in Co2FeAl Heusler alloy for sensor applications. *Sensors*, *20*(5), 1387.

[88] Yu, J., Xia, K., Zhao, X., & Zhu, T. (2018). High performance p-type half-Heusler thermoelectric materials. *Journal of Physics D: Applied Physics*, *51*(11), 113001.

[89] Lewis, G. N., & Randall, M. (1963). *Thermodynamics* (No. 44). Krishna Prakashan Media.

[90] Jain, R. K., &Simha, R. (1980). On the statistical thermodynamics of multicomponent fluids: equation of state. *Macromolecules*, *13*(6), 1501-1508.

[91] Tallon, J. L. (1980). The thermodynamics of elastic deformation—I: equation of state for solids. *Journal of Physics and chemistry of solids*, *41*(8), 837-850.

[92] Kholiya, K., & Pandey, K. (2019). High pressure compression behaviour of bulk and nanocrystalline SnO2. *Journal of Taibah University for Science*, *13*(1), 592-596.

[93] Singh, M., Tlali, S., & Narayan, H. (2012). Pressure dependent volume change in some nanomaterials using an equation of state.

[94] Chandra, J., Kandpal, D., & Gupta, B. R. K. (2008). High temperature study of nanomaterials using integral form of equation of state (IFEOS). *High Temperatures-High Pressures*, *37*(4).

[95] Stacey, F. D. (2005). High pressure equations of state and planetary interiors. *Reports on progress in physics*, *68*(2), 341.

[96] Whitman, A. M. (2020). *Thermodynamics: basic principles and engineering applications* (pp. 1-320). Springer.

[97] Kumar, M. (1995). High pressure equation of state for solids. *Physica B: Condensed Matter*, *212*(4), 391-394.

[98] Shanker, J., Kushwah, S. S., & Kumar, P. (1997). Equation of state and pressure derivatives of bulk modulus for NaCl crystal. *Physica B: Condensed Matter*, *239*(3-4), 337-344.

[99] Tyuterev, V. G., & Vast, N. (2006). Murnaghan's equation of state for the electronic ground state energy. *Computational materials science*, *38*(2), 350-353.

[100] Guillermet, A. F. (1995). Thermodynamic properties of the generalized Murnaghan equation of state of solids. *International journal of thermophysics*, *16*, 1009-1026.

[101] Forbes, J. W., Lemar, E. R., & Brown, M. (2012, March). Solid and liquid equation of state for initially porous aluminum where specific heat and γ/v are constant. In *AIP Conference Proceedings* (Vol. 1426, No. 1, pp. 759-762). American Institute of Physics.

[102] Cheng, X., & Kong, Y. (2011). Comparison of Equation of State and the Four-Parameter li Equation of State in Alloy. *Modern Physics Letters B*, *25*(18), 1557-1568.

[103] Islam, T., Srivastava, A. K., Kaloo, M. A., &Wani, A. A. (2023). Study Of The Compression Behaviour Of Fe Cr Ti Sn And Fe Cr Ti Sb Materials Using Various Equation Of States. *Elementary Education Online*, *20*(6), 4961-4961.

[104] Kholiya, K. (2013). High pressure isothermal equation of state for nanomaterials. *Indian Journal of Physics*, *87*(4), 339-343.

[105] Neece, G. A., & Squire, D. R. (1968). Tait and related empirical equations of state. *The Journal of physical chemistry*, *72*(1), 128-136.

[106] Jain, R. K., &Simha, R. (1989). Theoretical equation of state: thermal expansivity, compressibility, and the Tait relation. *Macromolecules*, *22*(1), 464-468.

[107] Raju, S., Mohandas, E., & Raghunathan, V. S. (1997). The pressure derivative of bulk modulus of transition metals: An estimation using the method of model potentials and a study of the systematics. *Journal of Physics and Chemistry of Solids*, *58*(9), 1367-1373.

[108] Hofmeister, A. M. (1991). Pressure derivatives of the bulk modulus. *Journal of Geophysical Research: Solid Earth*, *96*(B13), 21893-21907.

[109] Kumar, M. (1996). Application of high pressure equation of state for different classes of solids. *Physica B: Condensed Matter*, *217*(1-2), 143-148.

[110] AL-FARİS, S. J., Al-Saqa, R. H., MOHHAMED, H. M., & KAREEM, S. (2022). High pressure effects on the structural properties of GaN compound using equations of state. *International journal of thermodynamics*, *25*(1), 79-84.

[111] Nazemi, N., Ahmadian, F., &Boochani, A. (2023). Investigation of half-metallic properties of full-Heusler alloys of O2BaX (X= Na, K, Rb, and Cs). *Chemical Physics Letters*, *830*, 140751.

[112] Al-Shiekh, A. M. (2020). Using Different Equations of States to Study Volume Ratio, Bulk Modulus and Energy Gap in Nano Ge Under High Pressure. *Rafidain Journal of Science*, *29*(2), 64-72.

[113] Bhatt, A., & Kumar, M. (2012). Size-Dependent Equation of State for Nanomaterials. *International Journal of Nanoscience*, *11*(01), 1250010.

[114] Sushil, K., Arunesh, K., Singh, P. K., & Sharma, B. S. (2004). Analysis of finite-strain equations of state for solids under high pressures. *Physica B: Condensed Matter*, *352*(1-4), 134-146.

[115] Kumar, M., & Kumar, M. (2008). Empirical high-pressure equation of state for nano materials. *Indian Journal of Pure and applied physics, 46*, 378-381.

[116] Kumar, R., & Kumar, M. (2013). Equation of state for nanomaterials from thermal expansion. *Indian Journal of Pure and applied physics,* 51, 87-93.

[117] Sharma, U. D., & Kumar, M. (2011). Analysis of equation of state for nanomaterials. Physica B: Condensed Matter, 406(4), 794-800.

[118] Bhatt, A., & Kumar, M. (2012). Size-Dependent Equation of State for Nanomaterials. International Journal of Nanoscience, 11(01), 1250010.

[119] Bhatt, J. C., Kholiya, K., & Kumar, R. (2013). High Pressure Equation of State for Nanomaterials. International Scholarly Research Notices, 1-5.

[120] Singh, M. and Kao, M. (2013) Study of Nanomaterials under High pressure. *Advances in Nanoparticles*, **2**, 350-357

[121] Singh, M., & Singh, M. (2015). Impact of size and temperature on thermal expansion of nanomaterials. Pramana, 84, 609-619.

[122] Greshnyakov, V. A., &Belenkov, E. A. (2014). Technique for calculating the bulk modulus. Russian Physics Journal, 57(6), 731-737.

[123] Chandra, J., &Kholiya, K. (2016). Compression of nanomaterials under pressure. Journal of Taibah University for Science, 10(3), 386-392.

[124] Singh, M. (2016). Behaviour of Isothermal Bulk Modulus of Nanomaterials under the Effect of Temperature. Journal of Nanoscience and Technology, 138-139.

[125] Goyal, M., & Gupta, B. R. K. (2019). Study of shape, size and temperature-dependent elastic properties of nanomaterials. Modern Physics Letters B, 33(26), 1950310.

[126] Hinna, A., Steiniger, F., Hupfeld, S., Brandl, M., &Kuntsche, J. (2014). Asymmetrical flow field-flow fractionation with on-line detection for drug transfer studies: a feasibility study. Analytical and bioanalytical chemistry, 406, 7827-7839.

[127] Alsheikh, A. M., & Issa, A. A. (2020, March). Theoretical study of bulk and nanomaterials under high pressure. In AIP Conference Proceedings (Vol. 2213, No. 1). AIP Publishing.

[128] Ghazal, A. I., & Al-sheikh, A. M. (2021, September). Thermo Elastic Properties of Nano-TiO2 Under High Pressure Using Different Equations of State. In Journal of Physics: Conference Series (Vol. 1999, No. 1, p. 012075). IOP Publishing.

[129] Latimer, K., Dwaraknath, S., Mathew, K., Winston, D., & Persson, K. A. (2018). Evaluation of thermodynamic equations of state across chemistry and structure in the materials project. npj Computational Materials, 4(1), 40.

[130] Mishra, A., & Dharmendra, K. (2021, August). Pressure-volume relationships of some solids based on double potential energy functions. In Journal of Physics: Conference Series (Vol. 2007, No. 1, p. 012007). IOP Publishing.

[131] M AL-Sheikh, A., & S Hameed, K. (2011). Theoretical study of energy gap for silicon and germanium under high pressure. Rafidain Journal of Science, 22(3), 58-68.

[132] Goyal, M., & Gupta, B. R. K. (2019). Study of shape, size and temperature-dependent elastic properties of nanomaterials. Modern Physics Letters B, 33(26), 1950310.

[133] Gupta, R., & Gupta, M. (2021). Bulk modulus of second-order pressure derivative for nanomaterials. Bulletin of Materials Science, 44(3), 218.

[134] Mebrek M. (2019). Study the Electronic, Magnetic and Elastic Properties of Ir2FeGe. Journal of Chemical and Pharmaceutical Research, 11(4):65-72

[135] Yahya, S. J., Abu-Jafar, M. S., Al Azar, S., Mousa, A. A., Khenata, R., Abu-Baker, D., &Farout, M. (2022). The Structural, Electronic, Magnetic and Elastic Properties of Full-Heusler Co2CrAl and Cr2MnSb: An Ab Initio Study. Crystals, 12(11), 1580.

[136] Yadav, D. K., Bhandari, S. R., &Kaphle, G. C. (2020). Structural, elastic, electronic, and magnetic properties of MnNbZ (Z= As, Sb) and FeNbZ (Z= Sn, Pb) semi-Heusler alloys. Materials Research Express, 7(11), 116527.

[137] Shabara, R. M. (2017). High pressure effect on structural, electronic and elastic properties of topological half-Heusler LaPdBi compound. *Materials Research Express*, *4*(8), 086511.

[138] Aslan, M. (2022). Electronic and Structural Properties of Li1 -xKxMgN Half Heusler Alloy. International Journal of Science and Research, 11, 1210-1214.

[139] Khalfa, M., Khachai, H., Chiker, F., Baki, N., Bougherara, K., Yakoubi, A., ... &Khenata, R. (2015). Mechanical, electronic and thermodynamic properties of full Heusler compounds Fe2VX (X= Al, Ga). International Journal of Modern Physics B, 29(31), 1550229.

[140] Mishra, S., & Srivastava, A. K. (2015). Applicability of equation of state for prediction of mechanical properties of nanomaterials. *Journal of Chemical and Pharmaceutical Research*, *7*(6), 708-720.

[141] Singh, P. K. (2011). Pressure dependence of bulk modulus for solids based on the first-principles results. Indian Journal of Pure & Applied Physics 49(12), 829-832.

[142] Sharma, U. D., & Kumar, M. (2011). Analysis of equation of state for nanomaterials. Physica B: Condensed Matter, 406(4), 794-800.

[143] Singh, M. and Kao, M. (2013). Study of Nanomaterials under High pressure. *Advances in Nanoparticles*, **2**, 350-357.

[144] Tait, P. G. (1965). *Report on some of the physical properties of fresh water and of sea water*. Phys. Chem, 2, 1—76.

[145] Birch- Murnaghan, F. (1988). Elasticity and constitution of the Earth's interior. *Elastic Properties and Equations of State*, *26*, 31-90.

[146] Kholiya, K., & Chandra, J. (2014). Equation of state model for studying high-pressure compression behaviour of nanomaterials. *Journal of Taibah University for Science*, *8*(2), 137-141.

[147] Shanker, J., Kushwah, S. S., & Kumar, P. (1997). Theory of thermal expansivity and bulk modulus for MgO and other minerals at high temperatures. *Physica B: Condensed Matter*, *233*(1), 78-83.

[148] Goyal, M., & Gupta, B. R. K. (2019). Study of shape, size and temperature-dependent elastic properties of nanomaterials. Modern Physics Letters B, 33(26), 1950310.

[149] Srivastava, V., Kaur, N., Khenata, R., & Dar, S. A. (2020). Investigation of the electronic, magnetic, elastic, thermodynamic and thermoelectric properties of Mn_2CoCr Heusler compound: A DFT-based simulation. Journal of Magnetism and Magnetic Materials, 513, 167107.

[150] Kaur, N., Srivastava, V., & Dar, S. A. (2022). GGA based study on electronic structure and thermoelectric properties of Mn_2PtCo full-Heusler compound. Indian Journal of Physics, 96(1), 71-77.

[151] Güler, E., Güler, M., Uğur, Ş., &Uğur, G. (2021). First principles study of electronic, elastic, optical and magnetic properties of Rh_2MnX (X= Ti, Hf, Sc, Zr, Zn) Heusler alloys. International Journal of Quantum Chemistry, 121(10), e26606.

[152] Benichou, B., Bouchenafa, H., Nabi, Z., &Bouabdallah, B. (2022). Computational study of structural stability, elastic, electronic, magnetic and thermodynamic properties of the Rh2-based full-Heusler compounds: Rh2MnZ (Z= Sn, Pb, Tl) by FP-LAPW method. Revista Mexicana de Física, 68(6 Nov-Dec), 060502-1.

[153] Kaur, N., Srivastava, V., Dar, S. A., Khenata, R., & Sharma, R. (2023). A unified DFT exploration on transport and thermodynamic properties of L21 structure of Rh2XZn (X= Mn, Fe) ferromagnets. Materials Science and Engineering: B, 287, 116099.

[154] Srivastava, V., Kaur, N., & Dar, S. A. (2020, May). FP-LAPW calculations on electronic and thermoelectric properties of Mn2CoCr Heusler compound. In Journal of Physics: Conference Series (Vol. 1531, No. 1, p. 012031). IOP Publishing.

[155] Khandy, S. A., & Chai, J. D. (2020). Robust stability, half-metallic ferrimagnetism and thermoelectric properties of new quaternary Heusler material: a first principles approach. Journal of Magnetism and Magnetic Materials, 502, 166562.

[156] Bhattacharya, S., Pope, A. L., Littleton IV, R. T., Tritt, T. M., Ponnambalam, V., Xia, Y., & Poon, S. J. (2000). Effect of Sb doping on the thermoelectric properties of Ti-based half-Heusler compounds, TiNiSn 1− x Sb x. Applied Physics Letters, 77(16), 2476-2478.

[157] Raïâ, M. Y., Masrour, R., Hamedoun, M., Kharbach, J., Rezzouk, A., Hourmatallah, A., ... &Bouslykhane, K. (2022). Stability, magnetic, electronic, elastic, thermodynamic, optical, and thermoelectric properties of Co_2TiSn, Co_2ZrSn and Co_2HfSn Heusler alloys from calculations using generalized gradient approximation techniques. Journal of Materials Science: Materials in Electronics, 33(25), 20229-20256.

[158] Casper, F., Graf, T., Chadov, S., Balke, B., &Felser, C. (2012). Half-Heusler compounds: novel materials for energy and spintronic applications. Semiconductor Science and Technology, 27(6), 063001.

[159] Bennani, M. A., Aziz, Z., Terkhi, S., Elandaloussi, E. H., Bouadjemi, B., Chenine, D., ... &Bentata, S. (2021). Structural, electronic, magnetic, elastic, thermodynamic, and thermoelectric properties of the half-Heusler RhFeX (with X= Ge, Sn) compounds. Journal of Superconductivity and Novel Magnetism, 34, 211-225.

[160] Amraoui, R., Kadri, S., Meradji, H., Berkani, M., Bouaricha, A., Ghemid, S., ... & Ahmed, R. (2022). First-principles computational study on structural, elastic,

magnetic, electronic, and thermoelectric properties of Co2MnGe: a potential Heusler ternary compound. The European Physical Journal B, 95(12), 198.

[161] Charifi, Z., Ghellab, T., Baaziz, H., &Soyalp, F. (2022). Characterization of quaternary Heusler alloys CoFeYGe (Y= Ti, Cr) with respect to structural, electronic, magnetic, mechanical, and thermoelectric features. International Journal of Energy Research, 46(10), 13855-13873.

[162] Ahmed, T. (2013). Equations of state and PVT analysis. Elsevier.

[163] Zharkov, V. N., & Kalinin, V. A. (1971). Equations of state for solids at high pressures and temperatures (p. 257). New York: Consultants Bureau.

[164] Knittle, E., Kaner, R. B., Jeanloz, R., & Cohen, M. L. (1995). High-pressure synthesis, characterization, and equation of state of cubic C-BN solid solutions. Physical Review B, 51(18), 12149.

[165] Latimer, K., Dwaraknath, S., Mathew, K., Winston, D., & Persson, K. A. (2018). Evaluation of thermodynamic equations of state across chemistry and structure in the materials project. npj Computational Materials, 4(1), 40.

[166] Menikoff, R. (2007). Empirical equations of state for solids. ShockWave Science and Technology Reference Library, 143-188.

[167] Vinet, P., Rose, J. H., Ferrante, J., & Smith, J. R. (1989). Universal features of the equation of state of solids. Journal of Physics: Condensed Matter, 1(11), 1941.

[168] Yazdizadeh, M., Eslamimanesh, A., &Esmaeilzadeh, F. (2012). Applications of cubic equations of state for determination of the solubilities of industrial solid compounds in supercritical carbon dioxide: A comparative study. Chemical engineering science, 71, 283-299.

[169] Yazdizadeh, M., Eslamimanesh, A., &Esmaeilzadeh, F. (2011). Thermodynamic modeling of solubilities of various solid compounds in supercritical

carbon dioxide: Effects of equations of state and mixing rules. The Journal of Supercritical Fluids, 55(3), 861-875.

[170] Gross, J., & Sadowski, G. (2002). Application of the perturbed-chain SAFT equation of state to associating systems. Industrial & engineering chemistry research, 41(22), 5510-5515

[171] Shanker, J., Kushwah, S. S., & Kumar, P. (1997). Theory of thermal expansivity and bulk modulus for MgO and other minerals at high temperatures. Physica B: Condensed Matter, 233(1), 78-83.

[172] Gupta, R., & Gupta, M. (2021). Bulk modulus of second-order pressure derivative for nanomaterials. Bulletin of Materials Science, 44(3), 218.

[173] Sharma, U. D., & Kumar, M. (2011). Analysis of equation of state for nanomaterials. Physica B: Condensed Matter, 406(4), 794-800.

[174] Gupta, R., & Gupta, M. (2021). Bulk modulus of second-order pressure derivative for nanomaterials. Bulletin of Materials Science, 44(3), 218.

[175] Shakil, M., Mushtaq, S., Zeba, I., Gillani, S. S. A., Khan, M. I., Arshad, H., & Rafique, M. (2021). Structural, electronic, magnetic and thermoelectric properties of full heusler alloys Co2YZ (Z= S, Ge, Se): a first principles calculation. Physica B: Condensed Matter, 602, 412558.

[176] Latimer, K., Dwaraknath, S., Mathew, K., Winston, D., & Persson, K. A. (2018). Evaluation of thermodynamic equations of state across chemistry and structure in the materials project. npj Computational Materials, 4(1), 40.

[177] Wang, Z., Tait, K., Zhao, Y., Schiferl, D., Zha, C., Uchida, H., & Downs, R. T. (2004). Size-induced reduction of transition pressure and enhancement of bulk modulus of AlN nanocrystals. The Journal of Physical Chemistry B, 108(31), 11506-11508.

[178] Anderson, O. L. (1995). Equations of state of solids for geophysics and ceramic science (No. 31). Oxford University Press on Demand.

[179] Yahya, S. J., Abu-Jafar, M. S., Al Azar, S., Mousa, A. A., Khenata, R., Abu-Baker, D., &Farout, M. (2022). The Structural, Electronic, Magnetic and Elastic Properties of Full-Heusler Co2CrAl and Cr2MnSb: An Ab Initio Study. Crystals, 12(11), 1580.

[180] Menikoff, R. (2007). Empirical equations of state for solids. ShockWave Science and Technology Reference Library, 143-188.

[181] Vinet, P., Rose, J. H., Ferrante, J., & Smith, J. R. (1989). Universal features of the equation of state of solids. Journal of Physics: Condensed Matter, 1(11), 1941.

[182] Bhatt, S., & Kumar, M. (2017). Equation of state and lattice parameter of SnO2 nanomaterial. Materials Today: Proceedings, 4(9), 9547-9551.

[183] Zhu, K., Ju, Y., Xu, J., Yang, Z., Gao, S., & Hou, Y. (2018). Magnetic nanomaterials: Chemical design, synthesis, and potential applications. *Accounts of Chemical Research*, *51*(2), 404-413.

[184] Rao, C. N. R., & Cheetham, A. K. (2001). Science and technology of nanomaterials: current status and future prospects. *Journal of Materials Chemistry*, *11*(12), 2887-2894.

[185] Siddiqui, M. T. H., Nizamuddin, S., Baloch, H. A., Mubarak, N. M., Al-Ali, M., Mazari, S. A., ... & Griffin, G. (2019). Fabrication of advance magnetic carbon nano-materials and their potential applications: a review. *Journal of environmental chemical engineering*, *7*(1), 102812.

[186] Rao, C. N. R., & Cheetham, A. K. (2001). Science and technology of nanomaterials: current status and future prospects. *Journal of Materials Chemistry*, *11*(12), 2887-2894.

[187] Ahmadi, M., Ghoorchian, A., Dashtian, K., Kamalabadi, M., Madrakian, T., &Afkhami, A. (2021). Application of magnetic nanomaterials in electroanalytical methods: A review. *Talanta*, *225*, 121974.

[188] Cui, Z. (2016). *Printed electronics: materials, technologies and applications*. John Wiley & Sons.

[189] Chen, K. N., & Tu, K. N. (2015). Materials challenges in three-dimensional integrated circuits. *Mrs Bulletin*, *40*(3), 219-222.

[190] Kish, F., Lal, V., Evans, P., Corzine, S. W., Ziari, M., Butrie, T., ... & Welch, D. (2017). System-on-chip photonic integrated circuits. *IEEE Journal of Selected Topics in Quantum Electronics*, *24*(1), 1-20.

[191] Goldman, A. (2012). *Handbook of modern ferromagnetic materials* (Vol. 505). Springer Science & Business Media.

[192] Mamalis, A. G. (2007). Recent advances in nanotechnology. *Journal of Materials Processing Technology*, *181*(1-3), 52-58.

[193] Mamalis, A. G. (2007). Recent advances in nanotechnology. *Journal of Materials Processing Technology*, *181*(1-3), 52-58.

[194] Jun, B. H., Noh, M. S., Kim, J., Kim, G., Kang, H., Kim, M. S., ... & Lee, Y. S. (2010). Multifunctional silver-embedded magnetic nanoparticles as SERS nanoprobes and their applications. *small*, *6*(1), 119-125.

[195] Graf, T., Casper, F., Winterlik, J., Balke, B., Fecher, G. H., &Felser, C. (2009). Crystal structure of new Heusler compounds. *Zeitschriftfüranorganische und allgemeineChemie*, *635*(6-7), 976-981.

[196] Graf, T., Felser, C., & Parkin, S. S. (2011). Simple rules for the understanding of Heusler compounds. *Progress in solid state chemistry*, *39*(1), 1-50.

[197] Prakash, R., & Kalpana, G. (2023). First-principles study on novel Fe-based quaternary Heusler alloys, with robust half-metallic, thermoelectric and optical properties. *RSC advances*, *13*(16), 10847-10860.

[198] Baisnab, D. K., Mukherjee, S., & Das, S. (2021). A short review on inorganic thin films from device perspective. *Chemical Solution Synthesis for Materials Design and Thin Film Device Applications*, 231-275.

[199] Zharkov, V. N., & Kalinin, V. A. (1971). *Equations of state for solids at high pressures and temperatures* (p. 257). New York: Consultants Bureau.

[200] Amari, S., Mebsout, R., Méçabih, S., Abbar, B., &Bouhafs, B. (2014). First-principle study of magnetic, elastic and thermal properties of full Heusler Co2MnSi. *Intermetallics*, *44*, 26-30.

[201] Graf, T., Fecher, G. H., Barth, J., Winterlik, J., &Felser, C. (2009). Electronic structure and transport properties of the Heusler compound Co2TiAl. *Journal of Physics D: Applied Physics*, *42*(8), 084003.

[202] Garg, A. B., & Vijayakumar, V. (2011). Phase stability of Heusler compound Co2FeSi under pressure: An in-situ x-ray diffraction investigation. *Journal of Applied Physics*, *110*(8), 083523.

[203] Wiendlocha, B., Winiarski, M. J., Muras, M., Zvoriste-Walters, C., Griveau, J. C., Heathman, S., ... &Klimczuk, T. (2015). Pressure effects on the superconductivity of the Hf Pd 2 Al Heusler compound: experimental and theoretical study. *Physical Review B*, *91*(2), 024509.

[204] Joshi, H., Vu, T. V., Hieu, N. N., Khenata, R., & Rai, D. P. (2021). Mechanical and thermodynamical properties of Fe2CoAl a full-Heusler alloy under hydrostatic pressure: A DFT study. *Materials Chemistry and Physics*, *270*, 124792.

[205] Lei, Y., Deng, H., Lei, T., Yang, M., & Deng, J. (2013). First-Principles Study on Half-Metallic Full-Heusler Compound Mn 2 ZnSi. *Journal of superconductivity and novel magnetism*, *26*, 389-395.

[206] Abdullah, A., Husain, M., Rahman, N., Khan, R., Iqbal, Z., Zulfiqar, S., ... &Reshak, A. H. (2021). Computational investigation of structural, magnetic, elastic, and electronic properties of Half-Heusler ScVX (X= Si, Ge, Sn, and Pb) compounds. *The European Physical Journal Plus*, *136*(11), 1176.

[207] Abdullah, A., Husain, M., Rahman, N., Khan, R., Iqbal, Z., Zulfiqar, S., ... &Reshak, A. H. (2021). Computational investigation of structural, magnetic, elastic, and electronic properties of Half-Heusler ScVX (X= Si, Ge, Sn, and Pb) compounds. *The European Physical Journal Plus*, *136*(11), 1176.

[208] Joshi, H., Rai, D. P., Verma, K. D., Bhamu, K. C., & Thapa, R. K. (2017). Thermoelectric properties of tetragonal half-Heusler compounds, TiXSb (X= Ge, Si): a probe from Density Functional Theory (DFT). *Journal of Alloys and Compounds*, *726*, 1155-1160.

[209] Holzapfel, W. B., Hartwig, M., & Sievers, W. (2001). Equations of state for Cu, Ag, and Au for wide ranges in temperature and pressure up to 500 GPa and above. *Journal of Physical and Chemical Reference Data*, *30*(2), 515-529.

[210] Douglas, J. F., & Xu, W. S. (2021). Equation of state and entropy theory approach to thermodynamic scaling in polymeric glass-forming liquids. *Macromolecules*, *54*(7), 3247-3269.

[211] Menikoff, R. (2007). Empirical equations of state for solids. *ShockWave Science and Technology Reference Library*, 143-188.

[212] Ravindran, P., Fast, L., Korzhavyi, P. A., Johansson, B., Wills, J., & Eriksson, O. (1998). Density functional theory for calculation of elastic properties of

orthorhombic crystals: Application to TiSi 2. *Journal of Applied Physics*, *84*(9), 4891-4904.

[213] Kamiya, T., &Hosono, H. (2010). Material characteristics and applications of transparent amorphous oxide semiconductors. *NPG Asia Materials*, *2*(1), 15-22.

[214] Chizmeshya, A. V., Wolf, G. H., & McMillan, P. F. (1996). First-principles calculation of the equation-of-state, stability, and polar optic modes of CaSiO3 perovskite. *Geophysical research letters*, *23*(20), 2725-2728.

[215] Shanker, J., Kushwah, S. S., & Kumar, P. (1997). Theory of thermal expansivity and bulk modulus for MgO and other minerals at high temperatures. Physica B: Condensed Matter, 233(1), 78-83.

[216] Gupta, R., & Gupta, M. (2021). Bulk modulus of second-order pressure derivative for nanomaterials. Bulletin of Materials Science, 44(3), 218.

[217] Yahya, S. J., Abu-Jafar, M. S., Al Azar, S., Mousa, A. A., Khenata, R., Abu-Baker, D., &Farout, M. (2022). The Structural, Electronic, Magnetic and Elastic Properties of Full-Heusler Co2CrAl and Cr2MnSb: An Ab Initio Study. Crystals, 12(11), 1580.

[218] Menikoff, R. (2007). Empirical equations of state for solids. ShockWave Science and Technology Reference Library, 143-188.

[219] Vinet, P., Rose, J. H., Ferrante, J., & Smith, J. R. (1989). Universal features of the equation of state of solids. Journal of Physics: Condensed Matter, 1(11), 1941.

[220] Bhatt, S., & Kumar, M. (2017). Equation of state and lattice parameter of SnO2 nanomaterial. Materials Today: Proceedings, 4(9), 9547-9551.

[221] Borisenko, V. E., &Ossicini, S. (2013). *What is what in the Nanoworld: A Handbook on Nanoscience and Nanotechnology*. John Wiley & Sons.

[222] Joachim, C. (2009). *Nanosciences: The invisible revolution*. World Scientific.

[223] Wilson, M., Kannangara, K., Smith, G., Simmons, M., &Raguse, B. (2002). Nanotechnology: basic science and emerging technologies.

[224] Minnich, A., Dresselhaus, M. S., Ren, Z. F., & Chen, G. (2009). Bulk nanostructured thermoelectric materials: current research and future prospects. *Energy & Environmental Science*, *2*(5), 466-479.

[225] Yoon, H., & Jang, J. (2009). Conducting-polymer nanomaterials for high-performance sensor applications: issues and challenges. *Advanced Functional Materials*, *19*(10), 1567-1576.

[226] Tan, J. C., &Cheetham, A. K. (2011). Mechanical properties of hybrid inorganic–organic framework materials: establishing fundamental structure–property relationships. *Chemical Society Reviews*, *40*(2), 1059-1080.

[227] San-Miguel, A. (2006). Nanomaterials under high-pressure. *Chemical Society Reviews*, *35*(10), 876-889.

[228] Roduner, E. (2007). *Nanoscopic materials: size-dependent phenomena*. Royal Society of Chemistry.

[229] Ali, N., Teixeira, J. A., &Addali, A. (2018). A review on nanofluids: fabrication, stability, and thermophysical properties. *Journal of Nanomaterials*, *2018*.

[230] Cao, G. (2004). *Nanostructures & nanomaterials: synthesis, properties & applications*. Imperial college press.

[231] Guo, D., Xie, G., & Luo, J. (2013). Mechanical properties of nanoparticles: basics and applications. *Journal of physics D: applied physics*, *47*(1), 013001.

[232] Goyal, M., & Gupta, B. R. K. (2019). Study of shape, size and temperature-dependent elastic properties of nanomaterials. *Modern Physics Letters B*, *33*(26), 1950310.

[233] Wu, Q., Miao, W. S., Zhang, Y. D., Gao, H. J., & Hui, D. (2020). Mechanical properties of nanomaterials: A review. *Nanotechnology Reviews*, *9*(1), 259-273.

[234] Kiio, T. M., & Park, S. (2021). Physical properties of nanoparticles do matter. *Journal of Pharmaceutical Investigation*, *51*, 35-51.

[235] Paras, Yadav, K., Kumar, P., Teja, D. R., Chakraborty, S., Chakraborty, M., ... & Hang, D. R. (2022). A Review on Low-Dimensional Nanomaterials: Nanofabrication, Characterization and Applications. *Nanomaterials*, *13*(1), 160.

[236] Palit, S. (2018). Carbon Nanotubes and its Applications in Diverse Areas of Science and Engineering: A Critical Overview. *Engineered Carbon Nanotubes and Nanofibrous Material*, 1-27.

[237] Madkour, L. H. (2019). *Nanoelectronic materials: fundamentals and applications* (Vol. 116). Springer.

[238] Abdelsalam, H., & Zhang, Q. F. (2022). Properties and applications of quantum dots derived from two-dimensional materials. *Advances in Physics: X*, *7*(1), 2048966.

[239] Cardoso, V. F., Francesko, A., Ribeiro, C., Bañobre-López, M., Martins, P., &Lanceros-Mendez, S. (2018). Advances in magnetic nanoparticles for biomedical applications. *Advanced healthcare materials*, *7*(5), 1700845.

[240] Nasrollahzadeh, M., Sajadi, S. M., Sajjadi, M., &Issaabadi, Z. (2019). An introduction to nanotechnology. In *Interface science and technology* (Vol. 28, pp. 1-27). Elsevier.

[241] Suhag, D., Thakur, P., & Thakur, A. (2023). Introduction to nanotechnology. In *Integrated Nanomaterials and their Applications* (pp. 1-17). Singapore: Springer Nature Singapore.

[242] Binns, C. (2021). *Introduction to nanoscience and nanotechnology*. John Wiley & Sons.

[243] Lahiff, E., Lynam, C., Gilmartin, N., O'Kennedy, R., & Diamond, D. (2010). The increasing importance of carbon nanotubes and nanostructured conducting polymers in biosensors. *Analytical and bioanalytical chemistry*, *398*, 1575-1589.

[244] Morris, J. E., &Iniewski, K. (Eds.). (2013). Graphene, carbon nanotubes, and nanostructures: techniques and applications.

[245] Dresselhaus, M. S., Dresselhaus, G., &Jorio, A. (2004). Unusual properties and structure of carbon nanotubes. *Annu. Rev. Mater. Res.*, *34*, 247-278.

[246] Mansur, H. S. (2010). Quantum dots and nanocomposites. *Wiley Interdisciplinary Reviews: Nanomedicine and Nanobiotechnology*, *2*(2), 113-129.

[247] Dahman, Yaser. *Nanotechnology and functional materials for engineers*. Elsevier, 2017.

[248] Yang, G. Z. (Ed.). (2018). *Implantable sensors and systems: From theory to practice*. Springer.

[249] Chen, H., Zhang, W., Li, M., He, G., & Guo, X. (2020). Interface engineering in organic field-effect transistors: principles, applications, and perspectives. *Chemical reviews*, *120*(5), 2879-2949.

[250] Avouris, P., Freitag, M., &Perebeinos, V. (2008). Carbon-nanotube photonics and optoelectronics. *Nature photonics*, *2*(6), 341-350.

[251] Veetil, J. V., & Ye, K. (2009). Tailored carbon nanotubes for tissue engineering applications. *Biotechnology progress*, *25*(3), 709-721.

[252] Zondlo, J. W. (2012). Graphite: structure, properties, and applications. *Graphite, Graphene, and Their Polymer Nanocomposites*, 1-56.

[253] Wissler, M. (2006). Graphite and carbon powders for electrochemical applications. *Journal of power sources*, *156*(2), 142-150.

[254] Wen, Jianping, Dan Zhao, and Chuanwei Zhang. "An overview of electricity powered vehicles: Lithium-ion battery energy storage density and energy conversion efficiency." *Renewable Energy* 162 (2020): 1629-1648.

[255] Di Lecce, D., Verrelli, R., & Hassoun, J. (2017). Lithium-ion batteries for sustainable energy storage: recent advances towards new cell configurations. *Green Chemistry*, *19*(15), 3442-3467.

[256] Liu, Y., Shi, H., & Wu, Z. S. (2023). Recent status, key strategies and challenging perspectives of fast-charging graphite anodes for lithium-ion batteries. *Energy & Environmental Science*, *16*(11), 4834-4871.

[257] Asenbauer, J., Eisenmann, T., Kuenzel, M., Kazzazi, A., Chen, Z., &Bresser, D. (2020). The success story of graphite as a lithium-ion anode material–fundamentals, remaining challenges, and recent developments including silicon (oxide) composites. *Sustainable Energy & Fuels*, *4*(11), 5387-5416.

[258] Writer, B. (2019). Anode materials, SEI, carbon, graphite, conductivity, graphene, reversible, formation. In *Lithium-ion batteries* (pp. 1-71). Springer, Cham.

[259] Wen, Y., He, K., Zhu, Y., Han, F., Xu, Y., Matsuda, I., ... & Wang, C. (2014). Expanded graphite as superior anode for sodium-ion batteries. *Nature communications*, *5*(1), 4033.

[260] Anderson, O. L. (1984). A universal thermal equation-of-state. *Journal of Geodynamics*, *1*(2), 185-214.

[261] Ross, M., & Young, D. A. (1993). Theory of the equation of state at high pressure. *Annual Review of Physical Chemistry*, *44*(1), 61-87.

[262] Martin, J. J., & Hou, Y. C. (1955). Development of an equation of state for gases.

[263] Canuto, V. (1975). Equation of state at ultrahigh densities. *Annual Review of Astronomy and Astrophysics*, *13*(1), 335-380.

[264] Menikoff, R. (2007). Empirical equations of state for solids. In *ShockWave Science and Technology Reference Library* (pp. 143-188). Berlin, Heidelberg: Springer Berlin Heidelberg.

[265] Martin, J. J. (1967). Equations of state—Applied thermodynamics symposium. *Industrial & Engineering Chemistry*, *59*(12), 34-52.

[266] Redlich, O., &Kwong, J. N. (1949). On the thermodynamics of solutions. V. An equation of state. Fugacities of gaseous solutions. *Chemical reviews*, *44*(1), 233-244.

[267] Kontogeorgis, G. M., Liang, X., Arya, A., &Tsivintzelis, I. (2020). Equations of state in hree centuries. Are we closer to arriving to a single model for all applications? *Chemical Engineering Science: X*, *7*, 100060.

[268] Bina, C. R., &Helffrich, G. R. (1992). Calculation of elastic properties from thermodynamic equation of state principles. *Annual Review of Earth and Planetary Sciences*, *20*(1), 527-552.

[269] iovangigli, V., &Matuszewski, L. (2012). Supercritical fluid thermodynamics from equations of state. *Physica D: Nonlinear Phenomena*, *241*(6), 649-670.

[270] Tait, P. G. (1965). *Report on some of the physical properties of fresh water and of sea water*. Phys. Chem, 2, 1—76.

[271] Birch- Murnaghan, F. (1988). Elasticity and constitution of the Earth's interior. *Elastic Properties and Equations of State*, *26*, 31-90.

[272] Kholiya, K., & Chandra, J. (2014). Equation of state model for studying high-pressure compression behaviour of nanomaterials. *Journal of Taibah University for Science*, *8*(2), 137-141.

[273] Shanker, J., Kushwah, S. S., & Kumar, P. (1997). Theory of thermal expansivity and bulk modulus for MgO and other minerals at high temperatures. *Physica B: Condensed Matter*, *233*(1), 78-83.

[274] Restrepo, V. A. M. (2019). *Efficient Implementation of Advanced Molecularly-based Equation of State Models Out of the Documentation Level*. TechnischeUniversitaet Berlin (Germany).

[275] Dufal, S. (2013). Development and application of advanced thermodynamic molecular description for complex reservoir fluids containing carbon dioxide and brines.

[276] Sólyom, J. (2007). *Fundamentals of the Physics of Solids*. Springer-Verlag New York, Inc.

[277] Kontogeorgis, G. M., &Folas, G. K. (2009). *Thermodynamic models for industrial applications: from classical and advanced mixing rules to association theories*. John Wiley & Sons.

[278] Solon, A. P., Stenhammar, J., Cates, M. E., Kafri, Y., &Tailleur, J. (2018). Generalized thermodynamics of motility-induced phase separation: phase equilibria, Laplace pressure, and change of ensembles. *New Journal of Physics*, *20*(7), 075001.

[279] De Hemptinne, J. C., Kontogeorgis, G. M., Dohrn, R., Economou, I. G., Ten Kate, A., Kuitunen, S., ... &Vesovic, V. (2022). A view on the future of applied thermodynamics. *Industrial & Engineering Chemistry Research*, *61*(39), 14664-14680.

[280] Hendriks, E., Kontogeorgis, G. M., Dohrn, R., de Hemptinne, J. C., Economou, I. G., Zilnik, L. F., &Vesovic, V. (2010). Industrial requirements for thermodynamics and transport properties. *Industrial & engineering chemistry research*, *49*(22), 11131-11141.

[281] Prausnitz, J. M., & Tavares, F. W. (2004). Thermodynamics of fluid-phase equilibria for standard chemical engineering operations. *AIChE journal*, *50*(4), 739-761.

[282] Nishimori, H., & Ortiz, G. (2011). *Elements of phase transitions and critical phenomena*. Oxford university press.

[283] Hillert, M. (2007). *Phase equilibria, phase diagrams and phase transformations: their thermodynamic basis*. Cambridge university press.

[284] Hohenberg, P. C., & Halperin, B. I. (1977). Theory of dynamic critical phenomena. *Reviews of Modern Physics*, *49*(3), 435.

[285] Eliezer, S., Ghatak, A., & Hora, H. (2002). *Fundamentals of equations of state*. World Scientific.

[286] Tadmor, E. B., Miller, R. E., & Elliott, R. S. (2012). *Continuum mechanics and thermodynamics: from fundamental concepts to governing equations*. Cambridge University Press.

[287] Saumon, D., Chabrier, G., & van Horn, H. M. (1995). An equation of state for low-mass stars and giant planets. *Astrophysical Journal Supplement v. 99, p. 713*, *99*, 713.

[288] Hempel, M., Fischer, T., Schaffner-Bielich, J., &Liebendörfer, M. (2012). New equations of state in simulations of core-collapse supernovae. *The Astrophysical Journal*, *748*(1), 70.

[289] Özel, F., & Freire, P. (2016). Masses, radii, and the equation of state of neutron stars. *Annual Review of Astronomy and Astrophysics*, *54*(1), 401-440.

[290] Kothawale, M. M. (2013). *Study of Magnetic and Electrical Properties of Ultra-fine Ni-Zn Ferrite Materials Prepared by Novel Method* (Doctoral dissertation, Goa University).

[291] Gawas, S. G. (2018). *Synthesis, Study of Solid State and Spectral Properties of Substituted Ni-Zn Ferrites and their Application* (Doctoral dissertation, Goa University).

[292] Kundaiker, G. V. (2011). *Electrical and Magnetic Properties of Nanoparticle Mn-Zn Ferrites obtained from novel methods of Synthesis* (Doctoral dissertation, Goa University).

[293] Jowitt, S. M., Mudd, G. M., Werner, T. T., Weng, Z., Barkoff, D. W., & McCaffrey, D. (2018). The critical metals: An overview and opportunities and concerns for the future.

[294] Müller, E., Hilty, L. M., Widmer, R., Schluep, M., &Faulstich, M. (2014). Modeling metal stocks and flows: a review of dynamic material flow analysis methods. *Environmental science & technology*, *48*(4), 2102-2113.

[295] Shrivastava, P. (2018). Environmental technologies and competitive advantage. In *Business Ethics and Strategy, Volumes I and II* (pp. 317-334). Routledge.

Investigation of Compression Behavior of Heusler Compounds Using Various Equations of State

Tajamul Islam and A. K. Srivastava*

Department of Physics

Lovely Professional University, Phagwara, Punjab-144411

*Email: srivastava_phy@yahoo.co.in

Abstract

The compression behaviour of Heusler compounds viz, Rh_2MnZn, Rh_2FeZn, Co_2NbB, and Co_2TaB has been studied using various equations of state, namely Tait equation, Murnaghan equation, Shanker's equation and Kholiya and Chandra equation. It has been observed that the Tait equation of state generally fits best for the compression behaviour of the chosen materials, followed by the Murnaghan equation of state, whereas Kholiya and Chandra, and Shanker's equations of state are less accurate. All Heusler compounds exhibit similar patterns in compression behaviour with decreasing volume and increasing pressure with a slight deviation that may be due to their crystal structure and chemical composition. The obtained results are found to be in good agreement with the available experimental values. The results of this study can provide valuable insights into the compressibility and mechanical properties of Heusler compounds, which can inform their potential applications in various fields, including energy harvesting, spintronics, and thermoelectric devices.

1. Introduction

Intermetallic Heusler compounds have attracted significant attention in recent years due to their unique physical, electrical, and magnetic properties. Understanding the compression behaviour of these compounds is crucial for predicting their mechanical properties and for potential applications in fields such as energy storage, thermos-electrics, and spintronics. In this context, several studies have investigated the compression behaviour of different Heusler compounds using various equation of state (EOS) models. In recent days, various multi-component mixture compounds like Mn_2CoCr, Mn_2PtCo, Rh_2MnZn, and Rh_2FeZn are gaining more attention due to their extraordinary properties like compressible and structural properties by changing the pressure, volume and temperature [1-6]. These Heusler compounds are known for their exciting magnetic, electronic, and thermoelectric properties, making them capable materials for various technological applications [7-13]. Heusler compounds have various potential applications due to their unique combination of physical and chemical properties. Some of the major technological applications of such

İlkogretim Online - Elementary Education Online, 2021; Vol 20 (Issue 6): pp. 4961-4969
http://ilkogretim-online.org
doi: 10.17051/ilkonline.2021.06.482

Study Of The Compression Behaviour Of Fe Cr Ti Sn And Fe Cr Ti Sb Materials Using Various Equation Of States

Tajamul Islam[1,2], A.K Srivastava[1]* and Masood A Kaloo[3]* and Aijaz A Wani[4]

[1]Department of Physics, Lovely Professional University, Punjab-14441, India.
[2]Department of Physics, Govt. Degree College Shopian, J&K-192303, India.
[3]Department of Chemistry, Govt. Degree College Doda, J&K-182202, India.
[4]Department of Physics, Govt. Degree College Kulgam, J&K-192231, India.
Email id of Corresponding Author(s): srivastava_phy@yahoo.co.in, kaloomasood@gmail.com

Abstract

The Heusler compounds assert potential candidates for a variety of applications such as memory devices, spintronics, magneto resistive materials, and spin-value generators owing to their undeniable properties such as large magnetic moment, large ferromagnetism, Curie temperature, high polarization at the Fermi level, thermoelectric performance, etc. In this work, the theoretical approach wherein various equation of states such as Tait, Murnaghan, Shanker, Kohliya and Chandra have been employedto investigate thecompression behaviour of the two Heusler compounds FeCrTiSn and FeCrTiSb in detail. It has been observed that both the compounds FeCrTiSn and FeCrTiSb exhibit a nearly linearly declining trend with the applied pressure and our theoretical results are in agreement with experimental calculated one reported in the literature.

Key words: Magnetic, Thermoelectric, Superconductivity, Materials, Equation of State.

1. Introduction

Electronic and magnetic materials have subsequent applications in different fields [1-5]. Electronic materials have vast applications in the semiconductor industry, particularly in mobile phones, integrated circuits, and electronic chips [6-8]. For instance, silicon has found its way into modern computers, digital timepieces, communication satellites, and pocket calculators. Additionally, magnetic materials are used in devices including magnets, generators, magnetic detectors, microphones, and magnetic separators [9-12]. On the scale of these applications, we considered the class of materials known as "Heusler compounds".

"Heusler compounds" refers to a class of intermetallic compounds with a definite crystal structure and composition. Heusler compounds classically consist of three elements: two transition metals (one from group VIII and the other from groups III-VI) and a main-

Journal of Neonatal Surgery

ISSN: 2226-0439 (Online); (ISSN-L): 2226-0439

Website: *https://www.jneonatalsurg.com/ojs/index.php/jns/index*

Dear (Tajamul Islam, A.K Srivastava)

We have reached a decision regarding your manuscript submission to **Journal of Neonatal Surgery** titled as – "Investigation of physical properties of nanomaterials at high pressure"

Our Decision is to: **Accept Submission**

Journal of Neonatal Surgery

Our Indexing Partner's

Accepted Manuscript (Author Version)

DOI: 10.57647/jtap.2026.2002.14

Research Article

Pressure-Volume Response in Nanomaterials: Contrasting Graphenic Sheets, Oxide Ceramics, and Transition Metal Architectures

Tajamul Islam[1], A.K Srivastava[1], Mudasir Mir[2], Santosh Chackrabarti[3*], R.A. Zargar[4]

[1]*Department of Physics, Lovely Professional University, Phagwara, Punjab-144411 India*
[2]*Department of Physics, Government Degree College, Shopian (J&K), Jammu and Kashmir-192303, India*
[3]*Centre for Nanoscience and Nanotechnology, Jamia Millia Islamia, New Delhi-110025 India*
[4]*Department of Physics, Guru Nanak University, Ibrahimpatnam, Telangana-501506 India*

***Corresponding Author:** dhrub.phy@gmail.com

Received: 14 October 2025
Revised: 21 November 2025
Accepted: 17 December 2025

ORCID:

Accepted Manuscript Author Version

Abstract

This investigation presents a comprehensive theoretical examination of pressure-induced volumetric compression characteristics in five structurally diverse nanomaterials: graphite, aluminium oxide (Al_2O_3), single-walled carbon nanotubes (SWCNTs), nano-epsilon-phase iron (nano-ε-Fe), and nano-nickel (nano-Ni), representing carbon allotropes, ceramic oxides, and transition metal systems. Four established equations of state (Tait, Murnaghan, Kholiya and Chandra, and Shanker) were employed using experimentally derived bulk modulus values and their pressure derivatives from literature to model relative volumetric changes under applied pressure up to 16 GPa. The analysis reveals material-specific compressibility behaviours dictated by bonding characteristics, atomic configuration, and dimensionality. Al_2O_3 demonstrates the highest incompressibility among studied materials due to its strong ionic-covalent bonding, while SWCNTs exhibit pronounced nonlinear compression attributed to structural instabilities under confinement. Nano-Ni and nano-ε-Fe show intermediate compressibility with enhanced sensitivity due to nanoscale effects including surface energy

© Author(s) 2026 CC BY 4.0 https://creativecommons.org/licenses/by/4.0/

10:49 AM

SEEJPH South Eastern European Journal of Public Health

Date:20/02/2025
ID: SEEJPH-4555

Letter of Acceptance

Dear Authors:
Tajamul Islam1* A.K. Srivastava

It is a great pleasure to inform you that your article titled " **nvestigation of Compression Behaviour of Bulk Inorganic Materials (Al, Cu, Pb, Ni, and Zn) Under High Pressure"** has been accepted for publication in "**South Eastern European Journal of Public Health" ISSN: 2197- 5248.**

The article is scheduled for publication in the upcoming issue, 2025. Kindly complete the required formalities and email us the final version along with the publication fee payment.

EDITORIAL OFFICE

SOUTH EASTERN EUROPEAN JOURNAL OF PUBLIC HEALTH
WWW.SEEJPH.COM
ISSN: 2197- 5248

Investigation of Compression Behaviour of Bulk Inorganic Materials (Al, Cu, Pb, Ni, and Zn) Under High Pressure

Tajamul Islam[1*] A.K. Srivastava

[1]*Department of Chemical Engineering and Physical science, Lovely Professional University, Phagwara, Punjab, India-144411.*
**Corresponding Author: islam786physics@gmail.com*

KEYWORDS

Equation of State; Bulk Modulus; Compression; Volume.

ABSTRACT

This study investigates the compression behavior of aluminum (Al), copper (Cu), lead (Pb), nickel (Ni), and zinc (Zn) under varying pressure conditions, as predicted by several equations of state (EOS), including the Tait, Murnaghan, Kholiya and Chandra, and Shanker's equations. Each metal exhibits a consistent trend in volumetric compression (V/V_0) as pressure increases from 0 to 16 GPa, indicating a decrease in volume relative to the original volume (V/V_0). The Tait equation generally shows higher volumetric values at corresponding pressures compared to the other EOS models for all metals. In contrast, the Murnaghan equation provides values closely aligned with those from Kholiya and Chandra's equation, with minor deviations observed, particularly in nickel and zinc at higher pressures. Shanker's equation consistently predicts the lowest (V/V_0) values across all pressures for most metals, suggesting a more conservative estimate of volume reduction under compression. The data reveals the unique response of each metal to applied pressure, which is critical for applications in material science and engineering, providing insights into their mechanical properties and stability under extreme conditions. This comparative analysis enhances our understanding of the mechanical behavior of these metals, facilitating better material selection for high-pressure applications.

1. Introduction

High-pressure studies of bulk materials are always necessary because they shed light on the behavior of these materials under harsh circumstances, exposing phase transitions, structural deformations, and other crucial phenomena [1-5]. Mechanical features including volume compression and heat expansion are described by a variety of equations of state (EOS), including Tait's equation, Murnaghan's equation, Kholiya and Chandra Equation, and Shanker's equation of state [6-11]. The theoretical research of EOS at high pressure and high temperature are essentially significant enabling the extrapolation and interpolation into zones where experimental data is insufficient [12-13]. The equations of state (EOS) provide researchers with valuable perceptions into the properties of gases, liquids, and solids, enabling them to predict and analyze phase transitions, critical points, and other thermodynamic processes [14-15]. These equations serve as essential tools for understanding the behavior of matter under varying conditions, facilitating advancements in fields such as condensed matter physics and materials science [14-17]. Furthermore, the use of these EOS is essential for explaining how matter behaves in a variety of pressure, temperature, and volume situations [18-20]. Owing to their special qualities, inorganic metallic materials in bulk form play important roles in a variety of industries and technology [21–22]. These applications range from electrical components to structural materials [23-25]. It's crucial to remember that changes in economic conditions, environmental concerns, and technological improvements can all affect how useful these metals become over time [26-27].

As a result of changes in atomic and molecular organization, bulk materials studied under high pressure show a variety of alterations in their physical and chemical properties [28-